

117332

NHTSA-98-3588

DEPT. OF TRANSPORTATION

NHTSA-98-3588-91

00 NOV 29 PM 2:38

ORVR Vapor Canister Testing and Evaluation

FINAL REPORT

for:

General Motors Corporation

March 2000

S.E.A. INC.

7349 Worthington-Galena Rd., Columbus, Ohio 43085

ORVR Vapor Canister Testing and Evaluation

Gary J. Heydinger, Ph.D., P.E.

Dale A. Andreatta, Ph.D., P.E.

Ronald A. Bixel

Acknowledgements

This work was funded by GM pursuant to an agreement between GM and the U.S. Department of Transportation.

The authors thank Dr. Scott W. Jorgensen from GM for his assistance and useful insights and suggestions. We also thank Scott for his patience in dealing with the numerous delays that occurred during the course of completing this work.

We also acknowledge David A. Coover, Sr. and Joonhong Park for their assistance with many portions of the experimental testing.

Table of Contents

Acknowledgements	i
Introduction	1
Section 1: Experimental Study of Canister Rupture	2
Canister Rupture Device and Testing Specifications	2
Canister Rupture Results	6
Section 2: Investigation of Possible Ignition Sources	12
Surrogate Ignition Sources Used During Crash Tests	15
Section 3: Canister Loading Specifications and Procedures	16
Canister (Break-In) Preparation	16
Canister Loading	19
Section 4: Ignition Tests of Unruptured Canisters	21
Section 5: Measurement of Vapor Concentration after Canister Rupture	22
Section 6: Demonstration of Ignition of Ruptured Canister	26
Section 7: Vehicle Crash Tests	27
Crash Test Specifications	27
Side Impact Crash Test Results	30
Rear Impact Crash Test Results	30
Section 8: Risk Analysis	39
Introduction	39
Analysis	39
Conclusions.....	48
Appendix A: Results from Canister Rupture Tests which Resulted in Spilled Carbon	
Appendix B: Results from Vapor Concentration Measurement after Canister Rupture Tests	

Introduction

The objective of the project was to study safety aspects of rear-mounted Onboard Refueling Vapor Recovery (ORVR) canisters. Safety aspects which were studied experimentally were:

1. **Canister Rupture:** Study the amount of energy necessary to rupture a canister, and study the spilling and spreading of the carbon grains after rupture. Determine if the energy required to rupture the canister depends upon which face is struck.
2. **Ignition Sources:** Determine possible ignition sources that might exist in a vehicular collision, and determine the effect of these on vapor-laden carbon particles.
3. **Vapor Concentration:** Measure the vapor concentration in the area of freshly ruptured canisters laden with vapor.
4. **Ignition of Unbroken Canisters:** Determine whether it is possible, and under what conditions, to ignite an unbroken canister with vapor-laden carbon.
5. **Ignition of Broken Canisters:** Determine whether it is possible to ignite a broken canister laden with vapor.
6. **Vehicle Crash Tests:** Perform two vehicle crash tests with laden canisters, measure the vapor concentration in the area of the canister, and have ignition sources present which can ignite the vapor.

Finally, the results of the above tests were combined with other data to perform a relative risk analysis for both a rear-mounted ORVR canister and a front-mounted similar canister at a specified location in the front of the vehicle. In production, the intent is to mount ORVR canisters in the rear of the vehicle, while the traditional evaporative emissions canister was typically mounted in the front of the vehicle. The outcome of this analysis was an estimated number of fires per year in U.S. vehicles caused by the presence of the canister.

The canisters used for all testing were GM 2100 cc ORVR canisters.

Section 1: Experimental Study of Canister Rupture

The purpose of this testing was to study the amount of energy necessary to rupture a canister, and study the spilling and spreading of the carbon grains after rupture. The energy required to rupture the canister was evaluated for the bottom, the wide face, and the narrow face.

Canister Rupture Device and Testing Specifications

The canisters used for all testing were General Motors 2100cc Onboard Refueling Vapor Recovery (ORVR) canisters. The canisters were ruptured in three orientations: narrow side impacts, wide side impacts, and bottom impacts.

The rupture device was designed so the impactor would generate impact speeds similar to those that might exist in actual vehicle crashes; the consensus being that impact speed influences carbon dispersal. Accordingly, the impactor was designed to provide a constant speed of approximately 30 mph for all impact energies.

Figure 1 contains three photographs of the canister rupture device. The main components of the impactor are indicated on the photographs. Figure 2 is a side view schematic of the impactor illustrating how the impactor operates.

The impactor is accelerated to speed by the action of a swing arm, the cam-shaped aluminum plate shown in its down position in the top photos. Weights can be added to the plate and impactor to increase the energy of the impact, while maintaining a constant impact speed. The plate pivots about a 2.0 inch diameter shaft shown near the center of the height of the rupture device. The plate is raised prior to impact and a steel cable is wrapped around the plate, fitting in a groove cut along its perimeter. The cable connects to the impactor through a series of pulleys, providing a 4:1 speed multiplication between the speeds of the center-of-gravity of the swinging weights and the impactor. Thus, 30 mph is achieved with a relatively short 2-foot swing arm radius (radius of the center of mass) and the whole device fits inside a room. To achieve 30 mph with a normal pendulum would require a swing height of 30 feet.

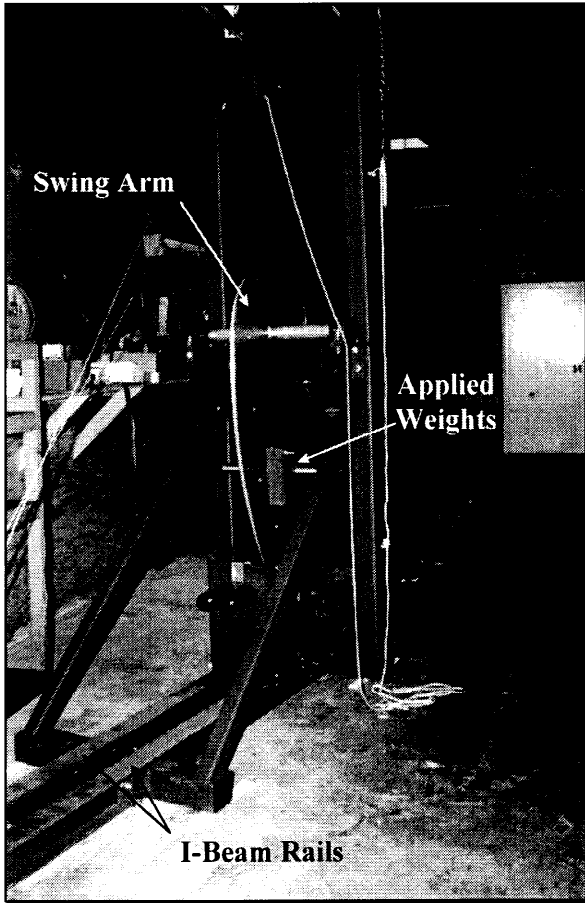
The impactor travels horizontally between a pair of 4-inch flange I-beams using six low-friction Teflon bearings built into the impactor. The impactor is moved to the rear of the rails before the rupture device is triggered. To generate the impact, the plate is swung down and the cable converts the energy of the falling weight of the plate into translational energy in the direction of travel of the impactor. Near the end of its travel the impactor disconnects from the cable and hits the canister.

The impactor itself is a 35 inch long, 3 inch diameter aluminum tube. The impactor has a 5 inch radius semispherical head at the impact end (front) and hardware for attaching various ballast at the rear. The impactor test weights ranged from 4.82 lb to about 40 lb. Achieving a particular impact energy and a 30 mph impact speed simultaneously is achieved by the proper adjustment of the weight of the swinging plate and the weight of the impactor.

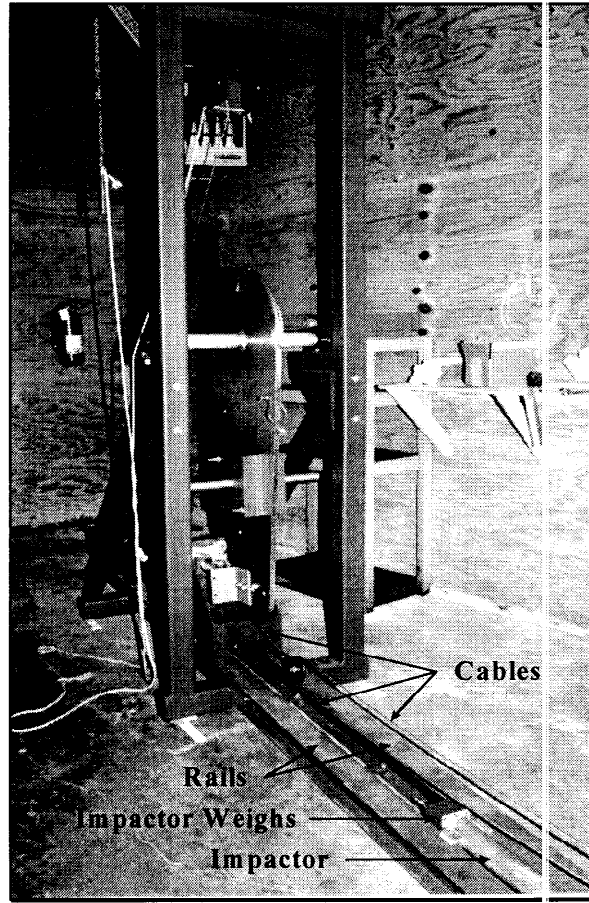
To confirm that the impactor was traveling at the proper speed, a Hi-8 video camera capable of recording 60 fields per second (2 fields are combined to make a frame) was used with a 1/10,000th second shutter speed. A surveyor's tape was placed in the camera field along the line of the impactor, and distinct images of the impactor could be achieved. The smallest subdivision of the surveyor's tape was 0.01 foot, thus the speed measurement was somewhat "discretized". Comparing the location of the impactor in two or three subsequent fields allowed calculation of the speed. This method proved to be repeatable, and is presumed to be accurate. Friction forces in the impactor accelerator were small, and were accounted for, since the camera recorded the speed of the impactor just before impact. The speed of the impactor was generally 90-94% of the theoretical speed assuming zero friction.

For the canister wide and narrow side tests the canister was hose-clamped to a 12 x 12 x 1/8 inch steel plate, which was set between two vertical rigid C-channels, 10 inches apart. This was to simulate the fact that the canister in a vehicle would not be on a rigid backing. Estimates were made of the energy absorbed by the plate, and these estimates were on the order of 20% of the test energy. The residual (plastic) deformation of the plate was measured after each test, and each test started with a nominally straight plate. After the plate would deform about 3 inches it would contact the frame of the machine and a 50-lb steel weight that was placed on the frame. The top of the frame was at about the centerline of the impactor, thus, the use of the 50 lb weight helped to even out the top to bottom distribution of forces on the impactor to prevent the impactor from rebounding at an upward angle.

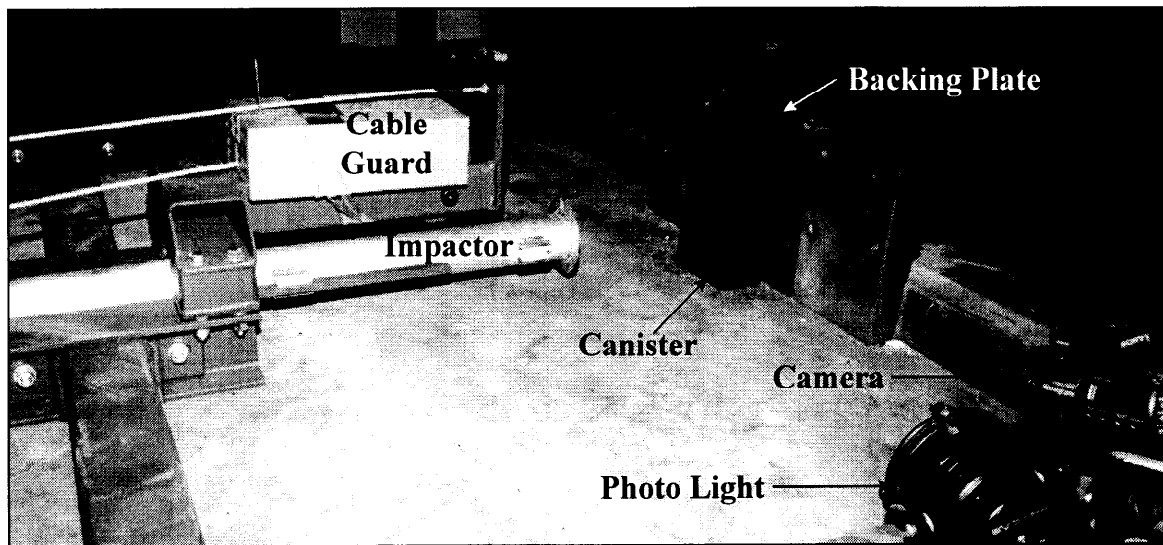
For the bottom impact tests the subframe was rigidly bolted to the frame of the machine below the level of the bottom of the impactor. A 3/16 inch steel cable was used near the top of the canister and a hose clamp was used near the bottom to secure the canister to the subframe during these tests. The cable was used to insure that the canister did not break free from its mounting, and to prevent impactor damage.



Canister Rupture Device - Rear View



Canister Rupture Device - Front View



Impact Area of Canister Rupture Device Showing Impactor

Figure 1: Canister Rupture Device

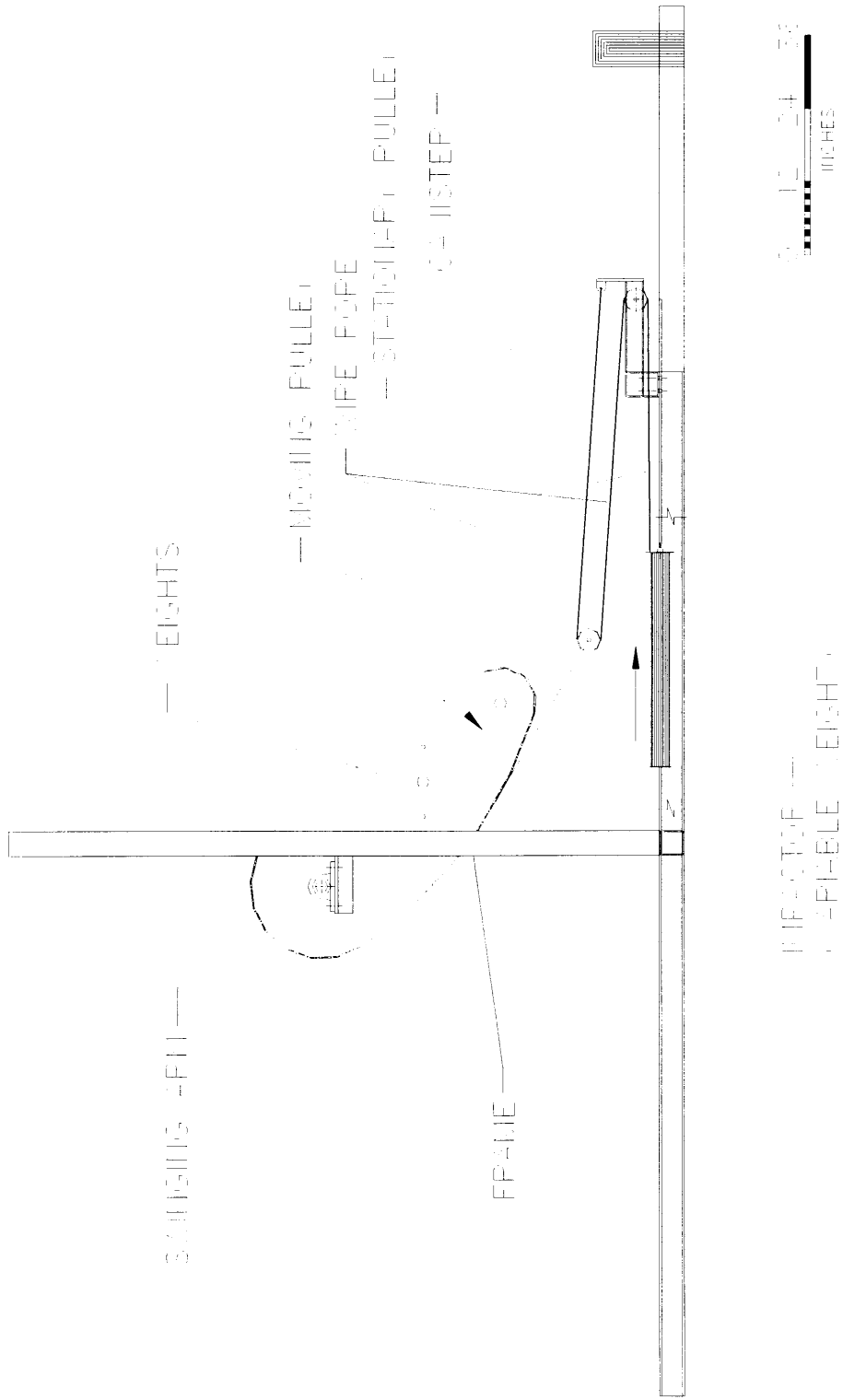


Figure 2: Schematic of Canister Rupture Device

Canister Rupture Results

Canister Rupture

The minimum energy required to break a canister and spill at least some carbon was measured in the preliminary testing phase. This was done for the wide side, the narrow side, and the bottom of the canister. Using data from the preliminary tests, a test matrix was made so the canisters would be subjected to impacts along the three axes at two and four times the minimum energy. Three tests were done at each direction at each energy level (a total of 18 tests). Carbon scatter in each test was noted.

Impacts were approximately in the center of the canister's carbon-loading section. Though no part of the canister appears to be particularly weak, the carbon loading section is probably the area which is most likely to rupture. This assumption was not tested in detail, and it may be that the shape of the impactor (relatively sharp versus relatively flat) may influence these results.

The minimum energy in each of the three directions was as follows:

Table 1: Minimum Impact Energy For Canister Rupture	
Impacted Side	Minimum Energy (ft-lbs)
Wide Side	129
Narrow Side	157
Bottom	79

The minimum energy possible while maintaining the 30 mph impact speed was 144.6 ft-lb (minimum impactor weight 4.82 lb). The minimum energy tests for the bottom and wide side tests were done with minimum impactor weight and less than 180° of swing arm motion, so the impactor speed was somewhat less than 30 mph. The impactor speed was directly measured by camera.

A complication arose in that there was considerable variation between canisters as to the minimum energy to break a canister. Also, during this phase of the testing, a limited number of canisters was available. Some unloaded (no gasoline vapor) canisters withstood impacts at four times the minimum energy determined earlier. For loaded canisters, some withstood up to six times the minimum energy with no carbon spill (canister loading is discussed in Section 3). There may be considerable variation between canisters, but our testing also suggests that the temperature of the plastic material may affect the breaking strength, with warm canisters being

stronger. Many plastics show an increase in ductility as temperature increases, which would allow the carbon particles to absorb more energy before the plastic ruptured. Lower breaking energies were typically observed in the winter months with a partially heated room, while higher breaking energies were achieved with the room warm, and the highest break energies were with the canisters warm from a recent fast-loading procedure. No canisters were tested at very low (sub-freezing) temperatures. Canister temperature was not understood to play a role in rupture prior to these tests; it was not included in the experimental protocol.

The variation in impact energy needed to rupture different canisters led to a change in procedure; the original test matrix was used with additional tests for “strong” canisters. In order to minimize the number of canisters used in the unloaded canister phase of the testing, if a canister did not break on the first test, the following procedure was used: Hit a canister with two times the minimum energy. If it does not break, turn the canister around and hit the same canister again, with three times the minimum energy. If this does not break the canister, turn it around and hit it with four times the minimum. Continue this until the canister breaks. If the canister breaks but does not spill carbon, record that as a break with no spillage, and discontinue testing on that canister, since its integrity is obviously compromised. On tests in which a canister did not crack, no change in the integrity of the canister was observed. If any bias was introduced by this procedure, it would lead to a lower energy to rupture the canister, and a conservative (high) estimate of the frequency with which carbon would be spilled.

When testing the bottoms of the canisters, all canisters broke and spilled carbon at twice the minimum energy. When testing the narrow and wide sides, some canisters withstood as many as three hits with 2, 3, and 4 times the minimum energy without breaking. In Table 2, these tests are given the same number. Thus, tests 5, 5b, 5c, and 5d were all done on the same canister, at, respectively, 2, 3, 4, and 5 times the minimum energy. The bottoms of the canisters were subsequently tested at four times the minimum energy, and the wide and narrow sides were tested at six times the minimum energy.

Table 2 below summarizes the results of the testing. In the table, some sequential numbers are missing, these are for tests that were judged to be invalid. Tests were deemed invalid if the test conditions, such as impact speed, were not achieved; which usually resulted from a mechanical problem. The invalid tests are included in the videotaped results, and thus already had numbers assigned to them.

Table 2: Summary of Canister Impact Tests

Canister/Test Number	Side Tested	V (mph)	E (ft-lbs.)	E/E_{min}	Break	Carbon Scatter
5	Wide	30.1	259	2.01	No	No
5/b	Wide	29.9	384	2.97	No	No
5/c	Wide	30.5	530	4.11	No	No
5/d	Wide	31.1	693	5.37	Yes	Yes
7	Narrow	30.7	331	2.10	No	No
7/b	Narrow	31.1	506	3.22	No	No
7/c	Narrow	30.3	638	4.06	Yes	Yes
8	Narrow	30.3	333	2.05	No	No
8/b	Narrow	30.3	481	3.06	No	No
8/c	Narrow	29.9	623	3.96	Yes	Yes
9	Narrow	30.3	333	2.05	No	No
9/b	Narrow	30.3	481	3.06	No	No
9/c	Narrow	29.9	623	3.96	Yes	No
10	Wide	29.7	253	1.96	Yes	No
11	Wide	29.7	253	1.96	No	No
11/b	Wide	29.9	387	2.97	No	No
11/c	Wide	30.7	537	4.16	Yes	Yes
13	Bottom	30.3	160	2.03	Yes	Yes
14	Bottom	30.3	160	2.03	Yes	Slight
15	Bottom	29.9	156	1.98	Yes	Yes
16	Bottom	30.3	323	4.09	Yes	Yes
17	Bottom	30.7	332	4.20	Yes	Yes
18	Bottom	30.3	323	4.09	Yes	Yes
19	Wide	30.3	788	6.11	Yes	Yes
20	Wide	30.3	788	6.11	Yes	Yes
21	Wide	30.3	788	6.11	Yes	Yes
22	Narrow	30.7	985	6.26	Yes	Yes
23	Narrow	30.7	985	6.26	Yes	Yes
24	Narrow	30.3	958	6.10	Yes	Yes

Carbon Scatter

The scatter of the charcoal was measured by using a series of 100 to 110 plastic trays, depending on the arrangement of the test. The trays were each about 5.3 inches (135 mm) square after a slight overlap was taken into account. These trays were arranged in a pattern to completely cover the area inside the frame of the impact area of the rupture device. This was generally from the canister back toward the machine (in the direction from which the impactor came) and also left and right. Figure 3 shows a photograph of a typical arrangement of the trays used to collect the scattered charcoal. In all cases the vast majority of the spilled carbon fell into the trays adjacent to the canister. In the higher energy tests a measurable amount of carbon fell outside the trays, either in front of the trays (in the direction to which the impactor was going) or to the left and right. The scatter outside the trays was weighed as a unit. In no cases was the scatter outside the trays concentrated.

Tabular results for the carbon scatter are shown in Table 3, and Figure 4 shows a graph of impact energy versus spilled carbon for all tests that resulted in carbon scatter.

As can be seen, in most cases at least half of the spilled carbon fell into one tray. Tests 16-24 were at four or six times the minimum energy, where the canister broke on the first hit. Tests up to number 15 were at two to five times minimum energy, depending on how much energy it took to break that particular canister. There appears to be no strong correlation between the energy level and the amount spilled, although the general trend is that higher energy levels resulted in greater carbon spillage. It is likely that in a vehicle, post-impact motions of the vehicle would have a large influence on the amount of carbon spilled from the ruptured canister.



Figure 3: Photograph of Typical Arrangement of Trays used to Collect Scattered Charcoal

Table 3: Summary of Carbon Scatter Measurement Tests

Canister/Test Number	Side Tested	Most Carbon in One Tray (grams)	Total Carbon in Trays (gram)	Total Carbon Outside Trays (grams)	Total Carbon Spilled (grams)
5/d	Wide	5.7	26.1	Negligible	26.1
7/c	Narrow	132.8	300.0	Negligible	300.0
8/c	Narrow	91.7	136.0	Negligible	136.0
11/c	Wide	228.9	340.3	Negligible	340.3
13	Bottom	78.5	147.6	Negligible	147.6
14	Bottom	8.2	8.2	Negligible	8.2
15	Bottom	6.5	16.0	Negligible	16.0
16	Bottom	51.3	62.6	Negligible	62.6
17	Bottom	25.3	52.1	Negligible	52.1
18	Bottom	48.0	94.9	Negligible	94.9
19	Wide	165.5	303.9	8.5	312.4
20	Wide	171.5	341.7	Negligible	341.7
21	Wide	60.2	130.7	Negligible	130.7
22	Narrow	54.6	198.0	42.0	240.0
23	Narrow	85.0	267.8	29.5	297.3
24	Narrow	31.1	277.0	52.7	329.7

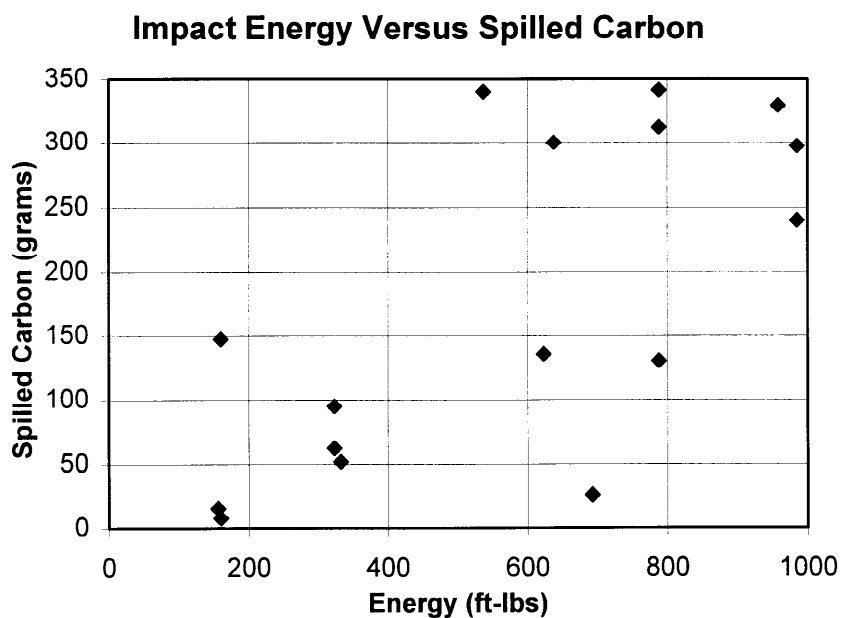


Figure 4: Impact Energy Versus Spilled Carbon (Charcoal)

Contour plots of the carbon scatter are shown in Appendix A for the 16 tests for which there was scatter. Along with each contour plot is a page with two photos showing the carbon spillage for each test. In all cases the vast majority of the scatter fell into the trays adjacent to the canister. In the plots, the origin ($x=0$, $y=0$) is the center of the impact zone. The view of the contour plot is an overhead view, with the impactor moving along the x-axis in the negative x-direction, and impacting the canister at (0,0). The x- and y-values are for the center of the trays, and each intersection in the plots in Appendix A represents the center of a tray. It is tempting to think of the squares on the plots as the trays themselves, but this is not correct. Some of the trays were trimmed to fit the corners around the canister. Note that each contour plot has its own scale. The positive x-direction was toward the machine or in the direction from which the impactor came, and the positive y-direction was to the left when looking in the positive x-direction.

In the higher energy tests the carbon dispersal was wider, that is, a larger fraction of the spilled carbon was thrown beyond the adjacent trays. In all cases, most of the carbon went into the trays adjacent to the impact zone. In most cases the contour plots show two "islands" of carbon scatter, one in the positive y-direction and the other in the negative y-direction. Usually, the positive y-island was bigger in area and heavier. In most cases the positive y-island had a larger positive x-coordinate.

When striking the bottoms of the canisters both the carbon distribution pattern and the damage to the canister were very consistent from test to test for a given energy level. For the other directions the damage and distribution pattern was not so consistent. As can be seen from the previous section, there was considerable variation from canister to canister in the amount of energy that it took to break a canister.

All tests were recorded by two video cameras. One was the Hi-8 camera that was used primarily to measure the speed of the impactor, though one can see the carbon dispersal to some extent. The damage to the canister can also be seen if the shutter opening occurred at a time so as to catch the impactor deflecting the canister. It was noted on some tests that at least 1 ½ inches of deflection could be imparted to the canister before the casing would break.

Section 2: Investigation of Possible Ignition Sources

The objective of this phase of the testing was to identify and test possible ignition sources that might be present in the vicinity of a canister at the time of an actual accident. The following four ignition sources were identified as being the most likely to be present:

1. Open flame
2. Hot metal such as a taillight or headlight filament
3. 12 V electrical spark
4. Mechanical spark

The goal of the testing of each likely ignition source was to determine in a “yes” or “no” manner whether the ignition source would cause ignition given certain worst case vapor/carbon conditions. As will be discussed later in this report, two different methods were used to load the canisters with vapor, a slow-load and a fast-load method. The fast-load method caused the carbon to heat up and thereby provided a worst case condition, so vapor laden carbon from a fast-load canister was used for ignition source testing. The test protocol for the fast-load canister testing was to test the canister within ten minutes of loading.

For all four sources tested, 20 ml samples of carbon from the same fast-load canister were used. The tests were performed by four people working in four separate stations and were performed concurrently so that all tests would be completed within ten minutes after the canister was loaded. Figure 5 contains photos of the test stations. To facilitate removing the vapor laden carbon from the canister, a door was cut into its side and taped shut prior to vapor-loading the canister. The ambient temperature was measured to be 70 degrees F in the test area.

Source No. 1 - Open Flame

The objective of this section was to determine whether an open flame - considered to be a “worst case” ignition source - could ignite a pile of carbon loaded with vapor using the fast load method.

A 20 ml sample of carbon was placed on a flat base in a pile about 8 cm in diameter. A small Bunsen burner flame (about 12 mm long) was placed at the level of the base and brought inward from 150 mm in 25 mm increments. The flame was held in position for 10 seconds before moving inward. This was performed three times with new 20 ml samples of carbon for each test.

Results:

Ignition occurred at 100 mm, 50 mm and 100 mm in three consecutive tests.

Source No. 2 - Hot Metal

Taillight filaments, from style 1157 bulbs, were used as the hot metal. To prepare the bulbs, the glass envelopes were broken to allow the filaments to be in direct contact with the surrounding environment. The life of such a filament is approximately six seconds. For each test, three bulbs were prepared such that their brake light filaments could be separately energized. A 20 ml

sample of carbon was placed in a pile approximately 8 cm in diameter. The bulbs were placed at varying distances from the carbon and were energized in order beginning with the furthest from the carbon. After a filament failed, the system was observed for about 2 seconds. Assuming no ignition had occurred, the next filament was energized. It was previously determined that the most effective vertical location of an ignition source was on the plane of the base of the carbon pile. Filaments were placed on the base surface at varying distances from the carbon pile. The distance from the edge of the pile ranged from 12 to 50 mm. A car battery producing 12.9 volts was used to energize the filaments.

Results:

For the first test, no ignition occurred at 50 mm. The next setting was 25 mm where ignition occurred. For the second test, with a fresh 20 ml of carbon, the increments were decreased so that filaments were placed at 50, 37.5, and 25 mm. Again, ignition did not occur until the 25 mm filament was energized.

Source No. 3 - Electrical spark

The test setup included carbon steel posts and a carbon steel hand-held electrode. The posts were connected to the negative pole of a 12 V car battery and the moving electrode was connected to the positive pole. The initial voltage was 12.9 V. A 20 ml pile of carbon was placed so that the posts were about 25, 50, and 62.2 mm from the pile. The sparks were made by brushing the hand-held electrode across the posts, beginning with the one farthest from the pile. If no ignition occurred after repeated sparking, the next closest post was used. This was repeated with a fresh 20 ml sample of carbon.

Results:

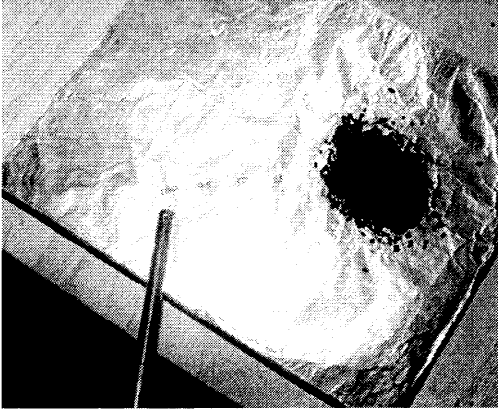
In the first test, ignition occurred at the 50 mm distance. In the second test, ignition occurred at the 25 mm post after about 10 seconds of sparking.

Source No. 4 - Mechanical spark

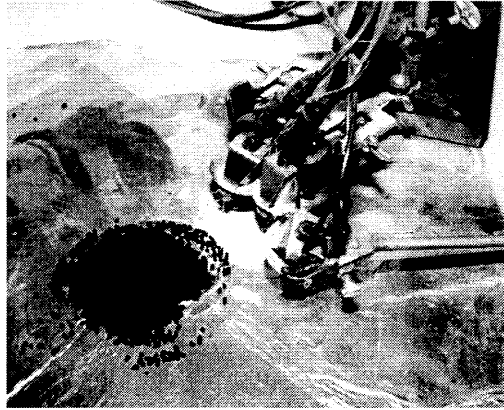
A flint/steel torch lighter (hand squeeze) was used to create the mechanical sparks. A 20 ml sample of carbon was placed on a flat surface in a pile about 8 cm in diameter. Locations for the spark source were marked on the surface at 25, 50, 75 and 100 mm. Sparks were created at the 100 mm location and, if no ignition occurred after 10 seconds, the process was repeated at the next closest location. The sparks traveled a significant distance from the source, and some actually touched the pile of carbon while they were still red hot.

Results:

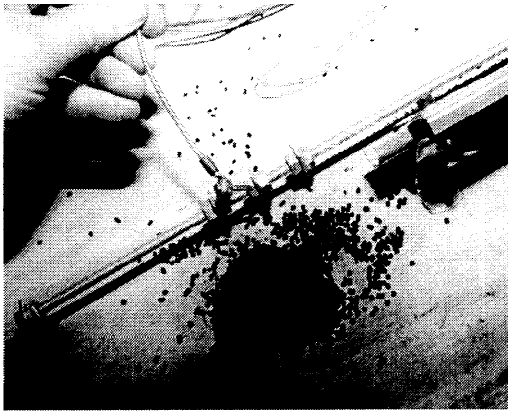
In three successive tests, ignition occurred at 75mm, 50mm and 75mm.



OPEN FLAME



HOT METAL TAILLIGHT FILAMENT



12 VOLT ELECTRICAL SPARK



MECHANICAL SPARK

Figure 5: Testing of Ignition Sources

Table 4 summarizes the results from the ignition source testing.

Table 4: Summary of Ignition Source Testing	
Ignition Source	Results
Open Flame	50 to 100 mm from pile
Hot Filament	25 mm from pile
12 V Electric Sparks	25 to 50 mm from pile
Mechanical Spark	50 to 75 mm from pile

Surrogate Ignition Source Used During Crash Tests

All four ignition sources tested ignited the piles of vapor laden carbon at a distance between 25 to 100 mm, with the open flame having the greatest distance.

For the crash tests it was necessary to have ignition sources mounted on the target vehicle in the vicinity of the canister that would survive the impact from the collision with the moving barrier. The test protocol was to keep the ignition sources active for two minutes after impact. The filaments tested survived for only about six seconds, and using any of the other three ignition sources during the crash tests appeared to be problematic.

As a surrogate to any of the likely ignition sources identified, automotive cigarette lighters were used as ignition sources during the crash tests. The cigarette lighter coils were tested for their ignition producing quality, and they were found to be comparable to the other sources tested, although not quite as likely to cause ignition as the open flame. The coils of the cigarette lighters were energized until red hot for over three minutes, more than enough time to meet the requirements of the test protocol. The lighter coils were removed from the outer jackets of the lighters and they were wired through a switch to a 12 V battery on the crash vehicle. Four of these sources were used for each crash test vehicle. Prior to the start of the crash tests, the lighter coils were energized. The coils had sufficient time to reach their red hot state, presumably near their steady-state temperature.

Section 3: Canister Loading Specifications and Procedures

Canister (Break-In) Preparation

During its use in a vehicle as well as in this test, the activated carbon in a canister will absorb certain heavy hydrocarbon vapors which can not be purged under reasonable purging conditions. This mass of heavy hydrocarbons is sometimes known as the “boot”. When working with laden canisters it is appropriate to first prepare or break-in the canisters by adding a mass of hydrocarbons to represent the “boot”.

General Motors provided the following as Delphi’s standard break-in procedure:

- Load to 2 gram breakthrough at 15 gm/hour of butane (about 6 liters of pure vapor per hour) or gasoline equivalent
- Purge at 23 liters/minute until 300 bed volumes are passed
- Repeat load and purge for a total of six cycles

This break-in procedure is very time consuming. Because the test plan projected loading up to 60 canisters, an alternative, faster, break-in procedure was needed. The following cycle was designed as a fast canister break-in cycle:

- Load to 2 gram breakthrough using air bubbled through gasoline at 2.8 liters/minute
- Purge at 23 liters/minute for 30 minutes (passing slightly more than 300 bed volumes)
- Repeat load and purge cycles until ‘stable’ canister weight gain after purge

A schematic of the hardware used to load the canisters during break-in is shown in Figure 6. Shop air was bubbled through gasoline held at a temperature of about 75-80°F by the water bath. The rate of air/vapor flow through the system was controlled using the rotameter. The gasoline used was first evaporated down to about 80% of its original volume to remove the lighter hydrocarbons in the vapor, which are relatively easily purged from the carbon in the canisters. The canister was weighed prior to break-in. A second canister, not shown in the schematic, was attached to the outlet air from the break-in canister. The 2 g breakthrough was achieved when the weight of the second canister gained 2 g. The actual hardware used consisted of plumbing to break in four canisters at a time. To purge the canisters, shop air was flowed through the canisters at the rates specified in the procedures above.

To compare the two canister break-in procedures, canisters were prepared using each of the two procedures. Figure 7 shows weight gain results from six load-purge cycles using each of the two procedures. These results indicated that the two procedures would result in similar canister weight gain. To further demonstrate that the two break-in procedures were comparable, we individually placed each of the two canisters in a small closed box, opened one side of the

canisters to allow vapors to escape, and measured the vapor concentrations using Figaro Model 822 organic solvent vapor sensors at six locations inside the box. Figure 8 shows a schematic of the sensor positions at the sides of the box. Figure 9 shows that the levels of vapor (%Lower Flammability Limit - %LFL) emanating from the slow and fast loaded canisters to be in the same range, verifying that the two canister break-in procedures were similar.

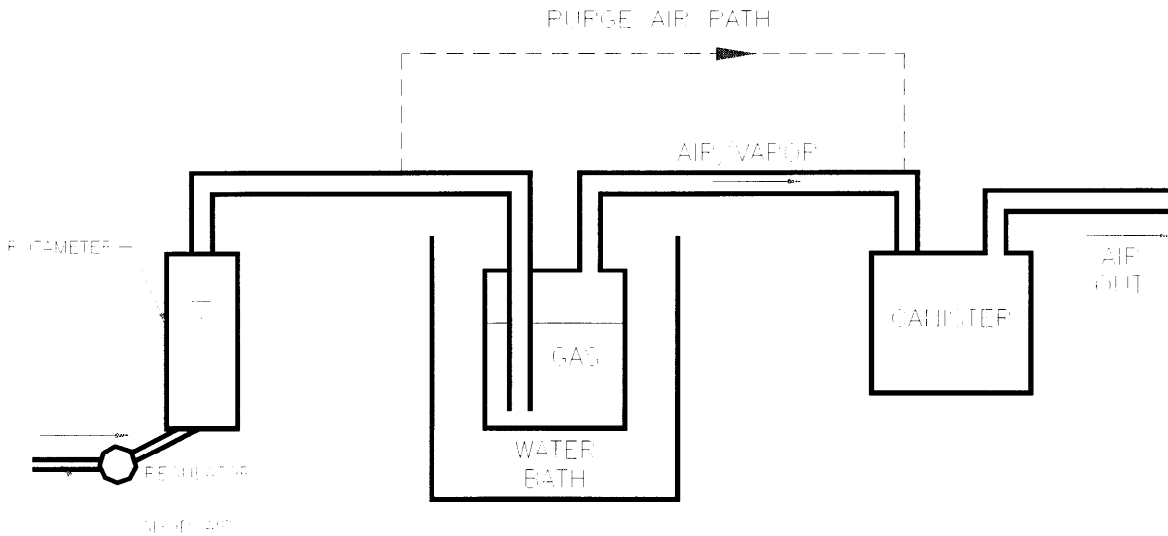


Figure 6: Schematic of Canister Break-In Hardware

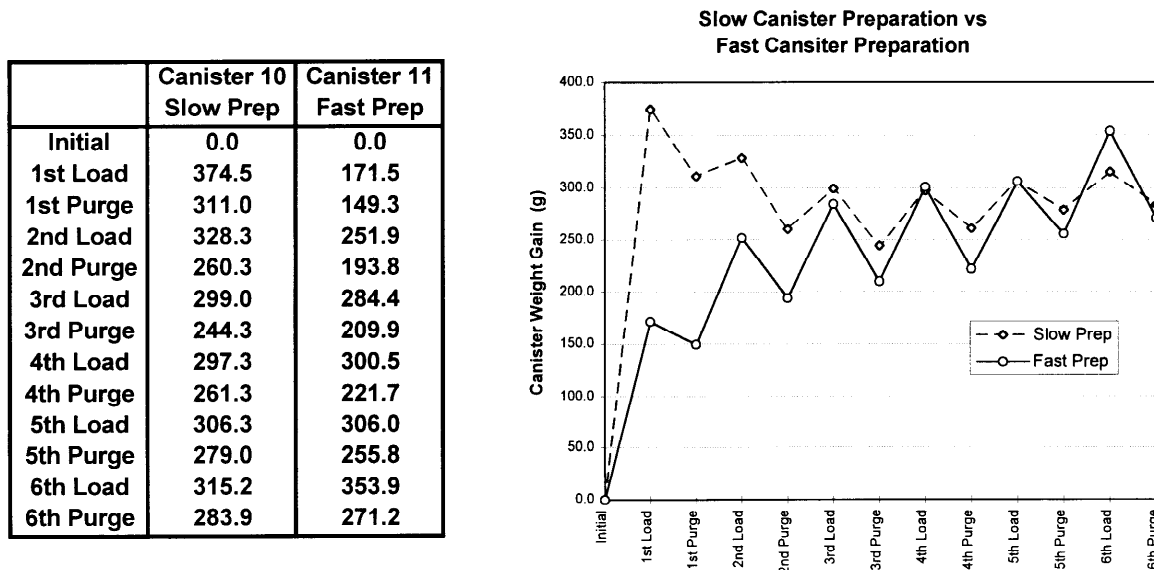


Figure 7: Comparison of Slow and Fast Canister Break-in Procedures: Canister Weight Gains

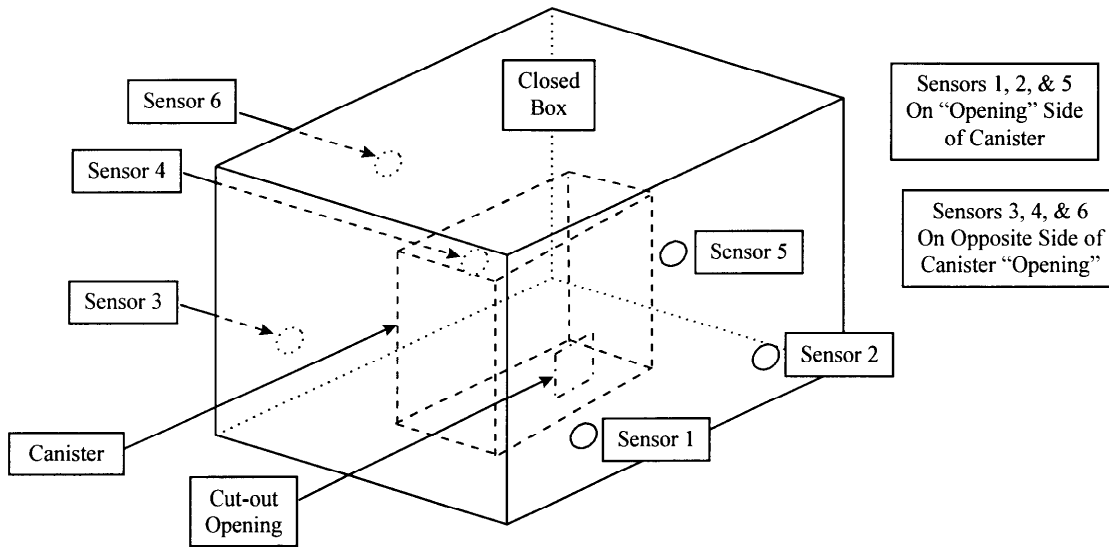


Figure 8: Schematic of Vapor Sensor Positions at Sides of Box

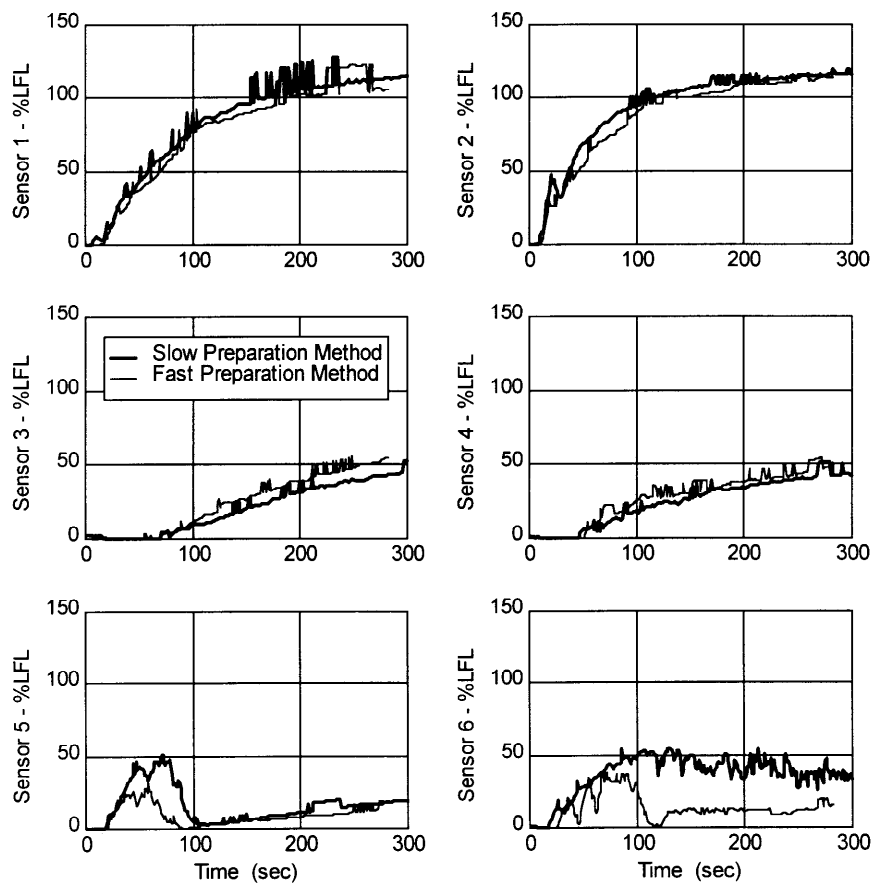


Figure 9: Comparison of Slow and Fast Canister Break-in Procedures: Concentration of Vapors Emanating from Opened Canister

Canister Loading

Two canister loading protocols were used during testing. The protocols are:

Fast Fill - To Simulate Canister Loading During Refueling

- Fill Until 2 gram Breakthrough Level
- 75°F, 9 RVP Gasoline
- 10 gal/minute Pump Rate, Nominal 22 Gallon Fill
- Test Loaded Canister within 0-10 Minutes of Filling
- Canister Warm from Loading

Slow Fill - To Simulate Canister Loading During Extended Periods of Slow Vapor Gain

- So-called '1.5x Enhanced' Fill
- 75°F, 9 RVP Gasoline
- 4 gal/minute Pump Rate, Nominal 22 Gallon Fill
- Soak One Hour
- Repeat Until 175 g Gain
- Soak One Hour
- Test Canister within 4 Hours of Loading
- Canister Nominally at Ambient Temperature

A valve at the exit to the pump was adjusted to deliver the proper flow rate of gasoline into the 32-gallon tank. The canisters, which were prepared using the break-in procedure described earlier, were connected to the system using flexible thin-wall tubes as shown so that the mass could be measured while vapors were being passed to the canister (Figure 10). This method proved very repeatable, and is believed to be accurate to about one gram.

Figure 10 shows a schematic of the canister loading hardware in the slow fill configuration. Prior to loading, the 55-gallon drum of gasoline was heated to 75-80° F and the fuel was pumped back and forth between the 32-gallon tank and the 55-gallon drum to generate a near-equilibrium concentration of vapor in the system. A separate pump and some 3-way valves were used to return the gasoline from the 32-gallon tank to the drum, and these are not shown in Figure 10. A gate valve at the outlet of the pump (also not shown in Figure 10) was adjusted to deliver the proper flow rate of gasoline into the 32-gallon tank, that is, either 10 gpm for fast fill or 4 gpm for slow fill. The canisters, which were prepared using the break-in procedure described earlier, were connected to the system using flexible thin-wall tubes as shown so that the mass could be measured while vapors were being passed to the canister. In the slow fill system the canister to be filled was placed on the balance as shown in Figure 10. In the fast-fill system, the so called breakthrough canister was placed on the balance and this canister absorbed the vapor breaking through the actual canister being filled. When the balance recorded a 2-gram weight gain of the breakthrough canister, the filling was stopped. These methods proved very repeatable, and are believed to be accurate to about one gram.

For the fast fill method, 2 gram breakthrough was typically achieved by pumping 20-25 gallons of gasoline from the drum into the tank. The breakthrough canister was used to measure the breakthrough, as in the technique used during canister preparation. Once breakthrough begins, the 2 gram level is achieved rapidly, usually in a few seconds. It is believed that, even if the mass of the breakthrough canister is not measured with great accuracy, this will have little effect on the mass of vapors remaining in the main canister.

The slow fill method typically required at least three series of pumping from the 55-gallon drum to the 32-gallon tank. The slow fill process takes a minimum of three hours. On some days when the slow fill canisters were being tested, the first one or more fill series would be done the day before the tests. The final fill series were always done on the test days.

The gasoline used was specified as 9 RVP test fuel. The RVP level of the gasoline was monitored periodically, and if the RVP dropped below 8, the entire drum was replaced with fresh 9 RVP fuel. Four drums were used during the project.

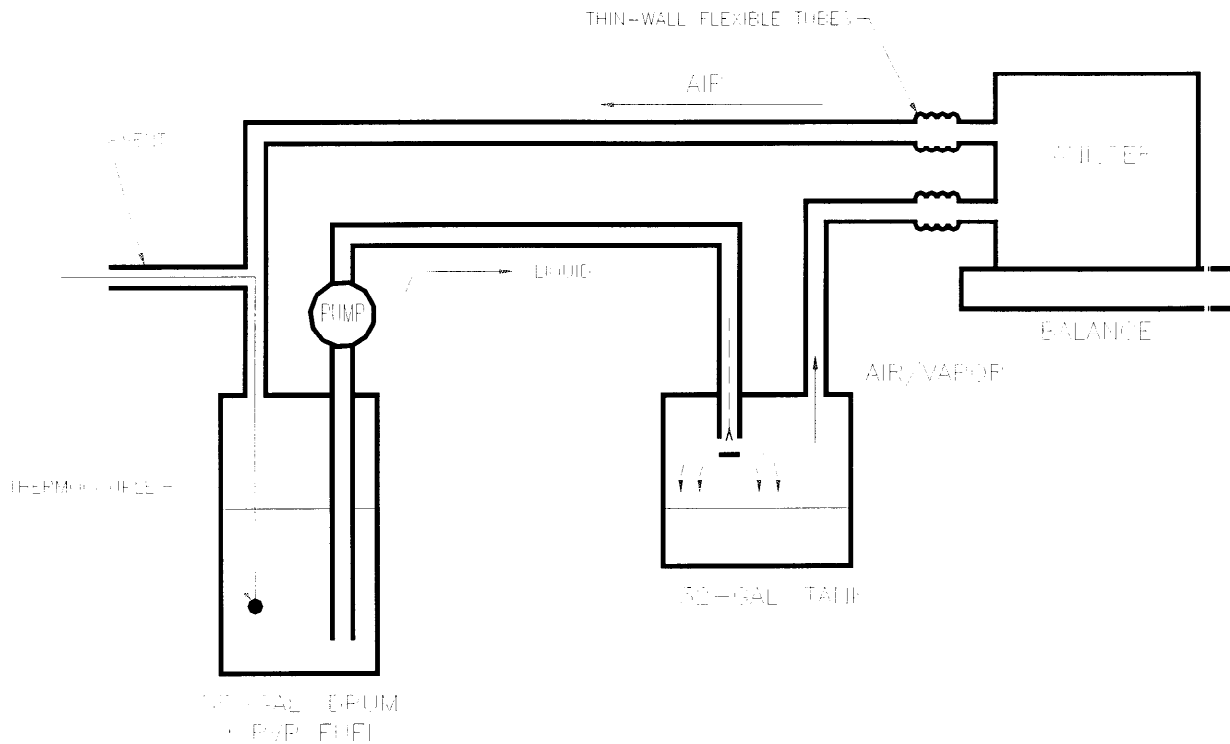


Figure 10: Schematic of Canister Loading Hardware (Slow Load Process Shown - without Breakthrough Canister)

Section 4: Ignition of Unruptured Canisters

A canister was prepared and loaded with vapor and it was placed on its narrow side on the concrete floor of the canister test laboratory. A burning candle was used as the ignition source. The height of the candle was set so that its flame was the height of one of the tubular openings on the canister.

The candle was lit several feet away from the canister and was pushed slowly toward the openings in the canister. When the flame reached a distance of approximately 75 mm (3 inches) from the opening, ignition of gases exiting the canister occurred in the form of a small 20 mm long flame coming from the opening (Figure 11). The flame stayed burning after the candle was removed. This process was repeated for the other two openings with the same result.

During the first several tests the flames were blown out after burning for several seconds. During later testing, the flames were left burning until the canister tube opening began to melt and burn. These tests demonstrated that vapors emanating from laden canisters are flammable and able to burn long enough to cause the canister material to ignite. Under their normal configuration, these canister tube openings are not open to the atmosphere.

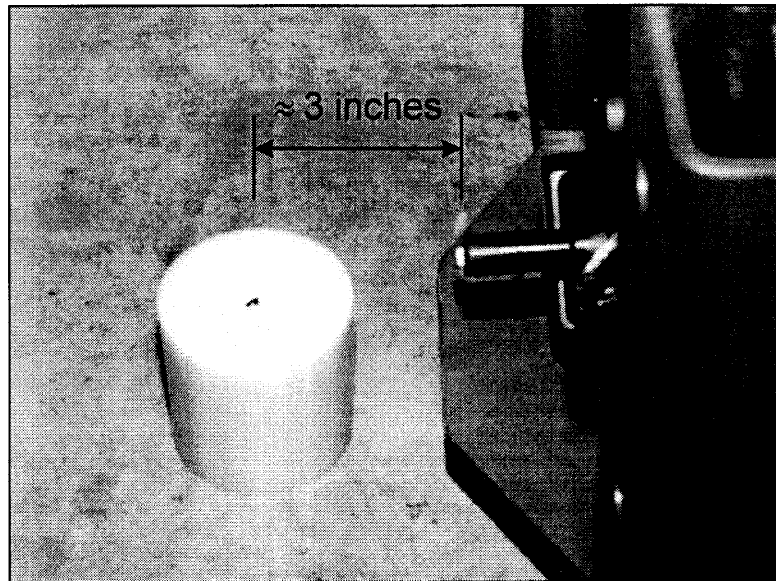


Figure 11: Demonstration of Ignition of Unruptured Vapor-Loaded Canister Showing Flame at the Candle and Tube Opening

Section 5: Measurement of Vapor Concentration after Canister Rupture

The vapor concentration levels in the vicinity of the ruptured canisters were measured using Figaro Model 822 organic solvent vapor sensors. The vapor sensors were supplied with 5 volt inputs, and circuitry was designed and built so the sensors' maximum output voltage would correspond to roughly 120-140% of the lower flammability limit (LFL).

The sensors were calibrated daily against a Bacharach Sentinel 44 LFL meter. To calibrate the sensors, they were placed in a sealed plastic bladder with the LFL meter and increasing amounts of gasoline vapor were injected into the bladder. Figure 12 shows a typical calibration for one of the sensors. Third-order polynomial fits of the measured data were found to represent the sensors' response characteristics well, and they were used in the calibrations. The sensors as configured for this research have low sensitivity below 10% LFL and high sensitivity in the range of 10-120% LFL. Also, as configured, the sensors saturate in the range of 120-140% LFL. Results shown in this section and in Appendix B indicate sensor saturation did occur in some tests.

Seven vapor concentration sensors were used to make measurements during the actual rupture tests. During preliminary testing one of the sensors was placed above the canister 400 mm off the floor, two were placed along side the canister 130 mm off the floor, and the other four were placed at floor level, arranged 60 degrees apart on a semicircle centered at the center of the canister with a radius of 250 mm. Figure 13 shows the preliminary sensor positions and vapor concentration measurement results from a rupture test. As Figure 13 shows, the three elevated sensors measured very little vapor concentration while the four sensors at floor level all saturated at LFL levels above 100% within 20 seconds. Three tests were done using these sensor positions, all with similar results. The vapor emanating from the ruptured canisters is heavier than air, so elevated sensors were not used for any of the final sensor positions.

Figure 14 shows the final sensor positions used for testing. The three previously elevated sensors were moved to ground level positions 500 mm from the canister as shown. During the preliminary tests, the canister rupture would sometimes result in a pile of carbon near the sensor. To prevent the sensors from becoming covered with carbon, the sensors were raised to 20 mm off the floor in their final positions.

Table 5 lists the configurations used for the vapor concentration after rupture measurements tests. The canister numbers used during this series of tests do not correspond to canister/test numbers used during the unladen impact tests. Tests were done using both the slow and fast canister fill methods and using impacts to all three canister impact positions; wide side, narrow side, and bottom. The last two tests were run with doors open at each end of the canister test laboratory to allow a slight breeze to flow across the test area. The wind speeds were measured using an anemometer and they are recorded in Table 5. The results of all of the tests listed in Table 5 are contained in Appendix B. For each test, the sensor measurements are provided as are photographs of the carbon spill from the rupture.

Canisters 20, 21, and 22 were all narrow side impacts using the fast fill method. Ruptures from these three tests resulted in fairly widespread dispersal of carbon in the region of the sensors. Most sensor recordings for all three of these tests indicate LFL levels of over 100%, indicating that the vapor concentration near the floor in the entire region of the sensors was at a combustible level. Some of the sensors did not quite reach 100% LFL, generally in areas where little carbon was spilled. In some instances, for the sensors farthest away from the canisters, the LFL level rise times were delayed relative to the closer sensors. This was judged to be due to a propagating “cloud” of vapor. This too was a function of the amount of carbon in the vicinity of the sensors. The results of these three tests also demonstrate that the process used is reasonably repeatable.

No conclusive differences were noted between the slow and fast fill methods, rather the measured LFL levels are a function of amount of carbon spilled and the distance from the carbon to the sensor.

The tests of canisters 24, 25, and 27, which were all bottom impacts, resulted in minor ruptures with small amounts of spilled carbon. None of the sensors recorded LFL levels above 50% during these tests. In general, the sensors reached their peak LFL levels about 30-60 seconds after the impacts of canisters 24, 25, and 27. This gives an indication of the rate and amount of vapor flow from broken canisters with a small amount of spilled carbon. After 2½-3 minutes the sensor recordings dropped to near zero as the vapors dispersed into the laboratory.

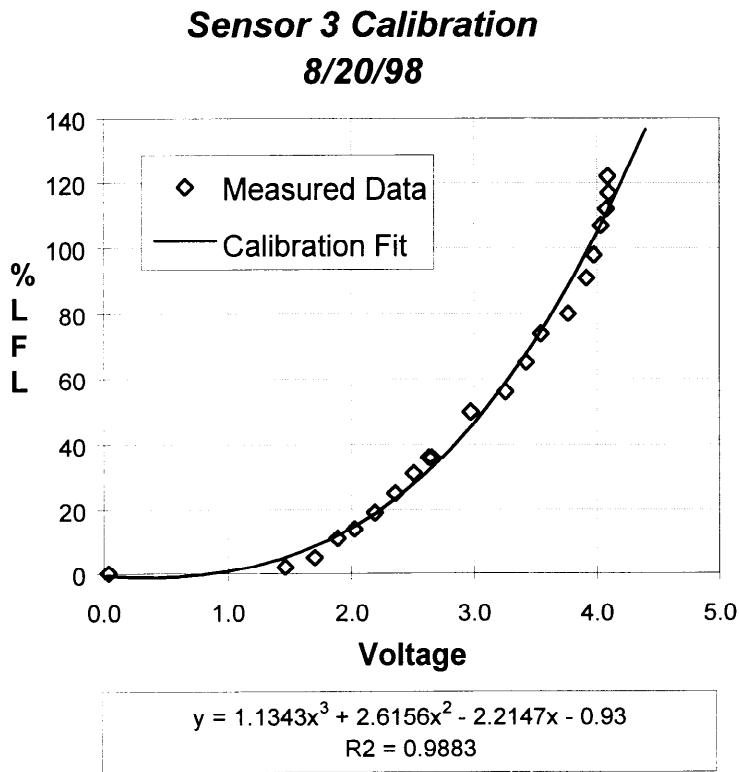


Figure 12: Representative Vapor Concentration Sensor Calibration

Note

- Canister #19
- Impact Date : Aug. 5, 1998
- Loading Method : Fast
- Impact Location : Wide Side

● Sensor Position

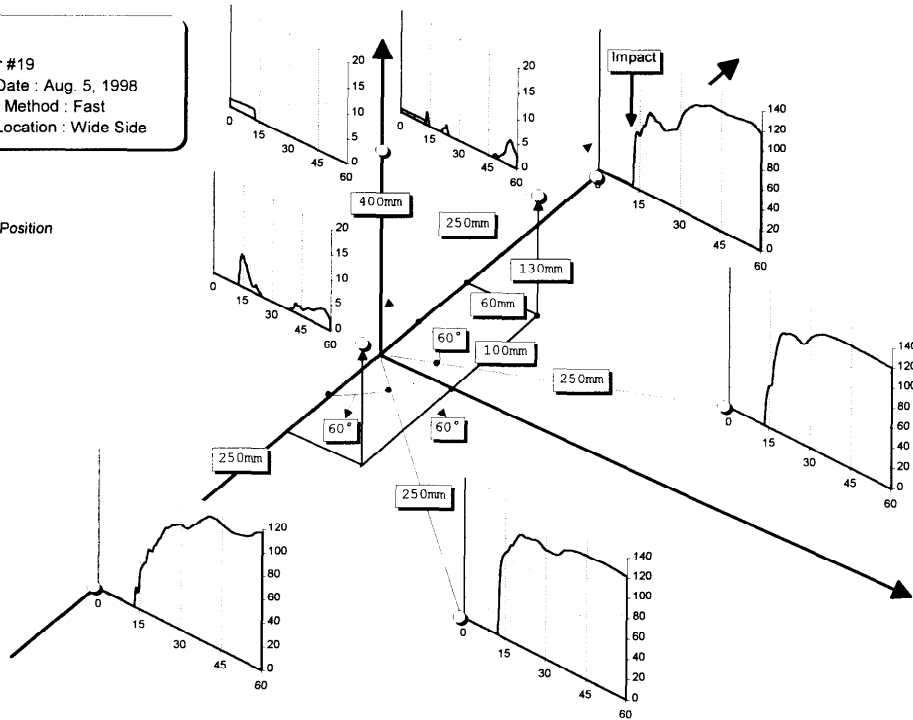


Figure 13: Preliminary Vapor Concentration Sensor Positions

Note

- Canister #31
- Impact Date : Aug. 20, 1998
- Loading Method : Slow
- Impact Location : Narrow Side

● Sensor Position

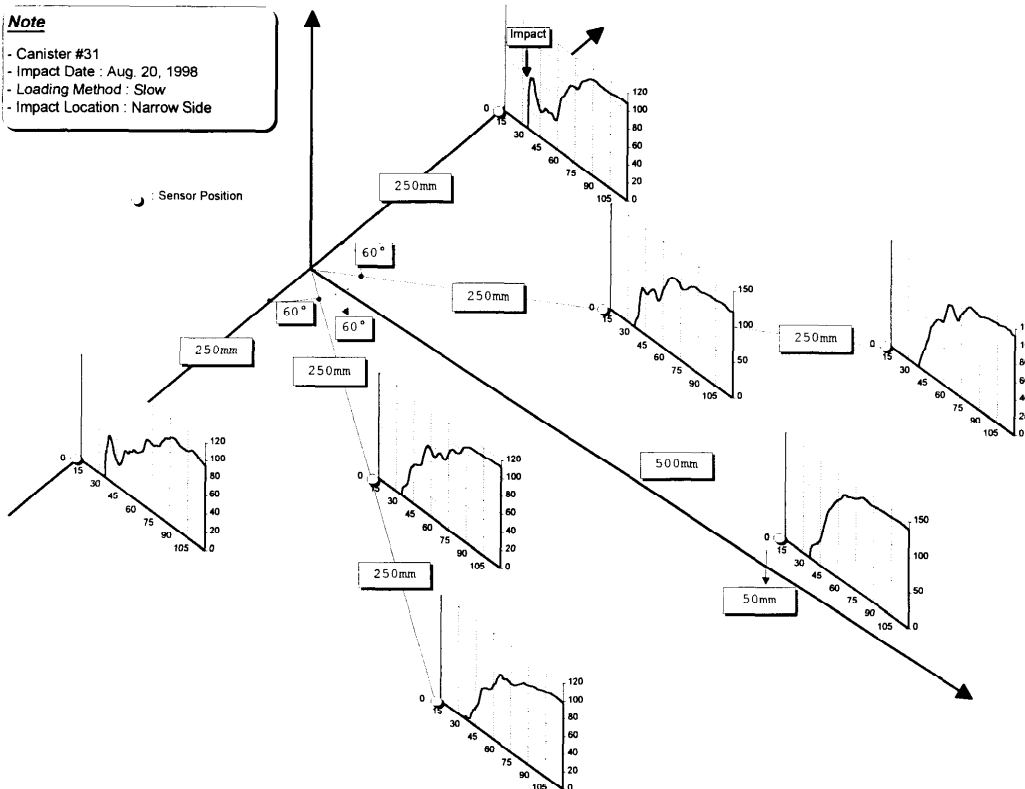


Figure 14: Final Vapor Concentration Sensor Positions

With the exception of canisters 32 and 28, all the vapor concentration measurements after rupture were done in an unventilated room with little air circulation. As mentioned, a door at each end of the room was left open for these two tests to study the effects of air flow on vapor concentrations. The rupture of canister 28 resulted in about 300 grams of spilled carbon. Only one of the sensors reached an LFL level above 100%, and only for a brief period of time. None of the sensors reached 60% after the rupture of canister 32, which spilled a moderate amount of carbon. Based on the amount of carbon spilled, had the doors been closed, LFL levels of over 100% at most sensor positions would be expected in the tests on canisters 32 and 28. This indicates that a breeze could significantly reduce the ground level vapor concentrations in the vicinity of a ruptured canister loaded with fully vapor-laden carbon. Also, the sensors farthest from canisters 32 and 28 had relatively low readings, further indicating that a breeze effectively disperses the vapors. During testing of canisters 32 and 28, the air speed in the area of canisters was measured using a hot-wire anemometer. Air speeds were always below 200 ft/min (2.3 mph) and were usually only a fraction of this.

Table 5: Summary of Vapor Concentration Measurement Test Configurations				
Date	Canister Number	Loading Method	Impact Location	Comments
8/11/98	20	Fast	Narrow Side	
"	21	Fast	Narrow Side	
"	22	Fast	Narrow Side	
8/20/98	23	Slow	Wide Side	
"	30	Slow	Wide Side	
"	31	Slow	Narrow Side	
9/3/98	24	Slow	Bottom	
"	25	Fast	Bottom	
"	27	Fast	Bottom	
9/11/98	32	Fast	Wide Side	Steady Wind 0-50 ft/min Wind Gusts to 200 ft/min
"	28	Fast	Narrow Side	Steady Wind <20 ft/min Wind Gusts 50-100 ft/min

Section 6: Demonstration of Ignition of Ruptured Canister

Two approximately two inch diameter opening flaps were cut into the wide side of a canister. The flaps were closed and taped shut, and the canister was prepared and loaded with vapor. After loading the canister, it was placed on its narrow side on an outdoor concrete slab, in an area with little breeze. Three taillight bulb ignition sources were prepared and positioned near the edge of the carbon pile, about 4-6 inches from the canister. The tape was removed from the flaps and the flaps opened allowing carbon to fall into a pile at the base of the canister. Once the sources were turned on the pile ignited and was left burning with a 2-3 foot high flame for several seconds until it was extinguished with a fire extinguisher. Figure 15 shows the results of igniting and extinguishing the ruptured canister. Much of the carbon scatter was caused by propellant from the fire extinguisher.

After pouring fresh carbon from the canister, the process was repeated using a burner, attached to a fuel supply with a ten foot long hose as the ignition source. This time the canister was left burning longer, about 20-30 seconds, until the plastic canister material caught fire.

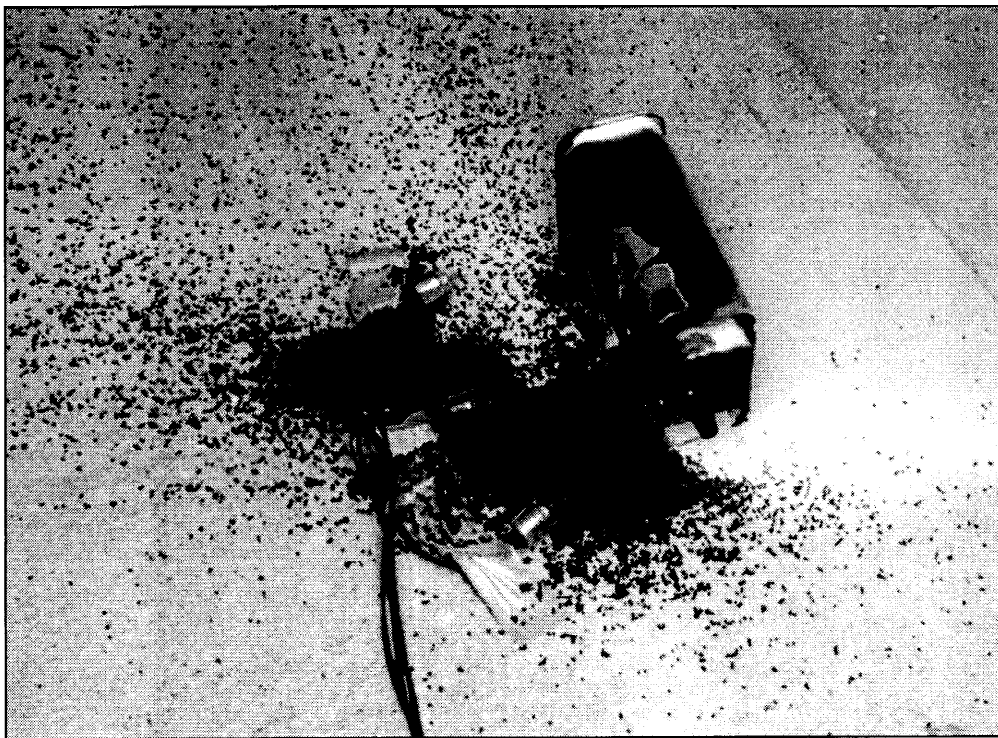


Figure 15: Photo After Demonstration of Igniting and Extinguishing the Ruptured Canister

Section 7: Vehicle Crash Tests

Crash Test Specifications

Two crash tests were run to test the rupture and ignition propensity of vapor loaded rear mounted ORVR canisters. The test conditions were based on the results of the previous canister rupture tests, vapor concentration measurements, and ignition source testing. The tests were designed to represent two plausible real world crash scenarios yet maximize the possibility of ignition.

Both tests used General Motors H-body vehicles (containing an ORVR canister) as the stationary target vehicles and the FMVSS 214 deformable movable barrier as the impacting vehicle. Table 6 provides details on the vehicle and barrier specifications and Figure 16 depicts the conditions for the two tests: the side impact test and the rear impact test. The side impact test vehicle was a 1997 Buick LeSabre and the moving barrier was positioned to strike the vehicle at an angle of 41° with a speed of 70 kph and with initial contact being the foremost corner of the barrier in line with the canister, as shown in Figure 16. The rear impact test used a 1997 Pontiac Bonneville SSE with a moving barrier speed of 85 kph and an impact zone of 50% overlap of the rear of the vehicle, again as shown in Figure 16. The fuel tanks of both vehicles were loaded with 100 lb of sand to emulate a nearly full fuel condition. The canisters used for tests were loaded using the slow fill method. Both crash tests were done on the same day, with the skies cloudy and the temperature between 50°F and 55°F.

The two vehicles used for the crash tests were not equipped with original equipment ORVR canisters. In production, it is expected that ORVR canisters will be placed near the fuel tank. To generically represent this in the crash tests, the canisters were placed near the fuel tanks. For the crash tests, the canisters were placed beside the fuel tank on the passenger's side of the vehicles as shown in Figure 17. To make room for the canisters, the fuel filter and fuel lines were removed from this space. Also, approximately ¼ inch of the edges of the fuel tanks were crimped down to make room for the canisters and to ensure that no sharp edges would be adjacent to the canisters.

For the side impact test, a single steel band was used to secure the canister. Two holes were drilled through the metal panel beneath the rear seat, and the strap was fed through the holes and wrapped around the canister and tightened from above. The steel band broke during the side impact test, so two bands were used during the rear impact test. Manufacturer's data states that the single strand strength of the strap was about 1630 lbs.

Figure 18 indicates the locations of the instrumentation and ignition sources used on the crash test vehicles. Consistent with the set-up used during the laboratory vapor concentration measurements, the vapor concentration sensors were mounted in the range of 13-19 inches (330-482 mm) from the center of the canister. Three sensors were used on each vehicle, and they were mounted as close to the ground as possible yet high enough to prevent them from being damaged during the crash, at a height of three inches. Four ignition sources were used: two in the vicinity of the canister to simulate ignition sources from a side impacting vehicle, one near the catalytic converter of the target vehicle, and one in the taillight region of the target vehicle. As discussed

Table 6: Crash Test Vehicles and Barrier Specifications

**SIDE IMPACT TEST
1997 Buick LeSabre**

VIN: 1G4HP52K7VH403603

Type: 4-Door Sedan

Wheelbase: 110.8 inches

Curb Weight Specification: 3,441 lb

Actual Test Weight: 4,030 lb

Overall Length: 200.8 inches

Overall Width: 74.4 inches

Overall Height: 55.6 inches

Front Track Width: 60.4 inches

Rear Track Width: 60.4 inches

Engine: V-6, 12 Valves, 3.8 Liter

Fuel Tank Capacity: 18.0 U.S. Gallons

Weight of Full Fuel Tank 109.8 lb
(Gasoline 6.1 lb/gal)

Nominal Weight of Sand/Gravel 100 lb

Nominal Volume of Sand/Gravel 1.83 ft³
Density of Sand/Gravel 60 lb/ft³

Canister 36 Used In This Test
Filled Using Slow Fill Method

**REAR IMPACT TEST
1997 Pontiac Bonneville SSE**

VIN: 1G2HZ52K1VH256746

Type: 4-Door Sedan

Wheelbase: 110.8 inches

Curb Weight Specification: 3,587 lb

Actual Test Weight: 4,030 lb

Overall Length: 202.1 inches

Overall Width: 74.5 inches

Overall Height: 55.7 inches

Front Track Width: 60.8 inches

Rear Track Width: 60.6 inches

Engine: V-6, 12 Valves, 3.8 Liter

Fuel Tank Capacity: 18.0 U.S. Gallons

Weight of Full Fuel Tank 109.8 lb
(Gasoline 6.1 lb/gal)

Nominal Weight of Sand/Gravel 100 lb

Nominal Volume of Sand/Gravel 1.83 ft³
Density of Sand/Gravel 60 lb/ft³

Canister 37 Used In This Test
Filled Using Slow Fill Method

Deformable Movable Barrier

FMVSS 214 Sled

Honeycomb Face

Test Weight: 3,015 lb

Side Impact Test

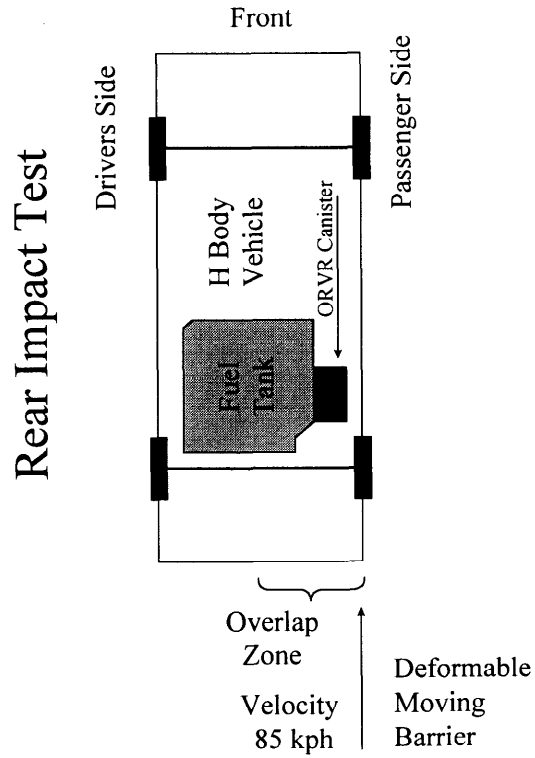
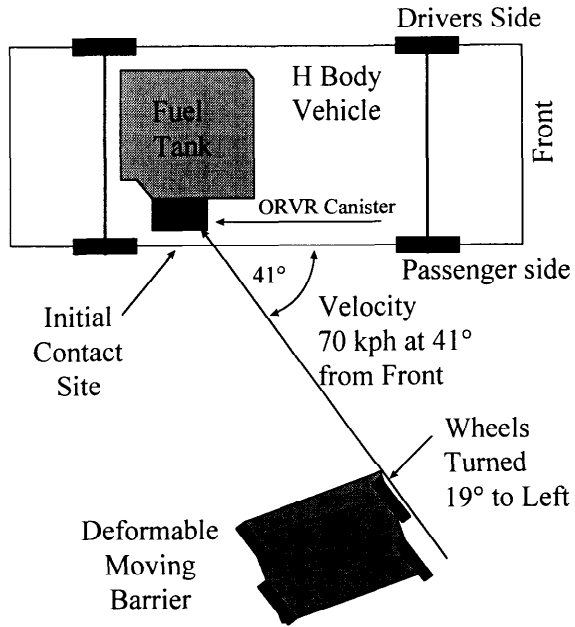


Figure 16: Side Impact and Rear Impact Test Specifications

in Section 2, automobile cigarette lighters were used as ignition sources. With the exception of the one in the taillight region mounted at 12 inches, the ignition sources were mounted four inches above the ground. Thermocouples were placed 6-7 inches off the ground nearby the canisters to detect the temperature rise in the event that ignition occurred. Two of the thermocouples were placed above the ignition sources in front of and behind the canister, and the third was placed directly to the inboard side of the canister.

Side Impact Crash Test Results

A pre-crash photo of the side impact test is shown in Figure 19. The side impact test was executed as planned, with impact occurring at the proper orientation and position at a speed of 69.5 kph. Figures 20 and 21 show the side impact post-crash vehicle and moving deformable barrier, respectively. Figure 22 shows the vehicle longitudinal and lateral accelerations measured during the test.

The metal band holding the canister in place broke during this test, and as a result the canister became detached from the vehicle and came to rest about seven feet from the vehicle. The impact from the barrier caused the metal underbody panel above the canister to buckle downward, presumably placing a large downward force on the canister and band that resulted in the band breaking. The vehicle underbody in the vicinity of where the canister was mounted is shown to be buckled downward in Figure 23. Figure 24 is a photo of the canister used in the side impact test showing abrasions sustained from the test, which were presumably caused by the buckling of the vehicle underbody. The lateral force from the impact resulted in the canister impacting the fuel tank and causing a ½ inch deflection in the fuel tank, as shown in Figure 23. This indicated that the canister experienced some level of direct impact force before it broke away from the vehicle.

Rear Impact Crash Test Results

Figure 25 contains pre-crash photos of the rear impact test. At a distance of about 20 feet from impact the skate connecting the moving barrier to the pull cable failed causing the barrier to prematurely disengage from the pull cable. For safety reasons, the test operator engaged a system stop when the problem occurred, which caused the brakes on the moving barrier to activate. This caused the barrier to pull slightly to the right and reduced the impact speed to approximately 74 kpm. (The barrier deviation to the right resulted in a failure of the hardware used to directly measure impact speed.) The overlap of the barrier with the vehicle was less than planned. About 40-45% of the rear of the vehicle was impacted by the moving barrier. The rear impact post-crash vehicle and moving deformable barrier are shown in Figures 26 and 27, respectively. Figure 28 shows the vehicle longitudinal and lateral accelerations measured during the test.

The canister did not break during the rear impact test. Although the rear of the vehicle was significantly crushed, the crush zone did not extend in front of the rear axle. There was no noticeable damage to the canister or its surrounding area. In spite of the test problems, this crash test represented a fairly severe rear impact and the fact that the canister did not break was not unexpected based on the extent of vehicle damage. Significantly more energy would be required to cause deformation into the canister region.

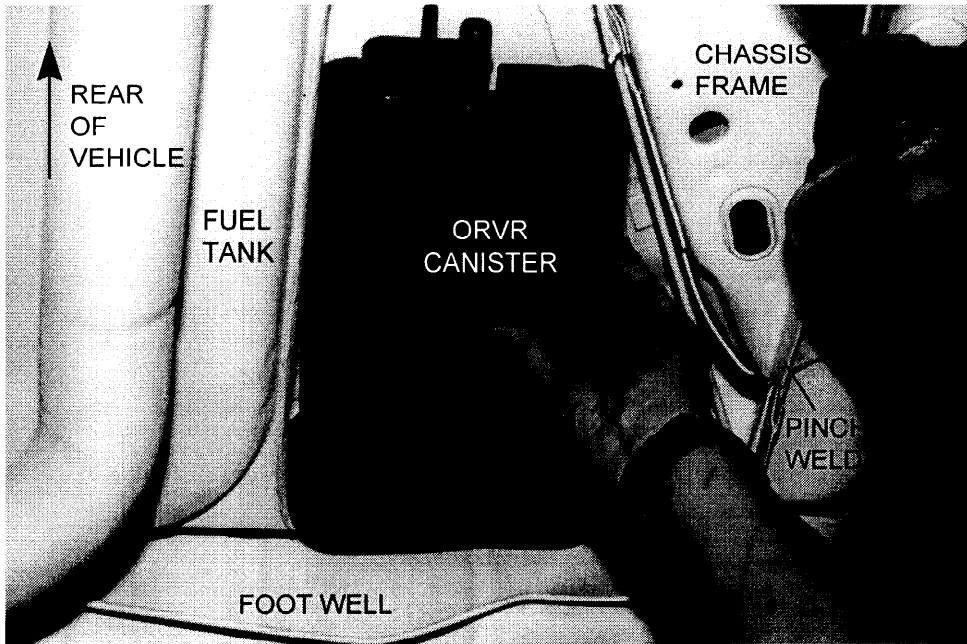


Figure 17: Position of Canisters As Mounted on Crash Test Vehicles



Figure 19: Pre-Crash Photo - Side Impact Test



Figure 20: Vehicle After Side Impact Test



Figure 21: Moving Deformable Barrier After Side Impact Test

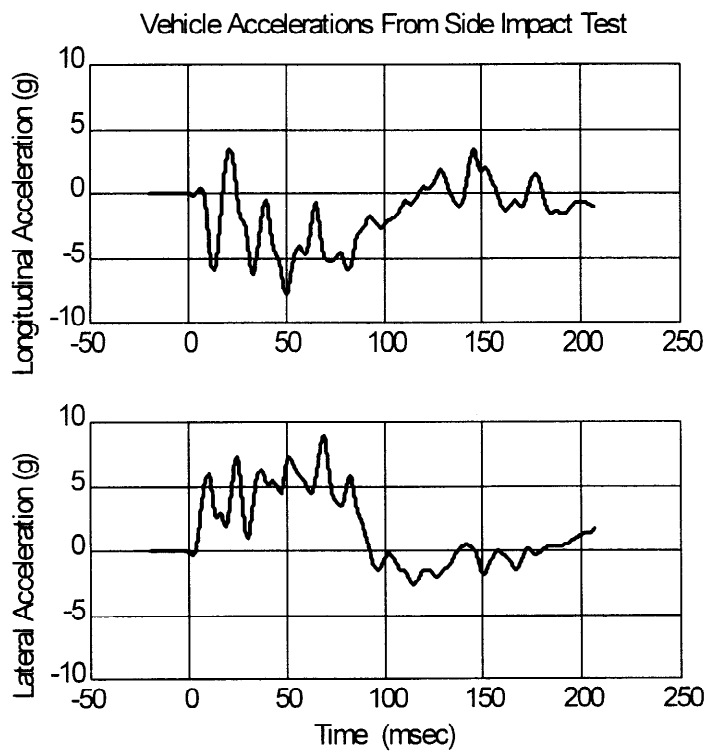


Figure 22: Accelerations from Side Impact Test



Figure 23: Post-Crash Side Impact Vehicle Showing Downward Buckling of Vehicle Underbody in Vicinity of Canister Mounting Location - Black Strap Shown Fuel Tank Edge at Top of Photo - Frame Rail at Bottom of Photo



Figure 24: Post-Crash Side Impact Canister Showing Abrasions Caused by Downward Buckling of Vehicle Underbody

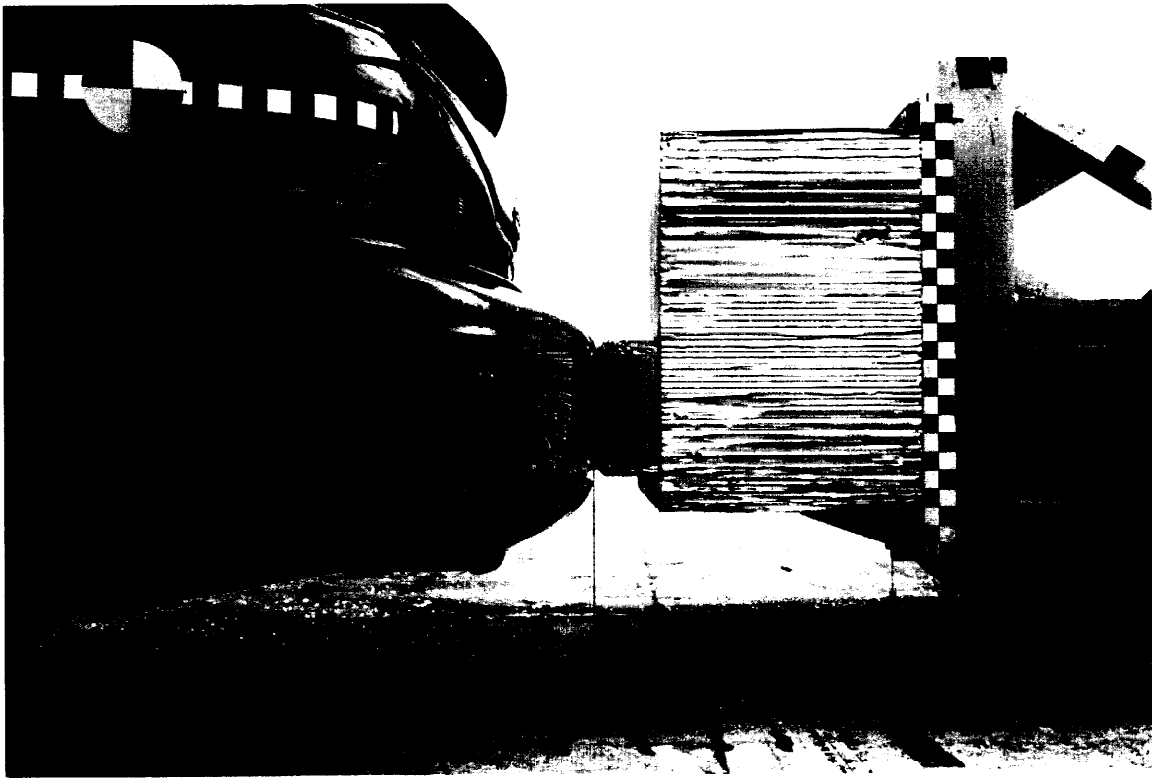
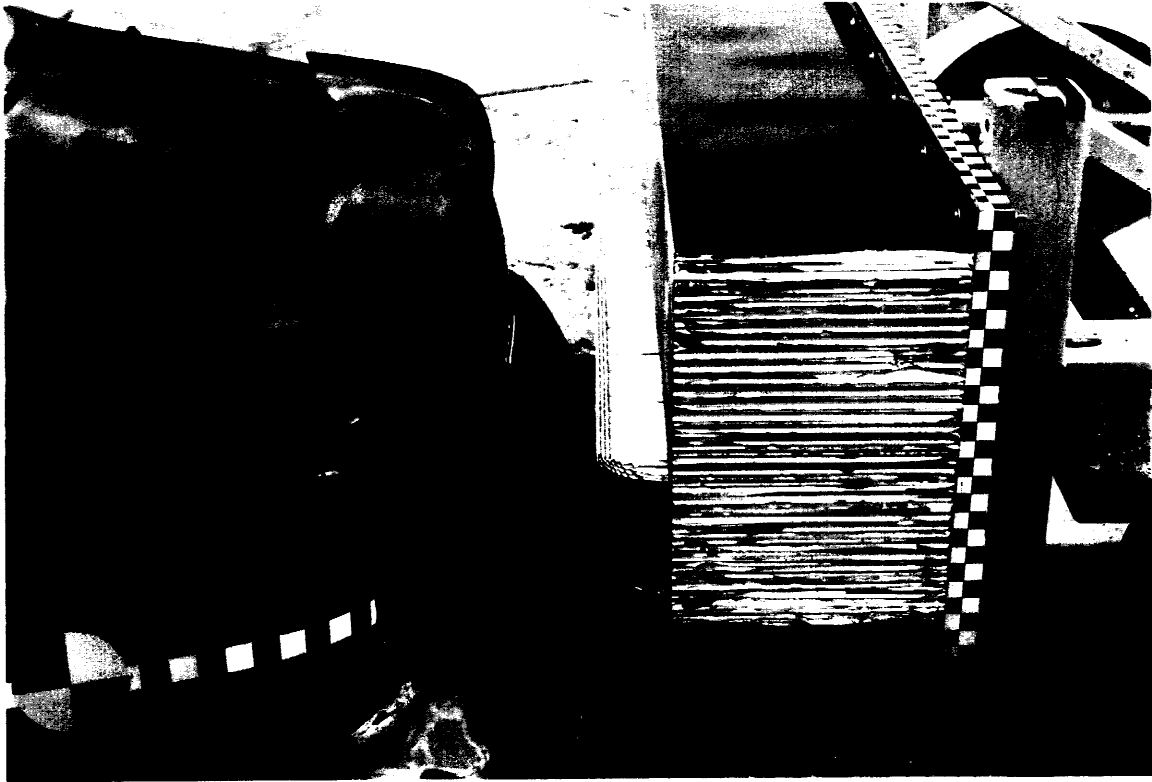


Figure 25: Pre-Crash Photos - Rear Impact Test

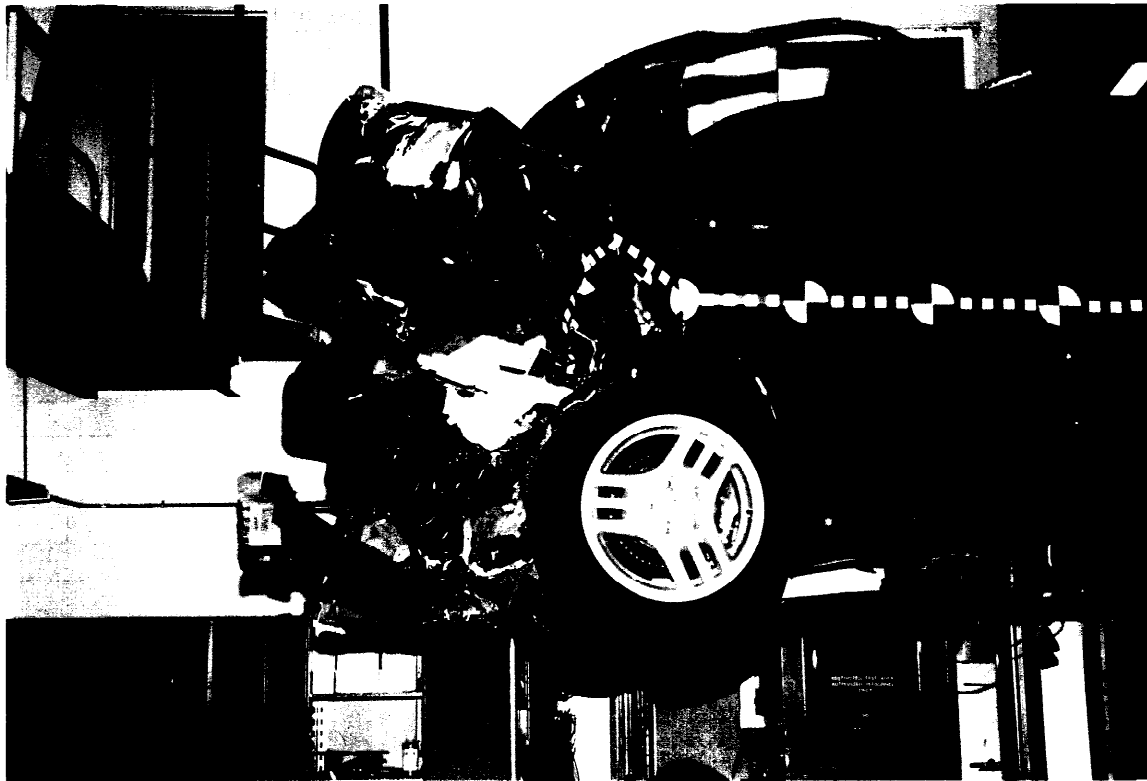


Figure 26: Vehicle After Rear Impact Test

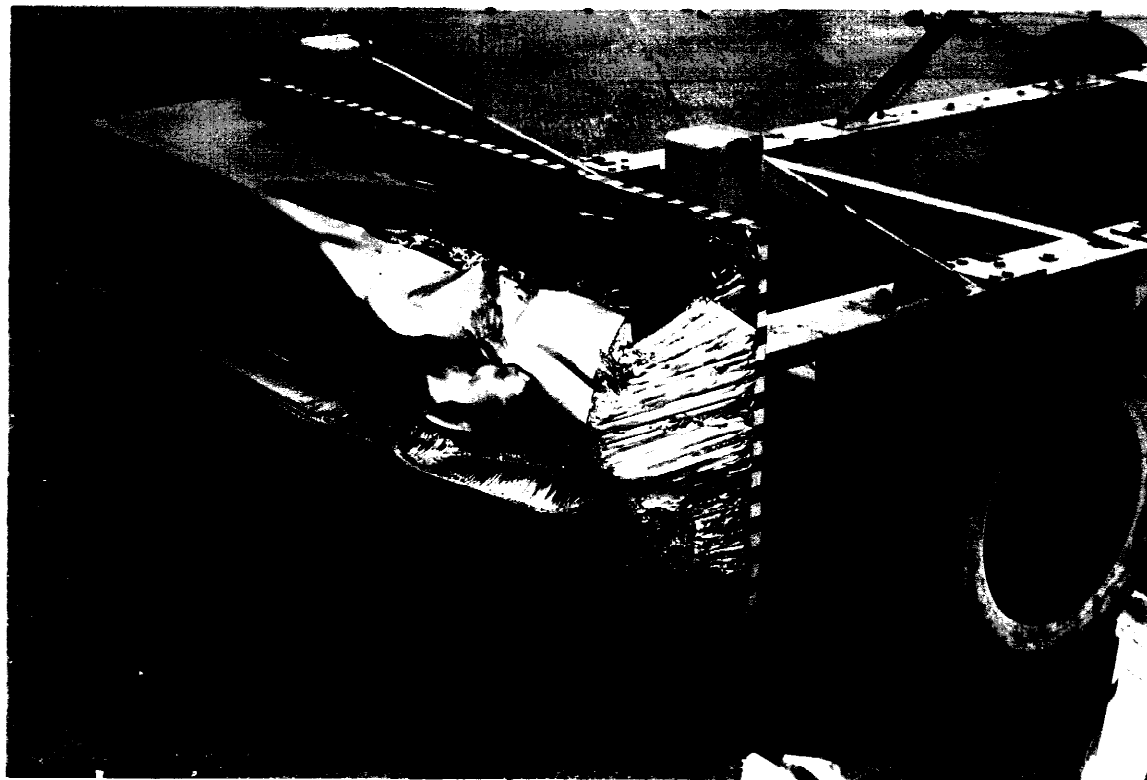


Figure 27: Movable Deformable Barrier After Rear Impact Test

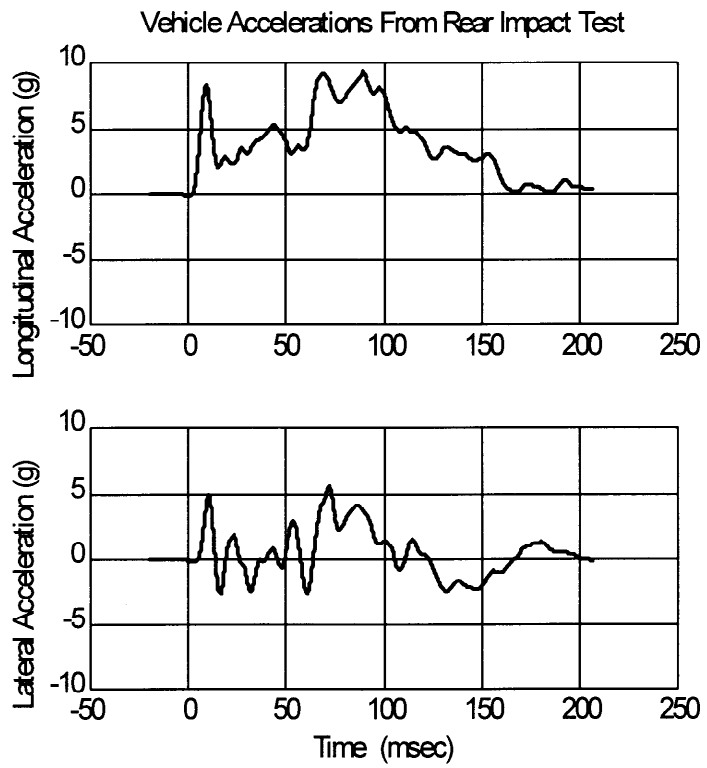


Figure 28: Accelerations from Rear Impact Test

Section 8: Risk Analysis

Introduction

The following risk analysis is intended to be an estimate only. The risk analysis is not exhaustive. Not all sources of ignition were studied thoroughly. This analysis is intended to be an upper bound of the risks associated with carbon canisters. Potential sources of error in the risk analysis are also mentioned.

Analysis

The number of canister-caused fires per year can be evaluated using the following formula:

$$N_{fires} = \sum_i N_i A_i B \quad (1)$$

where:

N_{fires} = number of canister-caused fires per year

N_i = number of collisions per year in one of the Collision Damage Classification (CDC) coded accidents that is in the region of the canister

A_i = probability of this collision causing the canister to break open and spill carbon

B = the probability of ignition if carbon is spilled

Each index “ i ” above refers to a certain Collision Damage Classification (CDC) damage level code. The CDC is a 7-digit (column) combination of letters and numbers and is a way of classifying collision damage based on the area of the vehicle damaged, depth of the damage, and direction of force. The first 2 digits are numbers and give the clock direction from which the force on the vehicle came. The third column is the general area of damage: front, rear, left, right, etc. The fourth column gives a more specific description of the damage area, such as the rear third of the side. Column 5 gives the vertical extent of the damage. Column 6 gives a general description of the damage area in terms of narrow or wide. Column 7 gives an indication of the depth of the residual crush. Columns 3 and 7 together can be used to convert a CDC to an approximate damage depth.

For the rear-mounted ORVR canisters only, collisions to the side of the vehicle and at the rear of the vehicle are considered. Based on both the crash test and the general experience that positions forward of the rear axle seldom incur damage in rear collisions (due to position, materials of construction, and protective design), rear collisions are highly unlikely to damage canisters. Subscript i refers to the damage level, which is the 7th column of the CDC. There are 9 damage levels, thus the above summation will include 9 terms for the ORVR, some of which may be zero.

For the front-mounted evaporative canister, collisions need to be considered from the front and from the side but at the front of the vehicle. Thus, 17 different CDC coded accidents need to be considered. Front-mounted canisters are mounted in the area behind one of the headlights.

The N_i 's in Equation (1), the estimated number of accidents per year with a CDC in one of the categories, were provided on request by the National Highway Traffic Safety Administration. To provide these numbers the National Accident Sampling Survey Collision Damage Survey database was used. This is a database of accidents involving a passenger vehicle that was damaged severely enough to be towed. This database has detailed records for selected sections of the United States, and then the results are extrapolated to cover the entire nation.

Factor A is the likelihood that the canister will break and spill carbon, and will be a number between 0 and 1. For the higher damage levels (larger values of i) A will be larger. It was assumed that for damage level 1, A was zero. It was also assumed that A could be no larger than 0.95 to reflect that even in the most severe accident there is a chance the canister will not rupture, if for no other reason than the canister could be broken loose and thrown clear of the accident.

Factor A was estimated by first producing a probability of rupture curve as a function of impactor energy, as shown in Figure 29. This data came from 45 impactor tests where either the wide or narrow sides of the canister were struck. Canister rupture will obviously be more likely at the higher energy levels, but there is considerable scatter in the data. In order to make the probability of rupture curve an increasing function of energy, the 2 ruptures and 15 non-ruptures below 500 ft-lb were lumped together in a single category. For energies below 500 ft-lb, the probability of rupture used is thus 2/17 (11.8%).

The scatter in the data is believed to come from two main sources. There seems to be some variation in the canisters themselves, and the strength of the canisters seems to be a strong function of temperature. Test temperatures were not recorded, but the tests done in warmer conditions seemed to provide more strength in the canisters. This is consistent with the fact that most plastics are more ductile at higher temperatures, allowing the carbon to absorb more energy before the plastic fractured.

As stated earlier, it was assumed that the probability of rupture was zero for damage level one. Mathematically, this means that $A_1 = 0$ for both front and rear canisters. We think that very minor collisions have a negligible chance of rupturing the canister. Collisions with a level 1 damage classification result in approximately 6 inches of crush, and this damage is unlikely to reach to the canister.

Energy (ft-lb)	Rupture	No Rupture
0-100	1	0
100-200	1	1
200-300	0	4
300-400	0	8
400-500	0	2
500-600	1	2
600-700	4	4
700-800	12	2
800-900	0	0
900-1000	3	0

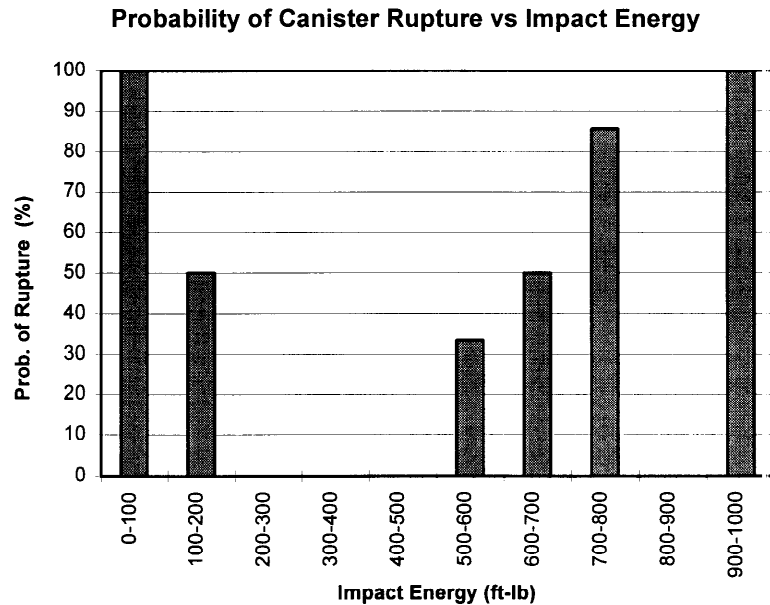


**Figure 29: Probability of Canister Rupture
Based on 45 Wide Side and Narrow Side Impacts**

The amount of energy in a collision per unit volume in the crush zone can also be estimated from the damage level in the CDC. It was assumed that the amount of energy absorbed by the canister was equal to the amount of energy per unit volume absorbed by the crush zone, provided the damage level was above 1. Thus, for a given damage level, one can calculate the energy per unit volume of the crush zone, and relate this to a probability of canister rupture. This will depend to a large extent on what is around the canister. If the canister is attached rigidly to the vehicle structure, it will tend to absorb more energy than if the canister is loosely mounted or is mounted on a flimsy structure that allows it to be pushed out of the way. Also, the presence of any sharp corners was not accounted for, and any sharp corners could significantly increase the chance of rupturing or cutting into the canisters.

The total energy E (in in-lbs) absorbed in a collision can be estimated from (Reference: Barrier Equivalent Velocity, Delta V and CRASH3 Stiffness in Automobile Collisions, by Philip V. Hight, D. Bruce Lent-Koop, and Robert A. Hight, SAE paper 850437, 1985):

$$E = L \left(\frac{K_A}{2} (C + C) + \frac{K_B}{6} (3C^2) + \frac{K_A^2}{2K_B} \right) \quad (2)$$

where:

C is the average damage depth in inches

L is the length of the damage zone in inches

K_A and K_B are the stiffness parameters, which will vary from vehicle to vehicle, and be different for the front and sides of the vehicle.

The general form of Equation (2) which appears in the reference is an integral of crush depth C , over crush length L , weighted by stiffness parameters K_A and K_B . Equation (2) is valid where the crush depth is constant across length L .

K_A and K_B values are available for the front, rear, and sides of vehicles, and for a number of vehicle sizes. (Reference: EDCRASH User's Manual p. 125, Table 4). Average values of K_A and K_B for the front and side were used. For the frontal impacts, frontal values of K_A and K_B were used, and they were:

$$K_A = 349 \text{ in-lb/in}^2$$

$$K_B = 54.0 \text{ in-lb/in}^3$$

For the impacts to the side of the front, frontal values were again used, since the side values typically are for the door area, and vehicles are much stiffer at the front end. For the impacts to the rear side (rear-mounted canister) side values of K_A and K_B were used. These were:

$$K_A = 142 \text{ in-lb/in}^2$$

$$K_B = 51.6 \text{ in-lb/in}^3$$

The average crush depth, C , can be assumed to be about 0.75 of the maximum value, which can then be related to the damage level from the CDC. The assumed maximum crush depths for each damage depth (front and side) are summarized in Table 7.

Crush Depth Code	Maximum Side Crush (in)	Maximum Front Crush (in)
1	6.2	12.0
2	12.0	23.5
3	18.6	39.0
4	26.0	50.0
5	32.0	62.0
6	39.2	81.0
7	45.4	93.0
8	51.6	105
9	65.0	>105

The volume of the crush zone will be approximately LCh , where h is the height of the front structure of the striking vehicle. An approximate value of h is 22 inches, estimated by surveying vehicles in a nearby parking lot. In calculating the crush energy per unit volume of the crush zone, L drops out of the equation, and the formula for crush energy per unit volume (in in-lb/in³) is:

$$E / vol = \frac{K_A}{h} + \frac{3K_B C_{max}}{8h} + \frac{2K_A^2}{3K_B h} \frac{1}{C_{max}} \quad (3)$$

The energy per unit volume typically increases at higher crush levels, except at very low levels where the third term in the above equation dominates. For each damage level from the CDC code a C_{max} is calculated, a crush energy per unit volume is calculated from Equation (3), and a probability of rupture, A_i , is estimated from Figure 29.

For the front-mounted canisters, the same probability of rupture was assumed when related to absorbed energy per unit volume of the vehicle. This implicitly assumes that the volume of the front-mounted canister is the same as the ORVR canister.

Factor B is the probability of ignition once carbon is spilled. B is assumed to vary with the amount of vapor in the canister, thus B will vary with the season, with the drive time since the last fill up, and with the drive time since the last diurnal cycle which will put vapor into the carbon. The collision frequency should be nearly independent of these factors, and an average value of B can be used that takes into account the average amount of vapor in the carbon. The value of B used for all canisters, both front-mounted evaporation canisters and rear-mounted ORVR canisters, was 0.00024.

Factor B was calculated from the following methodology. Data was provided to S.E.A. regarding the typical loading of vapor in the canister as a function of time in winter, spring, and summer driving cycles, assuming typical seasonal temperatures and a typical driving and tank filling patterns. It was assumed that when the amount of vapor in the canister was zero or below, the chance for ignition was zero. This was consistent with our bench tests using lightly loaded carbon, where ignition was possible but only when the ignition source was directly on the pile of carbon. (Note that zero vapor in the carbon actually refers to the condition where the "boot" of the gasoline vapors, the heavy vapors that have strong tendency to stay absorbed in the carbon are present. A negative vapor loading condition means that a portion of the boot has evaporated.) It was then assumed that the chance of ignition was proportional to the volume of the ignitable vapor cloud, and that the size of the ignitable vapor cloud was proportional to the amount of vapor in the carbon, once the carbon was spilled.

The mathematical formula for B for a given season of the year is:

$$B = \frac{1}{T} \int_0^T \frac{m}{170} \frac{V_{ig,170}}{V_{source}} dt \quad (4)$$

where:

m = the mass of vapor in the canister (in addition to the boot) grams

$V_{ig,170}$ = the volume of the ignitable cloud when there are 170 grams of vapor in the canister

V_{source} = volume of a vehicle where ignition sources are assumed to be present

T = drive time between refueling cycles

A number of canisters were broken that were filled with approximately 170 grams of vapor in addition to the boot, and when these canisters were broken the vapor concentration in the area was recorded. The vapor, being heavier than air, was found to form a low-lying cloud along the floor, with little vapor more than about 50 mm above the floor. Ignitable vapor concentrations were found to exist within about 0.5 meters of the broken canister, and to a first approximation this was independent of the amount of carbon spilled, assuming the amount of carbon was reasonably large. The ignitable cloud is thus a thin disk, whose volume was:

$$V_{ig,170} = \pi(0.5^2)(0.05) \quad (5)$$

or 0.0393 m^3 .

It was assumed that in any collision there would be one ignition source within the vehicle, and that this source would be within the body of the vehicle, that is, not in the tires and not in the roof or roof pillars. (Some of these assumptions will be discussed later.) Using 1999 data for vehicles, this volume, V_{source} in Equation (4), was found to be about 5.05 m^3 . Thus, the ratio of $V_{ig,170}$ to V_{source} if the canister is loaded with 170 g of vapor and there a reasonably large amount spilled is $0.0393/5.05 = 0.0078$.

The integration in Equation (4) can be performed, yielding a value of B for each of the 3 seasons examined. They are 0.000275 for the winter season, 0.000219 for the summer season, and 0.000234 for the spring season, which was assumed to be the same as the fall. Averaging these together gives the average for B as 0.00024. Note that this analysis says that ignition is more likely in the colder seasons than in the warmer seasons. The amount of vapor going into the carbon, both from diurnal cycles and from refueling, is greater in the warmer seasons, however in the cooler seasons the purging process occurs more slowly, leading to a higher average vapor concentration in the carbon.

A number of assumptions limit the risk analysis. The most important of these is that wind effects were largely ignored. S.E.A. did a limited number of vapor concentration tests with a light wind blowing through the impact region, and even winds on the order of 200 ft/min (2.3 mph) brought the vapor concentration levels down below the lower flammability limit. Thus, it is expected that the probability of ignition, B , calculated above is significantly higher than would be seen in the

real world. This wind factor should effect both front and rear-mounted canisters equally, so any comparison between the two mounting locations are still appropriate.

Another factor is that the vapor cloud will typically be very close to the ground, while the ignition sources will be higher. This is especially true for the ORVR canister where the canister itself is likely to be close to the ground. Again, this will tend to make the value of B calculated above higher than it should be, especially for the ORVR canisters.

It was assumed that a single ignition source was present in all crashed vehicles, and that the chance of this source being close to the carbon was equal in all cases. In reality, the rear-mounted canisters are much less likely than the front-mounted to be close to an ignition source. There are a number of reasons for this. Our vapor concentration studies showed that it takes some seconds for the vapors to build up to the combustible limit, even close to the ground. Thus, carbon and vapors which come out in the second or so between impact and final rest usually will not ignite, and only carbon that spills and vapors that evolve at final rest will be concentrated enough to be combustible. In most rear or rear side impacts that are severe enough to break the canister, the impacting vehicles will usually separate by a considerable distance. Thus, only ignition sources at the rear of the vehicle with the canister will have any chance of igniting the vapor. Since there are relatively few ignition sources in this location (mainly just the taillights) ignition seems unlikely. During most daytime driving, some of these ignition sources will not be present at all, partly because the bulb filaments will be cold and partly because any wires that might cause short circuiting and/or sparking will not be energized.

Data on the likelihood of an ignition source being present is limited. The literature shows that an ignition source is likely in the front end of the vehicle (with electrical system damage reported in 8 of the 12 staged collisions analyzed) (Reference: An Assessment of Automotive Fuel System Fire Hazards, DOT Report HS 800 624, December 1971). Very few accidents result in fire (about 1%). Clearly, few accidents result in the correct combination of spilled fuel and ignitable vapors, but it is unclear whether the relative rarity of fires indicates a lack of fuel or a lack of ignition sources.

There are many more ignition sources at the front of the vehicle. One of these is the headlight, which will reportedly be just in front of the canister. Also, in a high percentage of frontal accidents the vehicles remain in contact, thus further increasing the likelihood of an ignition source being present for a front-mounted canister. Thus, this analysis probably significantly underpredicts the ratio of front-mounted canister ignitions to rear-mounted canister ignitions.

The chance of fire from the rear-mounted canister is overestimated in this analysis by the fact that a considerable number of the accidents which are severe enough to rupture the rear-mounted canister will also rupture the fuel tank, leading to a far greater cloud of vapor. The chance of fire from a front-mounted canister is also overestimated in this analysis. A smaller number of frontal accidents which lead to rupture of a front-mounted canister will also cause fuel tank ruptures or underhood fires from ruptures of the fuel lines around the engine.

Temperature effects were not taken into account. Presumably, during the warmer months the canister will be warmer and when its contents are spilled they will be warmer and evolve vapors

more quickly. All of our concentration tests were done in the summer, and so should represent a near-worst case, however we do not know if cold weather conditions are significantly different. To be complete, one should consider both the temperature of the contents of the canister and the temperature of the surface on which the contents fall.

Temperature effects on the strength of the canisters were not taken into account. It was noted, and has been mentioned several times in this report, that colder canisters seemed to break more easily than warmer canisters, however we do not know how far down in temperature this trend would continue.

Finally, the period of time immediately after refueling while the canister is hot has not been considered fully. The amount of vapor in the canister has been considered as part of the data provided by GM, but the effects of temperature have not been considered. On the one hand, the canister will be hot and any spilled contents will tend to evolve vapor quickly, but on the other hand, we believe that hot canisters may be nearly unbreakable. Since this period of time corresponds to perhaps only 1-2% of all driving, the effect of this simplification should be negligible.

The results of the risk analysis are provided in Tables 8 and 9 for the rear-mounted and front-mounted canisters, respectively. The tables reflect the fact that front-mounted canisters are vulnerable to impacts from both the front and side, while the rear-mounted canisters are vulnerable only from the side.

Table 8: Risk Analysis Results Rear-Mounted Canister				
Damage Level (<i>i</i>)	Accidents per Year in US (<i>N_i</i>)	Probability of Rupture (<i>A_i</i>)	Probability of Ignition (<i>B</i>)	Number of Fires per Year in US (<i>N_{fires}</i>)
2	12736	0.118	0.00024	0.359
3	8639	0.118	0.00024	0.243
4	614	0.19	0.00024	0.028
5	66	0.32	0.00024	0.005
6	11	0.71	0.00024	0.002
7	8	0.87	0.00024	0.002
8	104	0.95	0.00024	0.024
9	169	0.95	0.00024	0.039
			Total	0.702

Table 9: Risk Analysis Results Front-Mounted Canisters				
Frontal Impacts				
Damage Level (<i>i</i>)	Accidents per Year in US (<i>N_i</i>)	Probability of Rupture (<i>A_i</i>)	Probability of Ignition (<i>B</i>)	Number of Fires per Year in US (<i>N_{fires}</i>)
2	171403	0.63	0.00024	25.7
3	43469	0.95	0.00024	9.91
4	8021	0.95	0.00024	1.83
5	3609	0.95	0.00024	0.823
6	3424	0.95	0.00024	0.781
7	1903	0.95	0.00024	0.433
8	1828	0.95	0.00024	0.416
9	2036	0.95	0.00024	0.464
Side Impacts				
Damage Level (<i>i</i>)	Accidents per Year in US (<i>N_i</i>)	Probability of Rupture (<i>A_i</i>)	Probability of Ignition (<i>B</i>)	Number of Fires per Year in US (<i>N_{fires}</i>)
2	31858	0.33	0.00024	2.52
3	26596	0.50	0.00024	3.19
4	3572	0.70	0.00024	0.600
5	866	0.88	0.00024	0.182
6	29	0.95	0.00024	0.007
7	29	0.95	0.00024	0.007
8	35	0.95	0.00024	0.008
9	41	0.95	0.00024	0.009
			Total	46.9

To get the accidents per year column above, the total number of accidents for both left and right sides of the vehicle was taken and divided by two.

For a given damage level, the number of fires per year (Column 5 in Tables 8 and 9) is the product of the number of accidents per year (Column 2) times the probability of rupture (Column 3) times the probability of ignition (Column 4). The totals listed in Tables 8 and 9 represent the estimated total number of canister-caused fires per year in the United States for rear-mounted and front-mounted canisters, respectively.

Conclusions

If rear-mounted ORVR canisters are used it is predicted that these canisters will lead to less than 1 fire per year in the United States. If front-mounted canisters are used and the canisters are placed just behind the headlight, it is predicted that approximately 47 fires per year in the United States will result.

The relative risk analysis performed and the results obtained are intended to be estimates only. Selected risks were evaluated, but not all sources of ignition were studied thoroughly. The analysis done was intended to provide an upper bound of the risks associated with carbon canisters.

Appendix A

Results from Canister Rupture Tests which Resulted in Spilled Carbon

Canister/Test Number	Side Tested	V (mph)	E (ft-lbs.)	E/E _{min}	Break	Carbon Scatter
5/d	Wide	31.1	693	5.37	Yes	Yes
7/c	Narrow	30.3	638	4.06	Yes	Yes
8/c	Narrow	29.9	623	3.96	Yes	Yes
11/c	Wide	30.7	537	4.16	Yes	Yes
13	Bottom	30.3	160	2.03	Yes	Yes
14	Bottom	30.3	160	2.03	Yes	Slight
15	Bottom	29.9	156	1.98	Yes	Yes
16	Bottom	30.3	323	4.09	Yes	Yes
17	Bottom	30.7	332	4.20	Yes	Yes
18	Bottom	30.3	323	4.09	Yes	Yes
19	Wide	30.3	788	6.11	Yes	Yes
20	Wide	30.3	788	6.11	Yes	Yes
21	Wide	30.3	788	6.11	Yes	Yes
22	Narrow	30.7	985	6.26	Yes	Yes
23	Narrow	30.7	985	6.26	Yes	Yes
24	Narrow	30.3	958	6.10	Yes	Yes

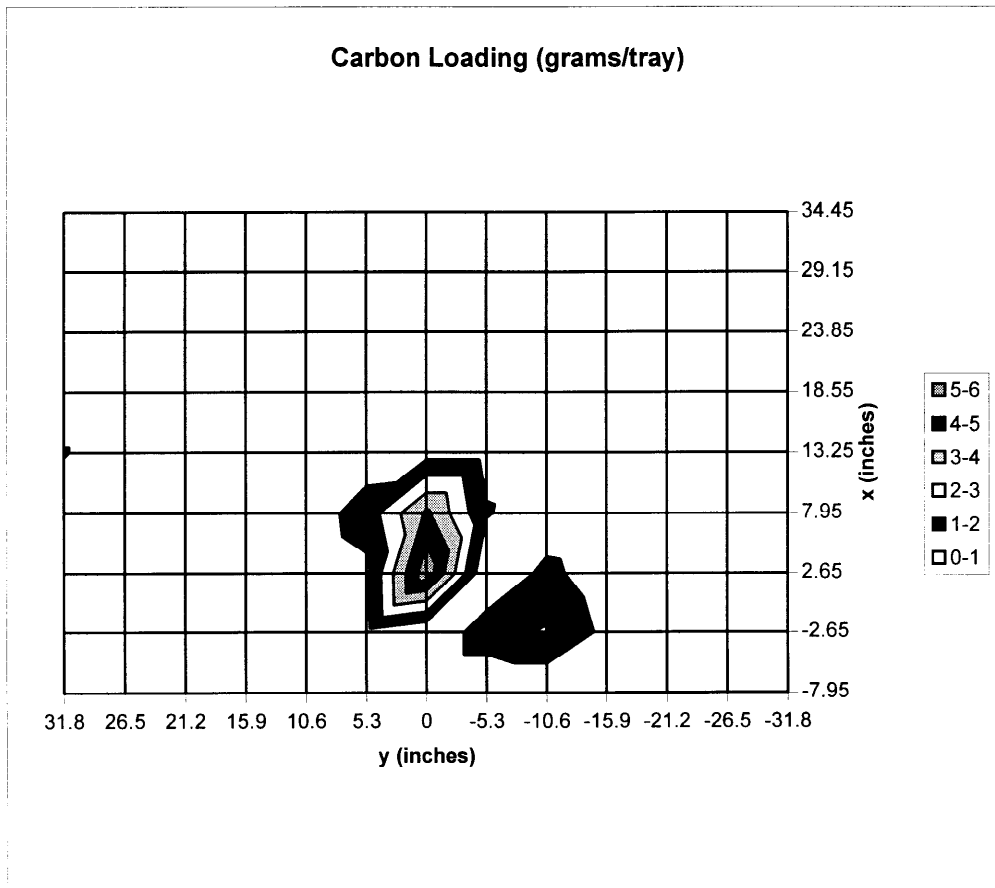
Test 5d-Wide Side

E = 693 ft-lbs

E/E_{min} = 5.37

x ==>	-7.95	-2.65	2.65	7.95	13.25	18.55	23.85	29.15	34.45
-31.8	0	0.2	0	0	0	0	0	0	0
-26.5	0	0.4	0	0	0	0	0	0	0
-21.2	0	0.5	0.2	0	0	0	0	0	0
-15.9	0	0.7	0.3	0	0	0	0	0	0
-10.6	0	2.1	1.3	0.2	0.4	0	0	0	0
-5.3	0	1.6	0	1.1	0.6	0	0	0	0
0	0	0	5.7	4.2	0.6	0	0	0	0
5.3	0	0.7	0.8	1.4	0.5	0	0	0	0
10.6	0	0.3	0.4	0.5	0.3	0	0	0	0
15.9	0	0	0	0	0	0	0	0	0
21.2	0	0	0	0	0	0	0	0	0
26.5	0	0	0	0	0	0	0	0	0
31.8	0	0	0	0	1.1	0	0	0	0

Total 26.1





**Test 5d:
Wide Side Impact**

Test 7c-Narrow Side

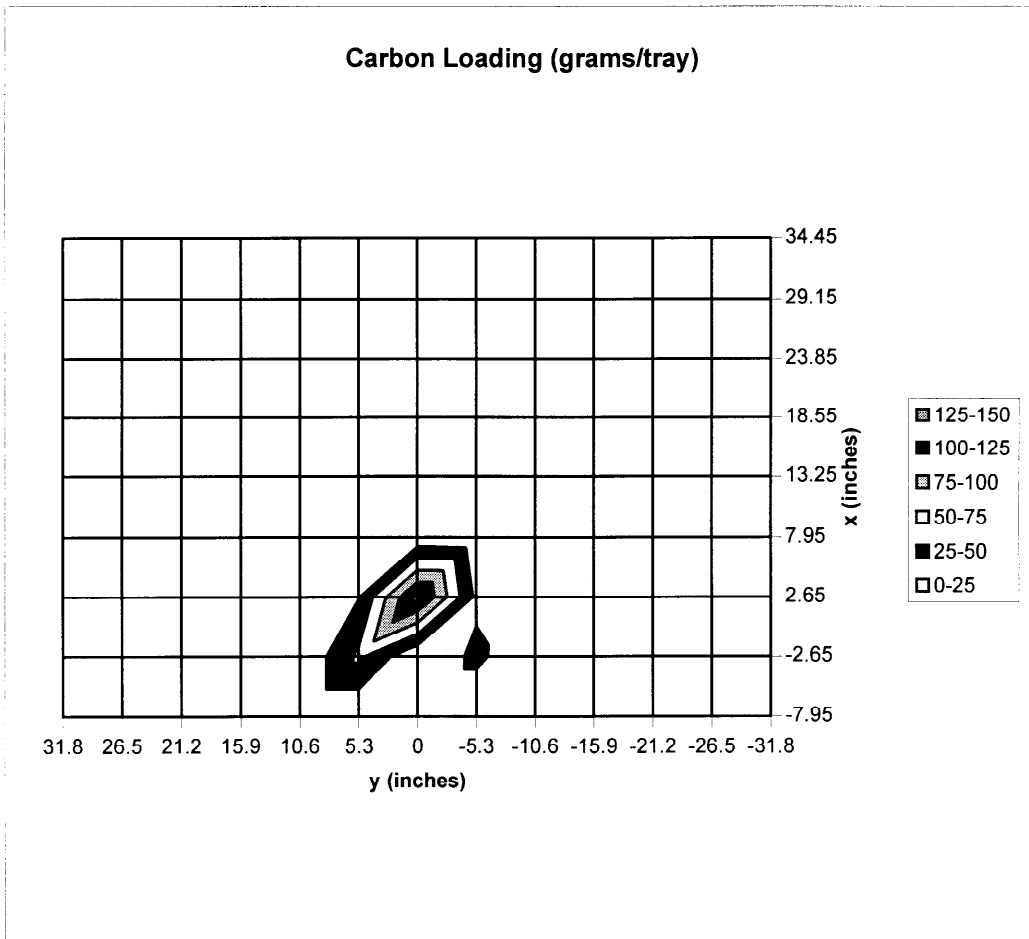
E = 638 ft-lbs

E/E_{min} = 4.06

x====>	-7.95	-2.65	2.65	7.95	13.25	18.55	23.85	29.15	34.45
-31.8	0	0	0	0	0	0	0	0	0
-26.5	0	0	0	0	0	0	0	0	0
-21.2	0	0	0	0	0	0	0	0	0
-15.9	0	0	0	0	0	0	0	0	0
-10.6	0	0	0.7	0.6	0.7	0.5	0.5	0	0
-5.3	0	31.4	18.9	2.8	1.7	1.3	0.6	0	0
0	0	0	132.8	6.3	1.5	1.7	1.2	0	0
5.3	0	55.4	23.8	4.6	3.2	3	2.3	0	0
10.6	0	0.2	0.5	0.8	1.1	1.1	0.8	0	0
15.9	0	0	0	0	0	0	0	0	0
21.2	0	0	0	0	0	0	0	0	0
26.5	0	0	0	0	0	0	0	0	0
31.8	0	0	0	0	0	0	0	0	0

y

Total 300





Test 7c:
Narrow Side Impact

Test 8c-Narrow Side

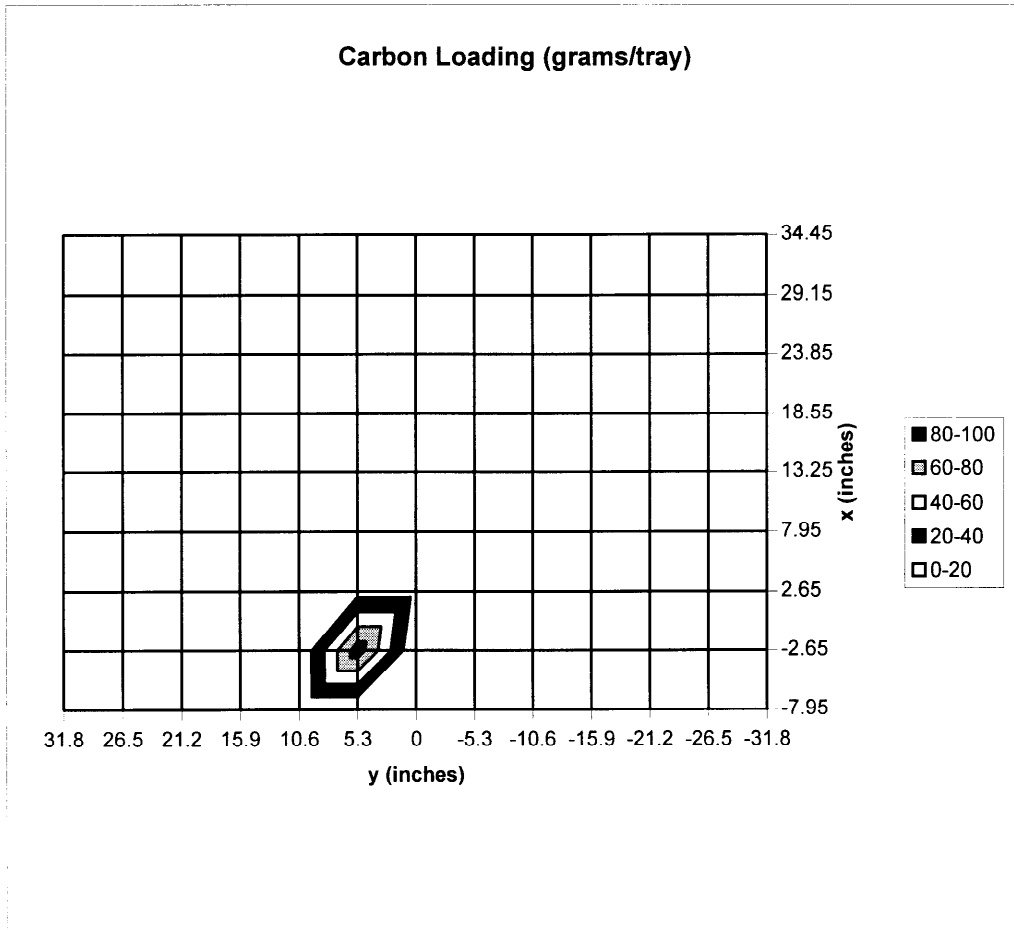
E = 623 ft-lbs

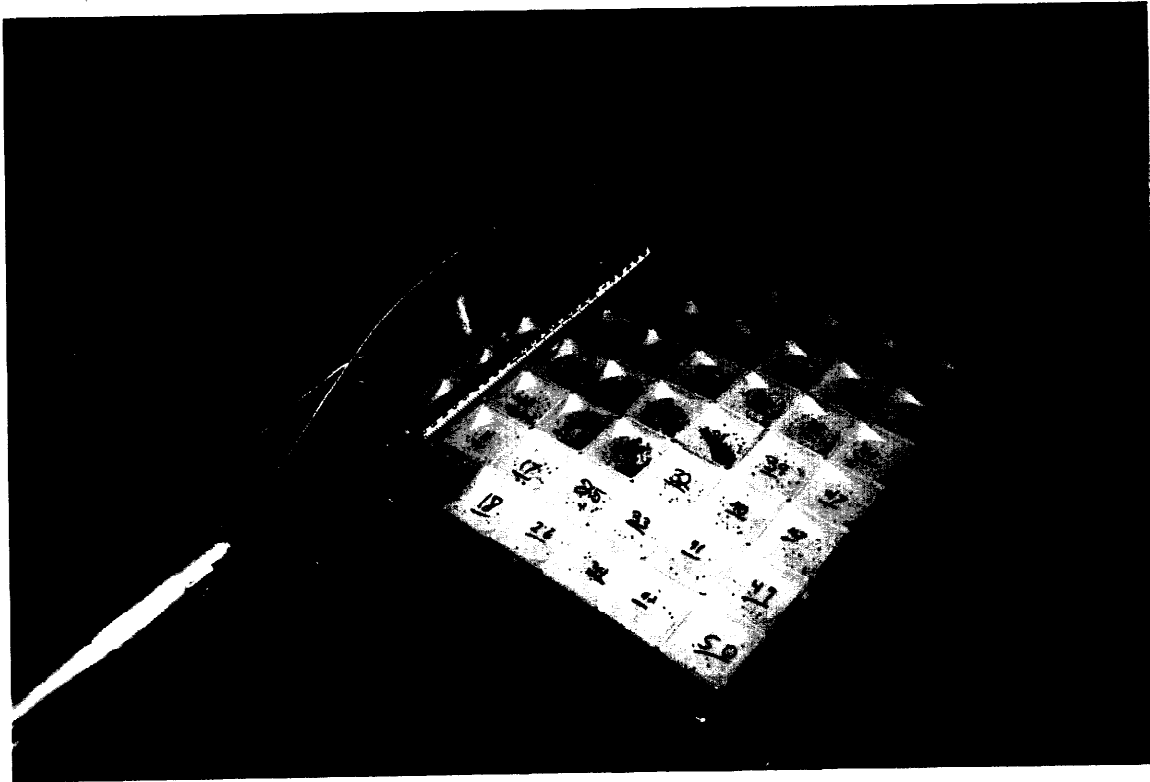
E/E_{min} = 3.96

x ==>	-7.95	-2.65	2.65	7.95	13.25	18.55	23.85	29.15	34.45
-31.8	0	0	0	0	0	0	0	0	0
-26.5	0	0	0	0	0	0	0	0	0
-21.2	0	0	0	0	0	0	0	0	0
-15.9	0	0	0	0	0	0	0	0	0
-10.6	0	0	0	0	0	0	0	0	0
-5.3	0	0	0	0	0	0	0	0	0
0	0	0	12.8	0.7	0.6	0	0	0	0
5.3	0	91.7	12.5	4	1.2	0	0	0	0
10.6	0	0.9	2.3	2.6	4.4	0.7	0	0	0
15.9	0	0.3	0.2	0.2	0.4	0.3	0	0	0
21.2	0	0	0.2	0	0	0	0	0	0
26.5	0	0	0	0	0	0	0	0	0
31.8	0	0	0	0	0	0	0	0	0

y

Total 136





Test 8c:
Narrow Side Impact

Test 11c-Wide Side

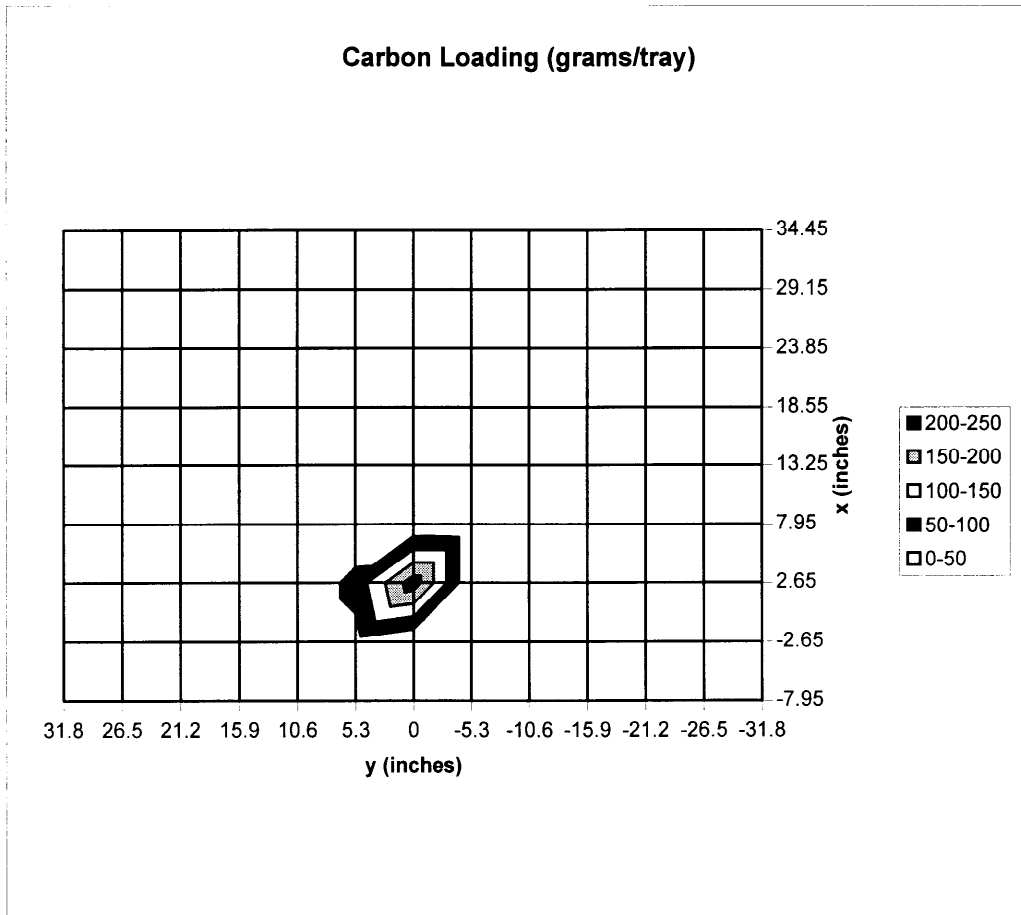
E = 537 ft-lbs

E/E_{min} = 4.16

x ==>	-7.95	-2.65	2.65	7.95	13.25	18.55	23.85	29.15	34.45
-31.8	0	0	0	0	0	0	0	0	0
-26.5	0	0	0	0	0	0	0	0	0
-21.2	0	0	0	0	0	0	0	0	0
-15.9	0	0	0	0	0	0	0	0	0
-10.6	0	0	0	0	0	0	0	0	0
-5.3	0	2.8	1.6	0.7	0	0	0	0	0
0	0	0	228.9	4.2	0.3	0	0	0	0
5.3	0	32.7	68.2	0.5	0.4	0	0	0	0
10.6	0	0	0	0	0	0	0	0	0
15.9	0	0	0	0	0	0	0	0	0
21.2	0	0	0	0	0	0	0	0	0
26.5	0	0	0	0	0	0	0	0	0
31.8	0	0	0	0	0	0	0	0	0

y

Total 340.3





Test 11c:
Wide Side Impact

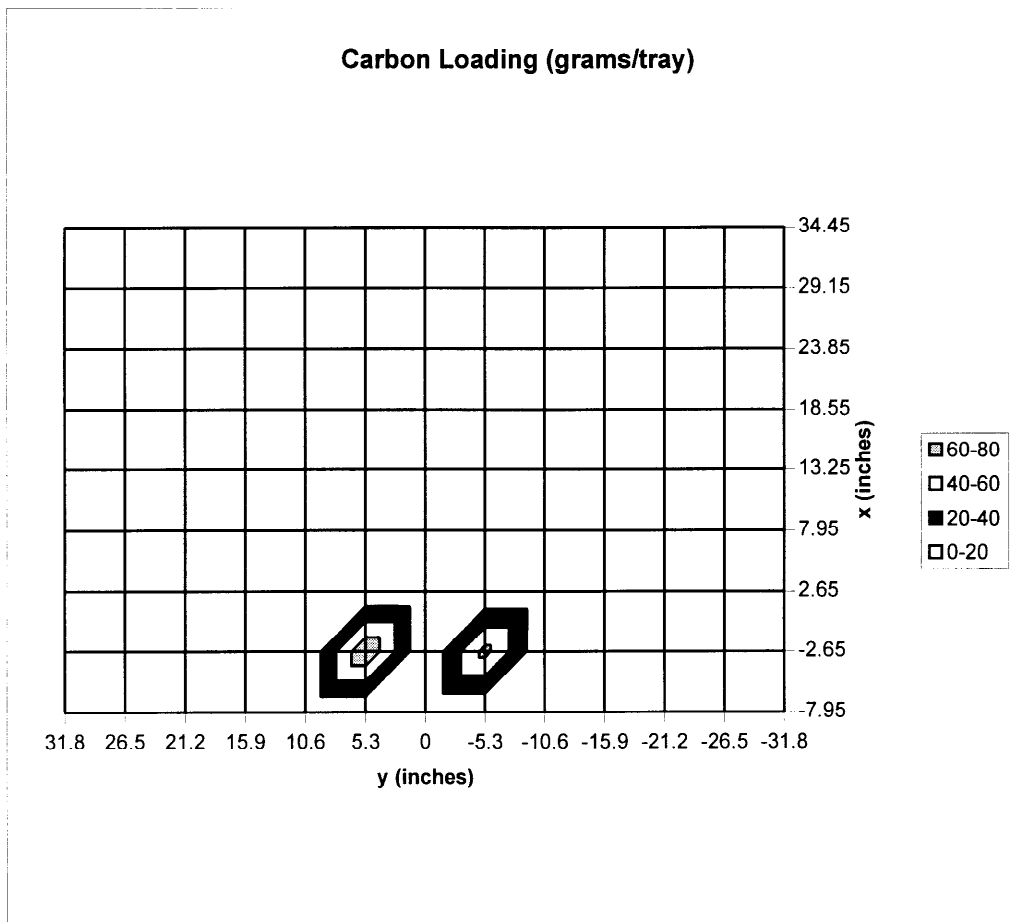
Test 13-Bottom

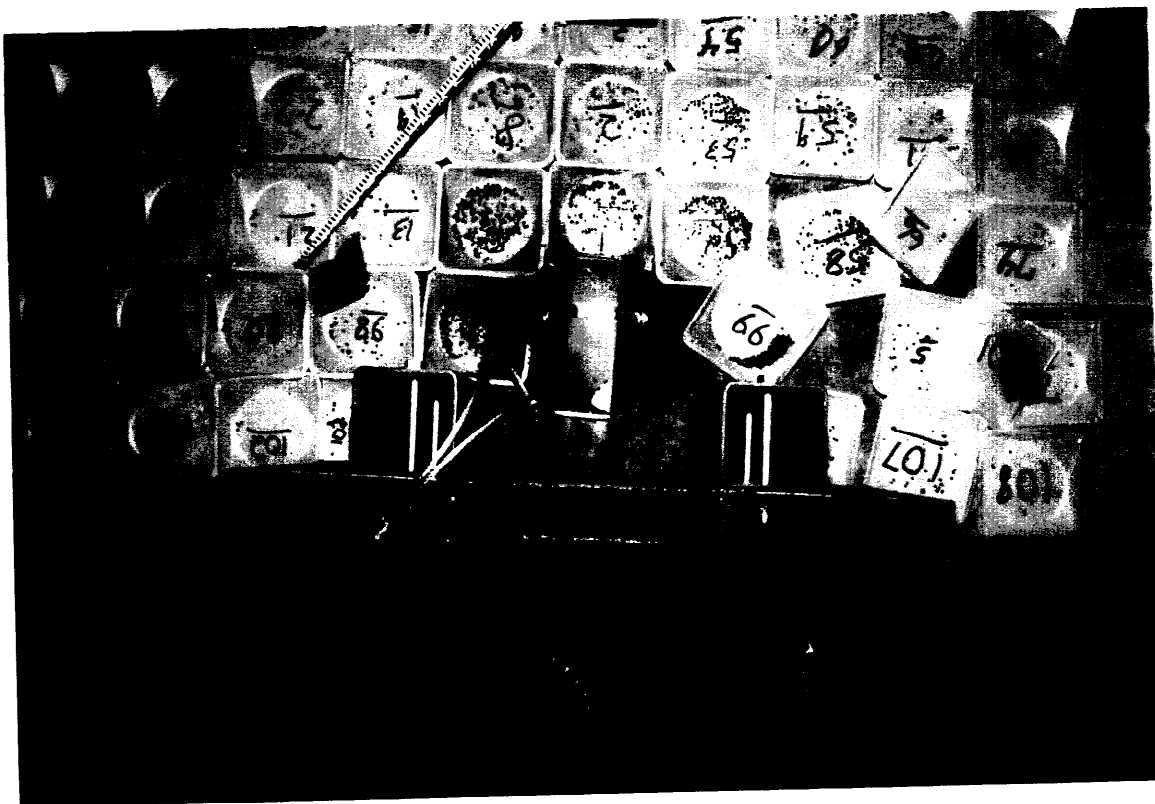
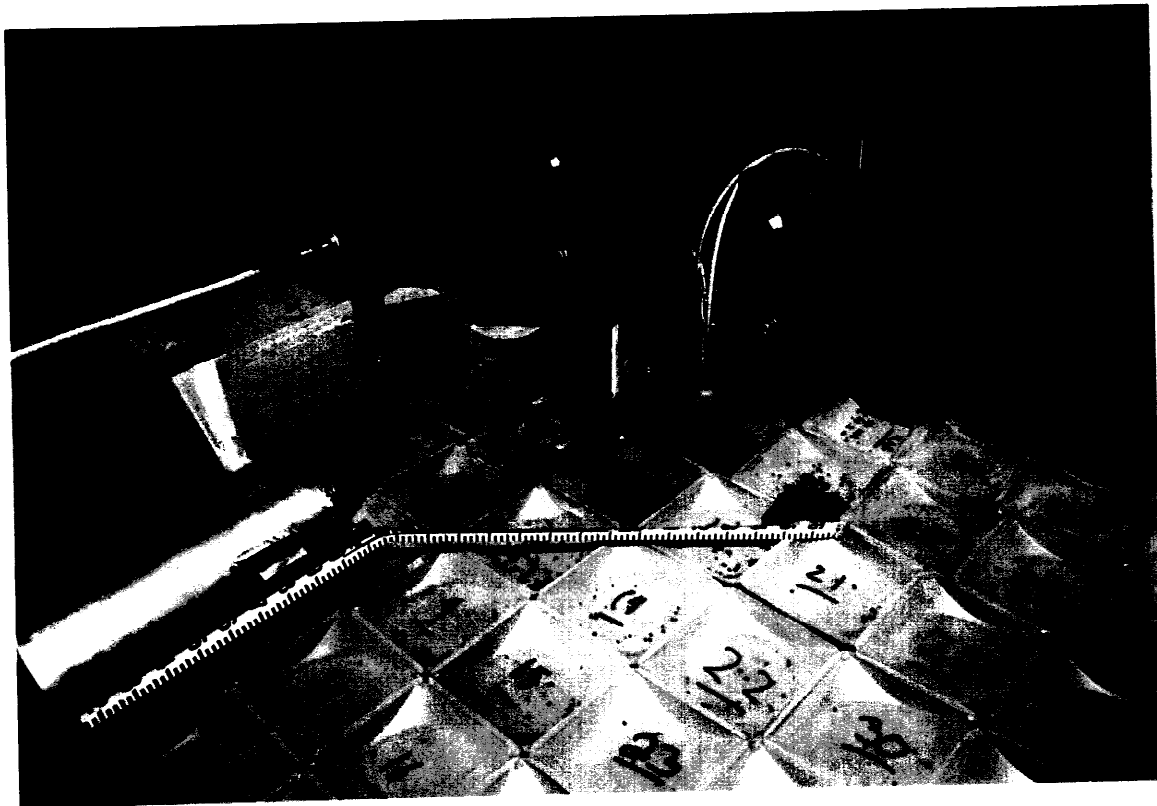
E = 160 ft-lbs

E/E_{min} = 2.03

x ==>	-7.95	-2.65	2.65	7.95	13.25	18.55	23.85	29.15	34.45
-31.8	0	0	0	0	0	0	0	0	0
-26.5	0	0	0	0	0	0	0	0	0
-21.2	0	0	0	0	0	0	0	0	0
-15.9	0	0	0	0	0	0	0	0	0
-10.6	0	0	0.6	0	0	0	0	0	0
-5.3	0	66.6	0.9	0	0	0	0	0	0
0	0	0	0	0	0	0	0	0	0
5.3	0	78.5	1	0	0	0	0	0	0
10.6	0	0	0	0	0	0	0	0	0
15.9	0	0	0	0	0	0	0	0	0
21.2	0	0	0	0	0	0	0	0	0
26.5	0	0	0	0	0	0	0	0	0
31.8	0	0	0	0	0	0	0	0	0

Total 147.6





Test 13:
Bottom Impact

Test 14-Bottom

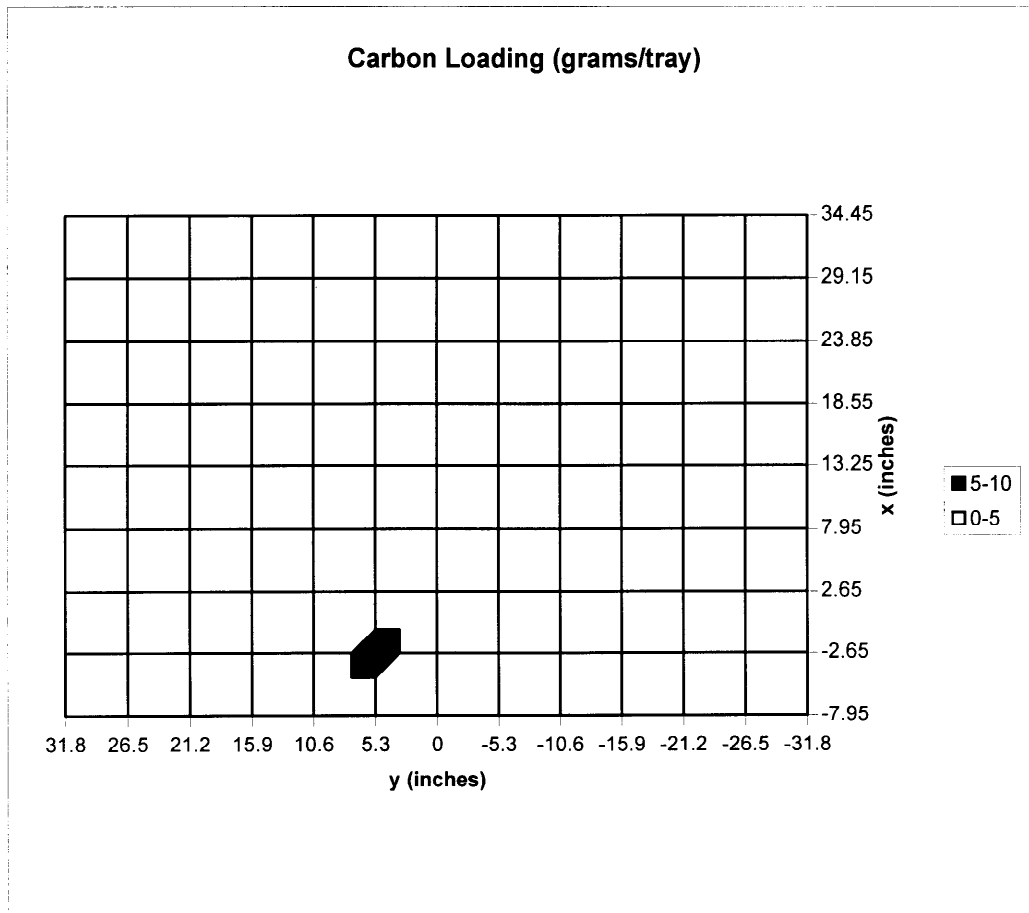
E = 160 ft-lbs

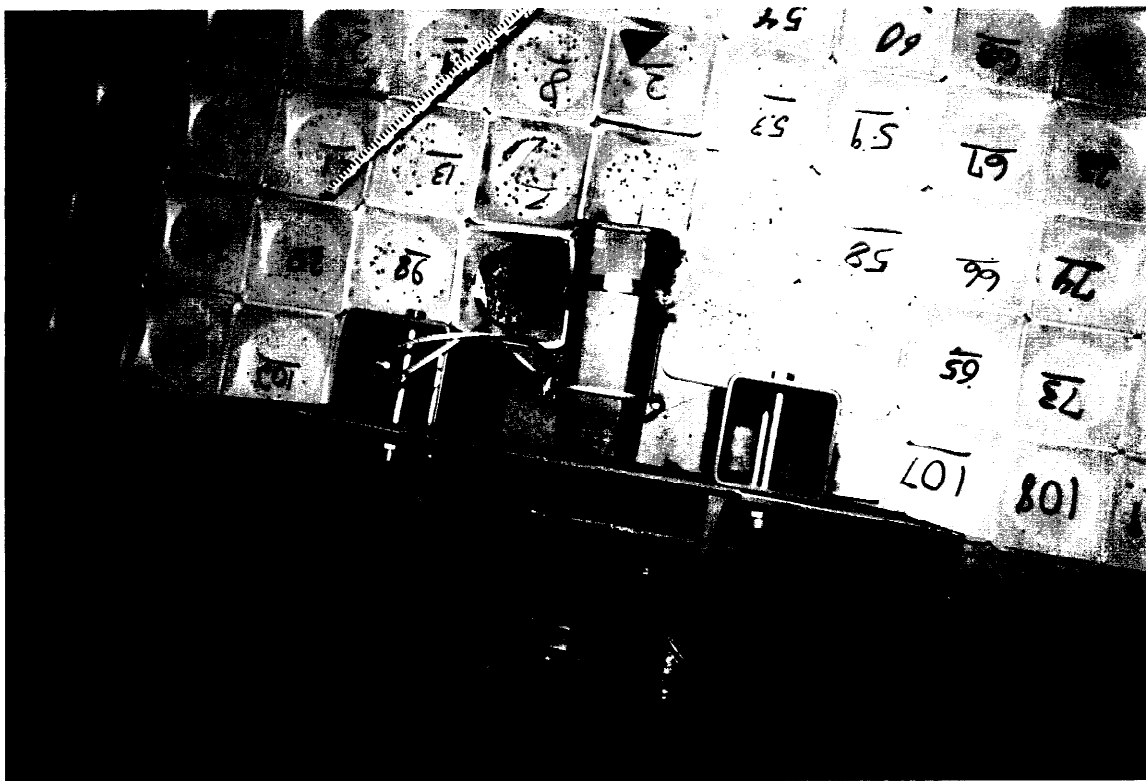
E/E_{min} = 2.03

x ==>	-7.95	-2.65	2.65	7.95	13.25	18.55	23.85	29.15	34.45
-31.8	0	0	0	0	0	0	0	0	0
-26.5	0	0	0	0	0	0	0	0	0
-21.2	0	0	0	0	0	0	0	0	0
-15.9	0	0	0	0	0	0	0	0	0
-10.6	0	0	0	0	0	0	0	0	0
-5.3	0	0	0	0	0	0	0	0	0
0	0	0	0	0	0	0	0	0	0
5.3	0	8.2	0	0	0	0	0	0	0
10.6	0	0	0	0	0	0	0	0	0
15.9	0	0	0	0	0	0	0	0	0
21.2	0	0	0	0	0	0	0	0	0
26.5	0	0	0	0	0	0	0	0	0
31.8	0	0	0	0	0	0	0	0	0

y

Total 8.2





Test 14:
Bottom Impact

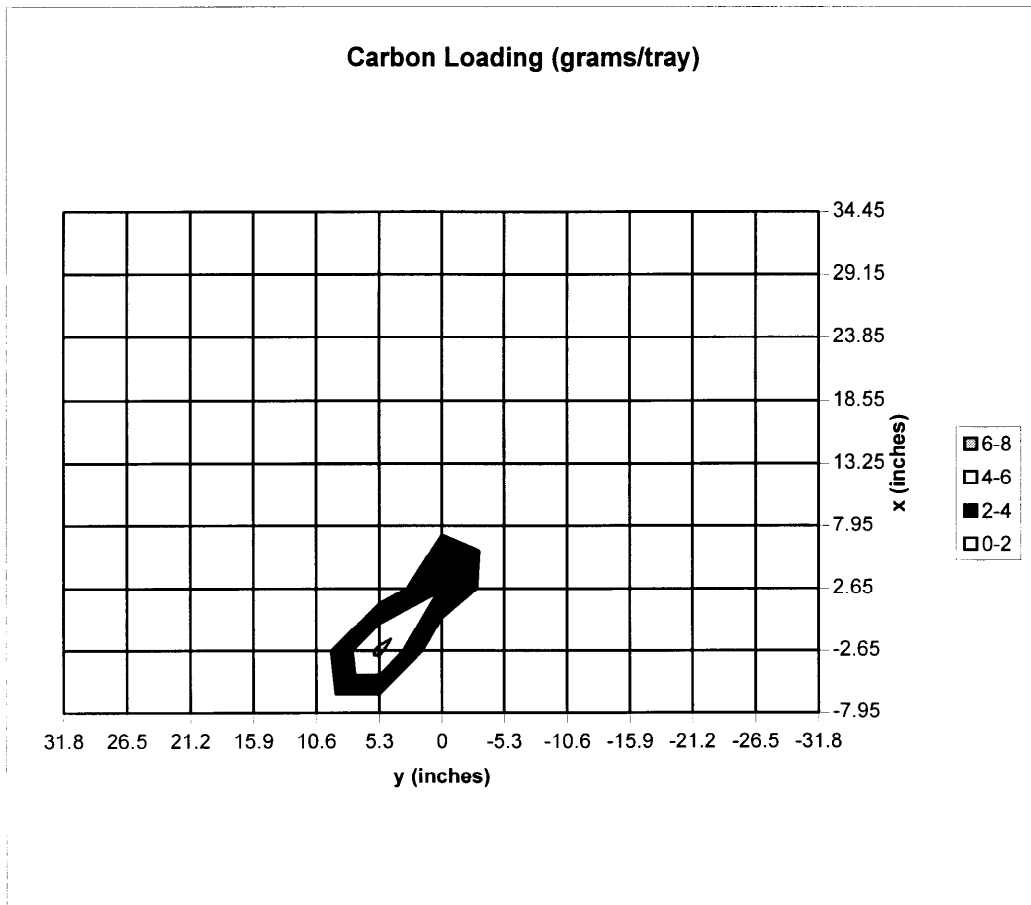
Test 15-Bottom

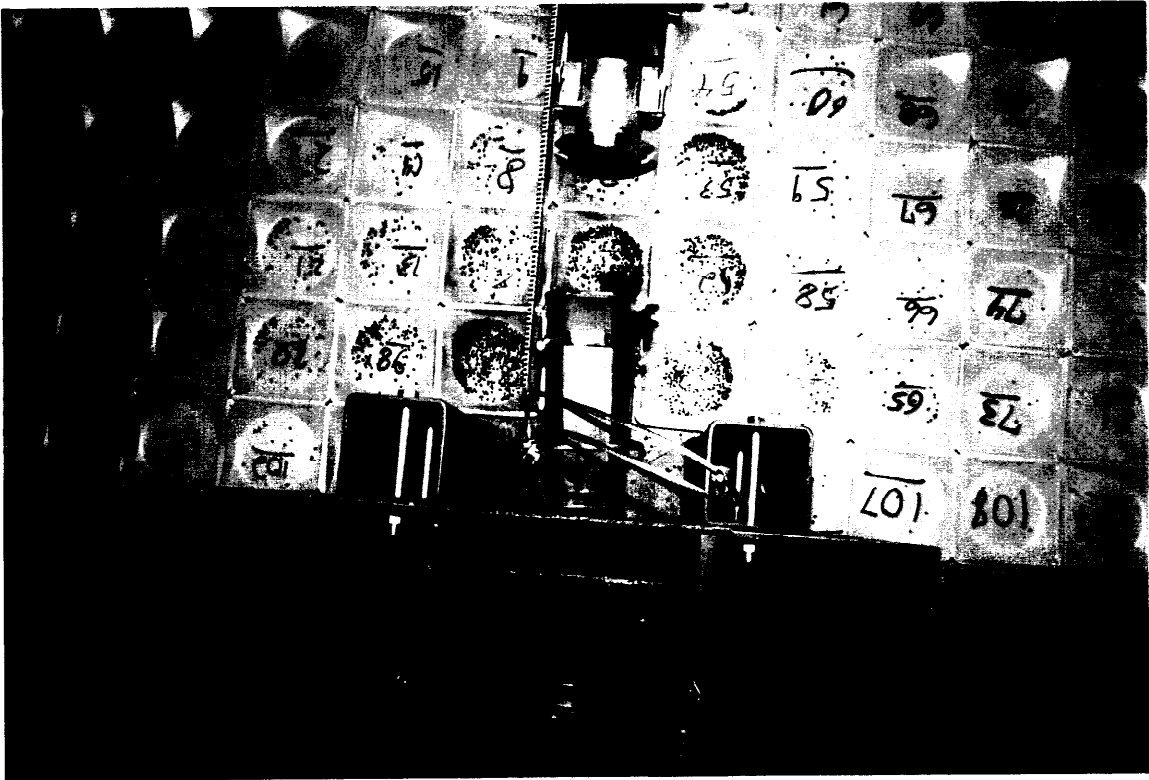
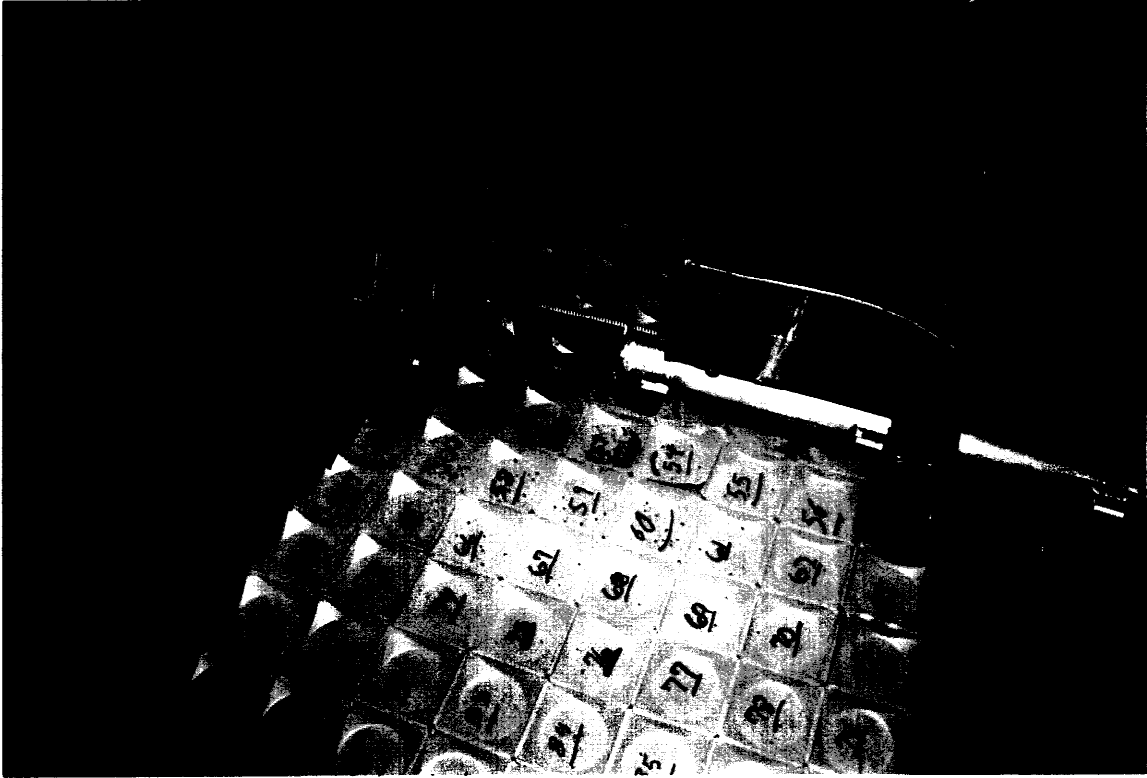
E = 156 ft-lbs

E/E_{min} = 1.98

x ==>	-7.95	-2.65	2.65	7.95	13.25	18.55	23.85	29.15	34.45
-31.8	0	0	0	0	0	0	0	0	0
-26.5	0	0	0	0	0	0	0	0	0
-21.2	0	0	0	0	0	0	0	0	0
-15.9	0	0	0	0	0	0	0	0	0
-10.6	0	0	0	0	0	0	0	0	0
-5.3	0	0.9	0.6	0.8	0	0	0	0	0
0	0	0	3.8	1.7	0	0	0	0	0
5.3	0	6.5	0.6	0	0	0	0	0	0
10.6	0	0.6	0.5	0	0	0	0	0	0
15.9	0	0	0	0	0	0	0	0	0
21.2	0	0	0	0	0	0	0	0	0
26.5	0	0	0	0	0	0	0	0	0
31.8	0	0	0	0	0	0	0	0	0

Total 16





**Test 15:
Bottom Impact**

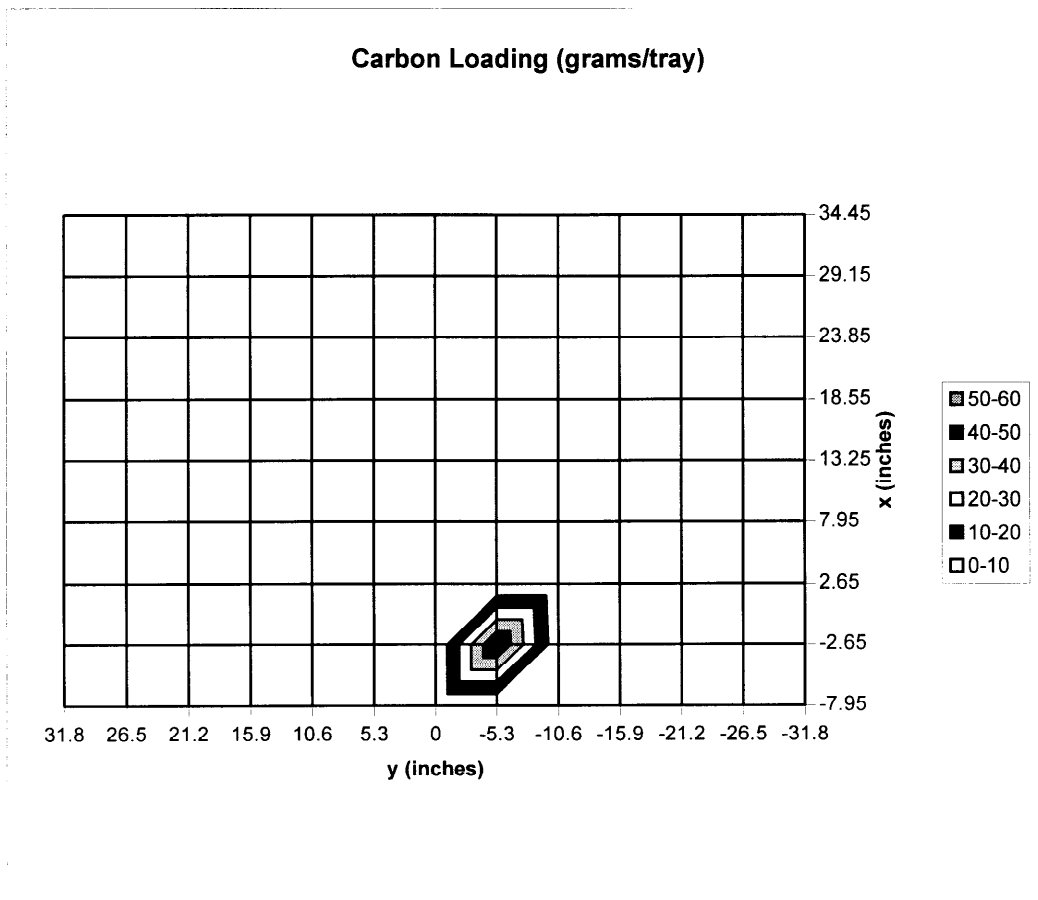
Test 16-Bottom

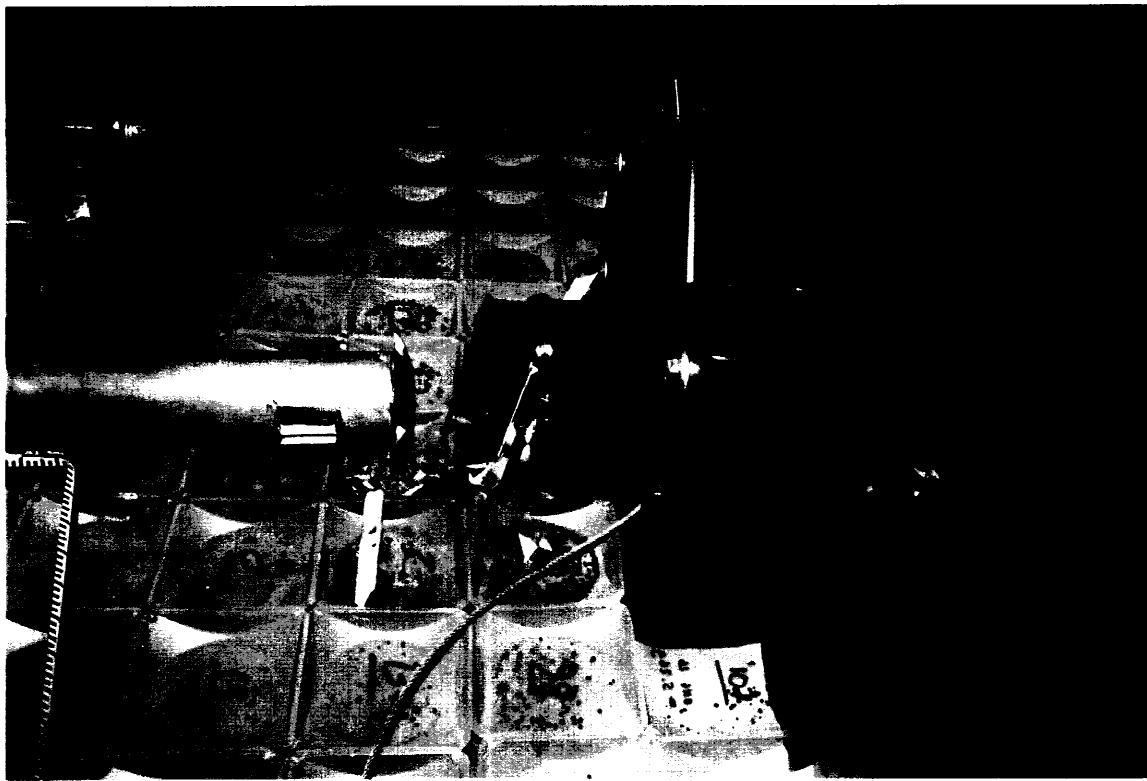
E = 323 ft-lbs

E/E_{min} = 4.09

x ==>	-7.95	-2.65	2.65	7.95	13.25	18.55	23.85	29.15	34.45
-31.8	0.6	0.5	0	0	0	0	0	0	0
-26.5	0.6	0.8	0	0	0	0	0	0	0
-21.2	0.5	1	0	0	0	0	0	0	0
-15.9	0.6	1.4	0	0	0	0	0	0	0
-10.6	0	1.9	0	0	0	0	0	0	0
-5.3	0	51.3	0	0	0	0	0	0	0
0	0	0	1.2	0	0	0	0	0	0
5.3	0	1.5	0.7	0	0	0	0	0	0
10.6	0	0	0	0	0	0	0	0	0
15.9	0	0	0	0	0	0	0	0	0
21.2	0	0	0	0	0	0	0	0	0
26.5	0	0	0	0	0	0	0	0	0
31.8	0	0	0	0	0	0	0	0	0

Total 62.6





**Test 16:
Bottom Impact**

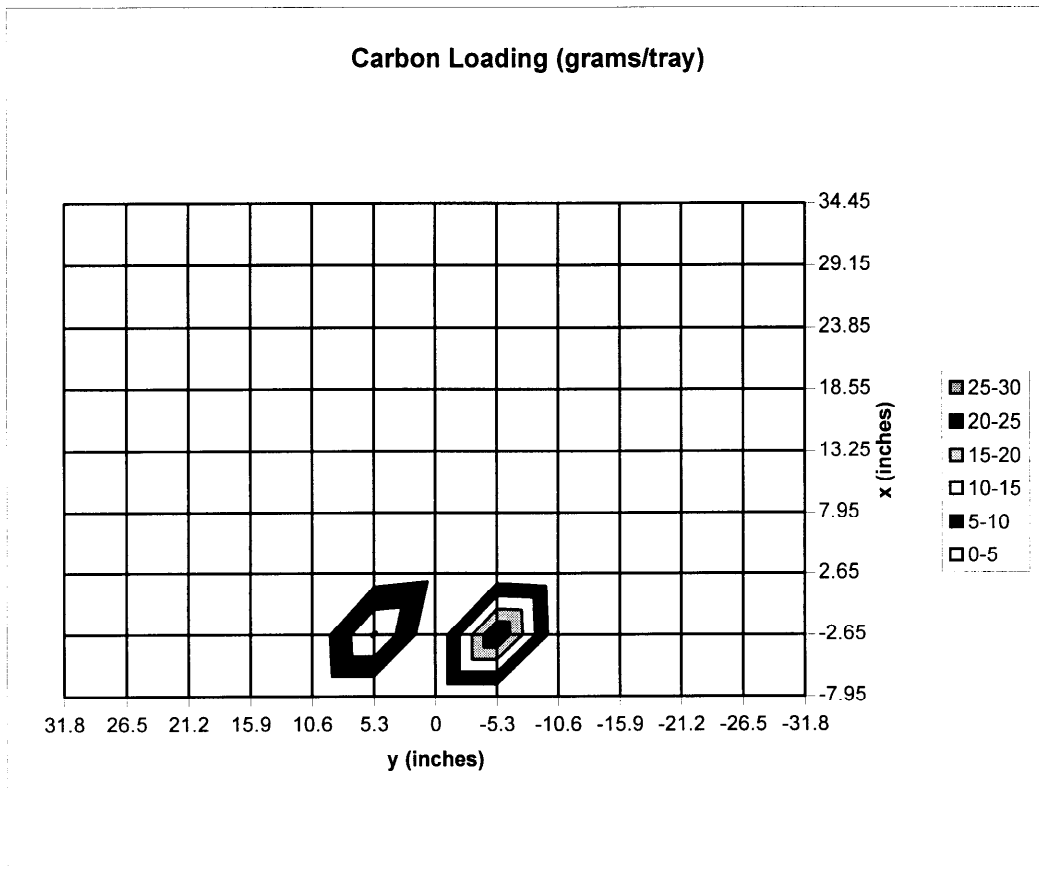
Test 17-Bottom

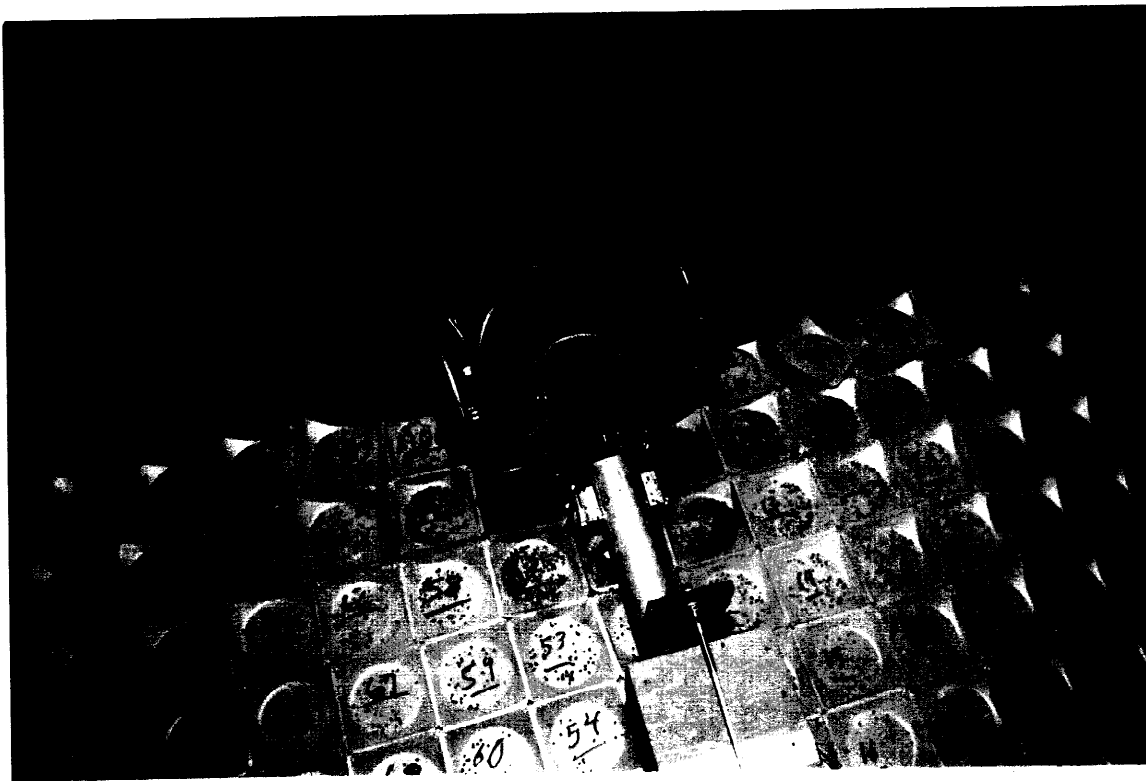
E = 332 ft-lbs

E/E_{min} = 4.20

x ==>	-7.95	-2.65	2.65	7.95	13.25	18.55	23.85	29.15	34.45
-31.8	0	0	0	0	0	0	0	0	0
-26.5	0	0	0	0	0	0	0	0	0
-21.2	0.4	0	0	0	0	0	0	0	0
-15.9	0.9	0.5	0	0	0	0	0	0	0
-10.6	0	0.9	0	0	0	0	0	0	0
-5.3	0	25.3	1.2	0	0	0	0	0	0
0	0	0	3.5	0	0	0	0	0	0
5.3	0	15.5	2.1	0	0	0	0	0	0
10.6	0	0.7	0.5	0	0	0	0	0	0
15.9	0	0.4	0.2	0	0	0	0	0	0
21.2	0	0	0	0	0	0	0	0	0
26.5	0	0	0	0	0	0	0	0	0
31.8	0	0	0	0	0	0	0	0	0

Total 52.1





Test 17:
Bottom Impact

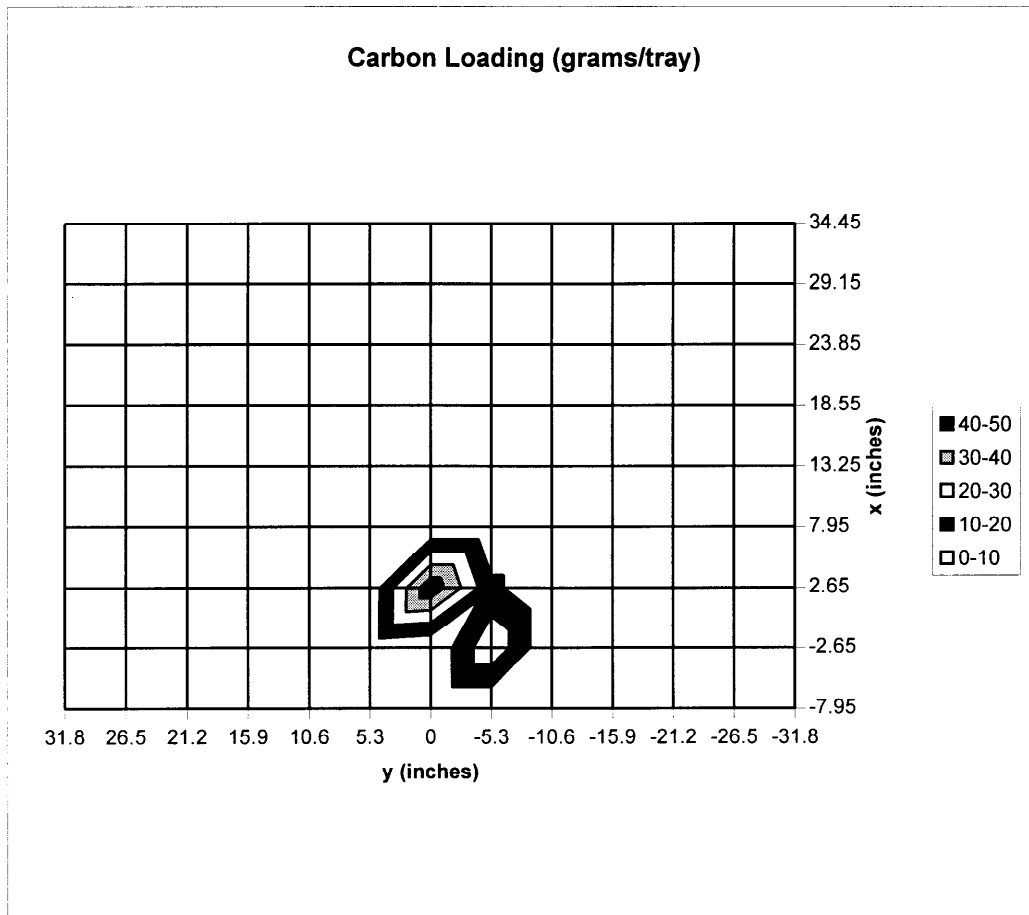
Test 18-Bottom

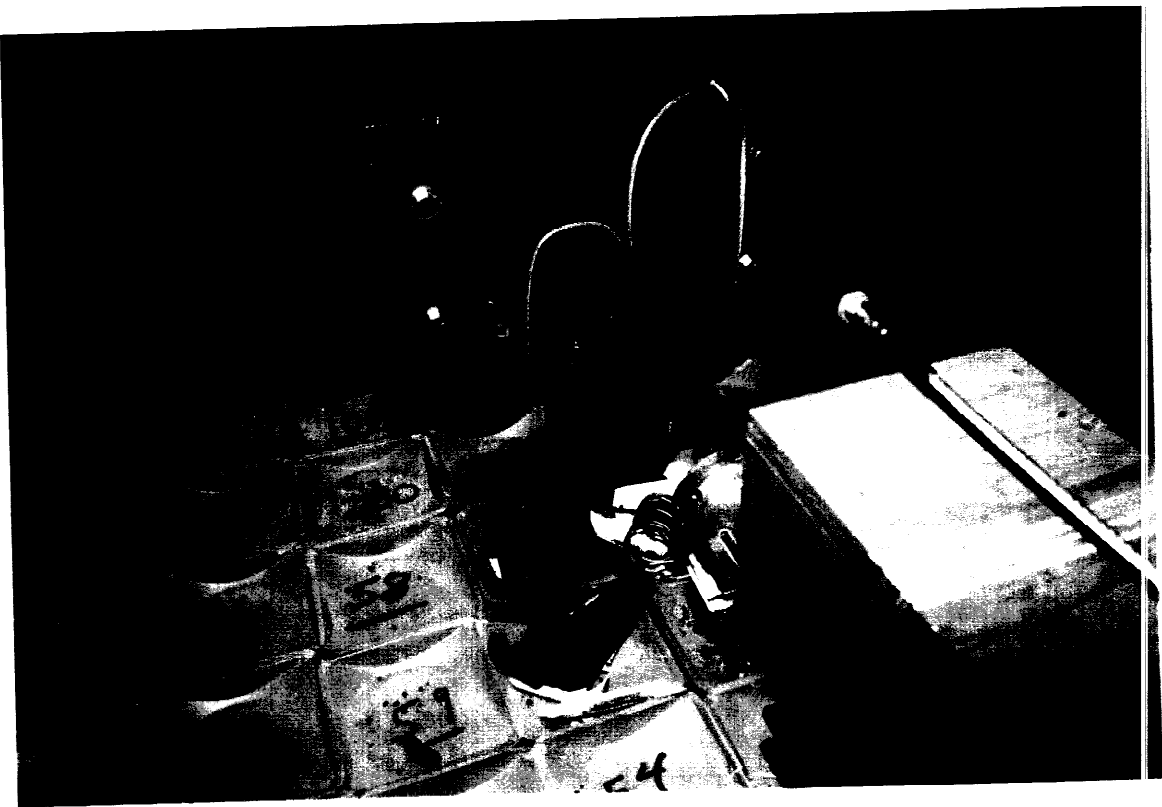
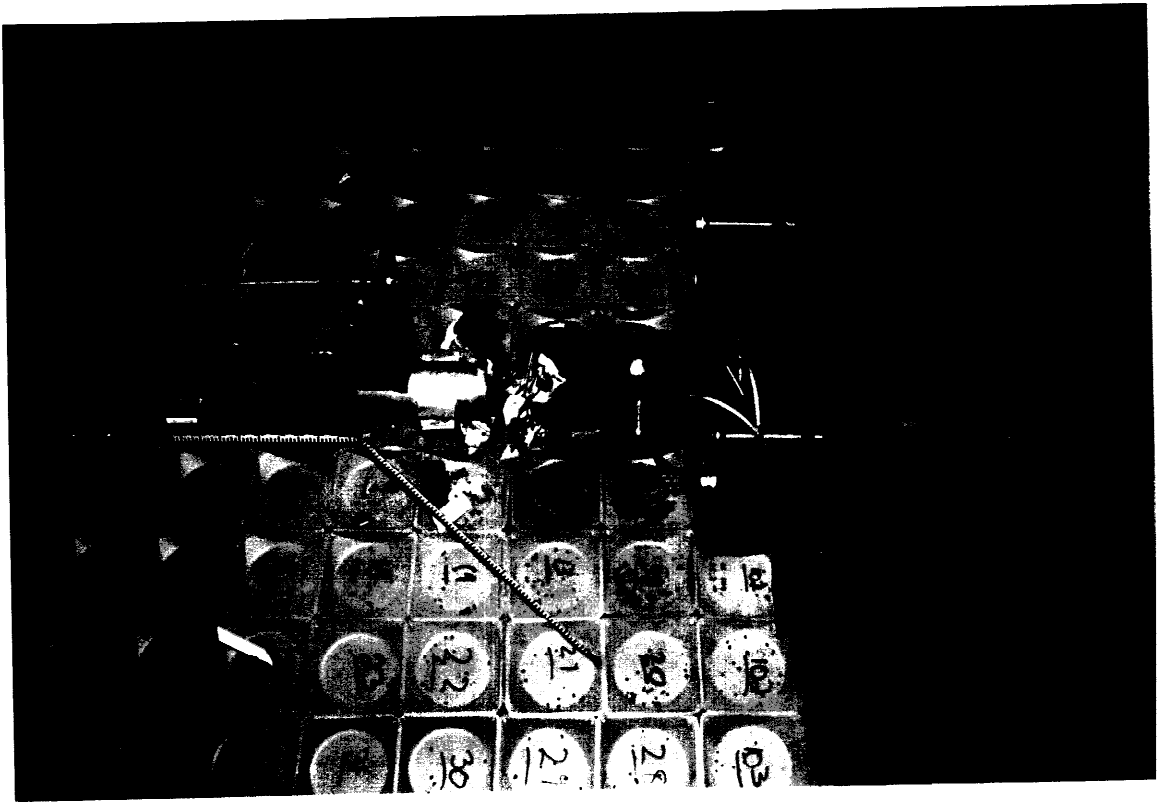
E = 323 ft-lbs

E/E_{min} = 4.09

x ==>	-7.95	-2.65	2.65	7.95	13.25	18.55	23.85	29.15	34.45
-31.8	0	0	0	0	0	0	0	0	0
-26.5	0	0	0	0	0	0	0	0	0
-21.2	0	0	0	0	0	0	0	0	0
-15.9	0	0	0	0	0	0	0	0	0
-10.6	0	0	0	0	0	0	0	0	0
-5.3	0	28.3	12.6	0	0	0	0	0	0
0	0	0	48	0	0	0	0	0	0
5.3	0	3.2	2.8	0	0	0	0	0	0
10.6	0	0	0	0	0	0	0	0	0
15.9	0	0	0	0	0	0	0	0	0
21.2	0	0	0	0	0	0	0	0	0
26.5	0	0	0	0	0	0	0	0	0
31.8	0	0	0	0	0	0	0	0	0

Total 94.9





Test 18:
Bottom Impact

Test 19-Wide Side

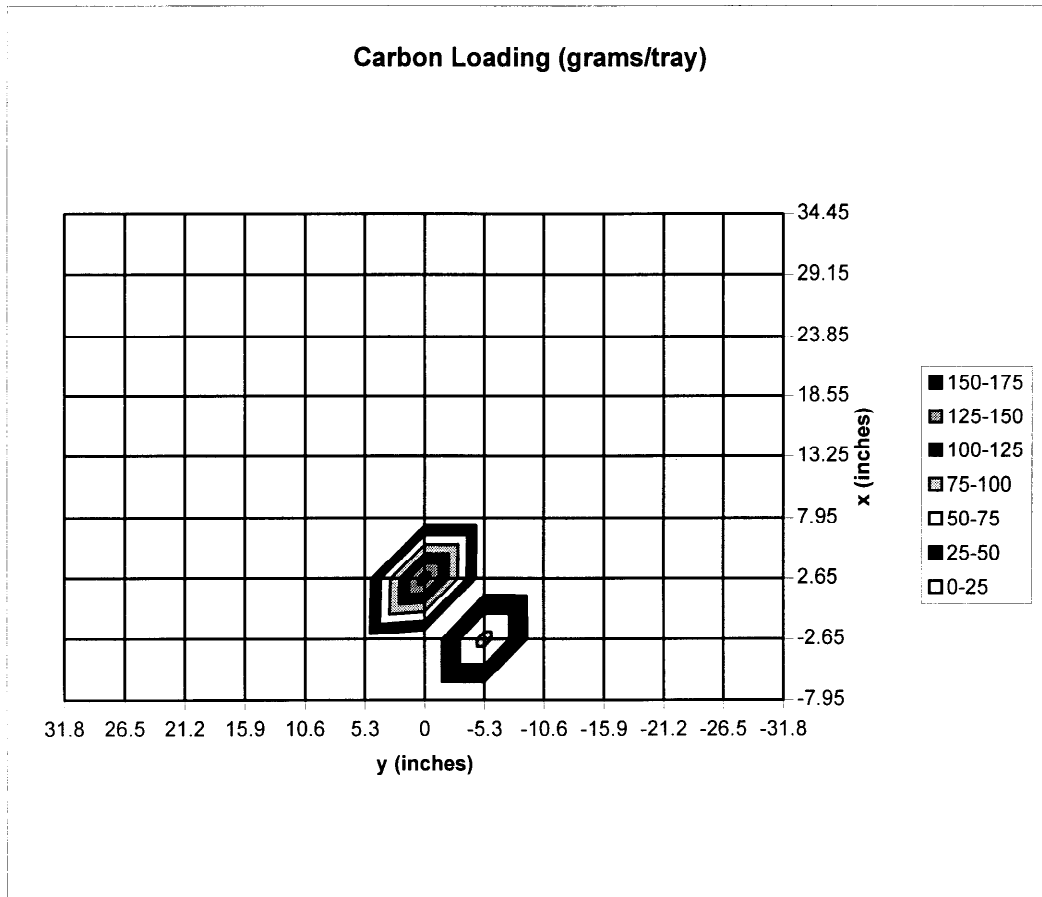
E = 788 ft-lbs

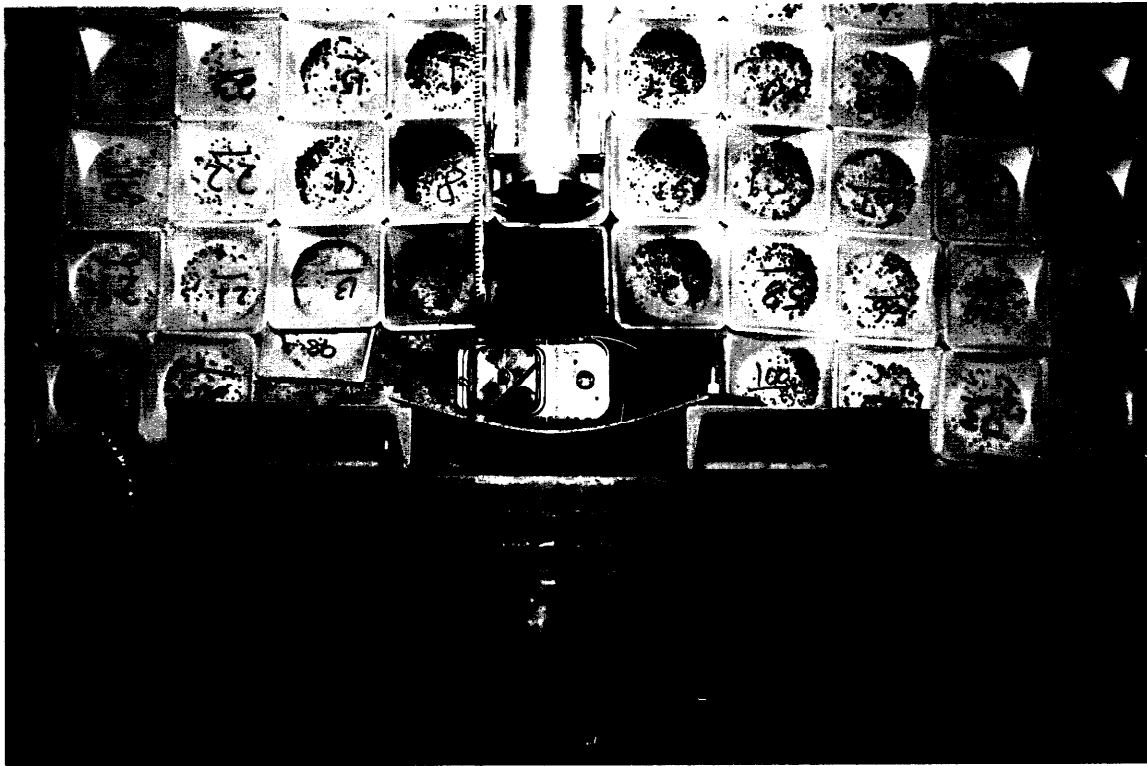
E/E_{min} = 6.11

x ==>	-7.95	-2.65	2.65	7.95	13.25	18.55	23.85	29.15	34.45
-31.8	0	0	0	0	0	0.7	0.7	0.3	0
-26.5	0	0	0	0	0.2	0.5	0.5	0	0
-21.2	0	0	0	0	0.5	0.7	0.2	0	0
-15.9	0	0	0	0	0.5	0.5	0.1	0	0
-10.6	0	1.1	1	0.8	1.1	0.7	0	0	0
-5.3	0	85.3	2.2	3.8	2.4	0	0	0	0
0	0	0	165.5	3.6	1.3	0	0	0	0
5.3	0	11.5	7.7	4.7	1.6	0	0	0	0
10.6	0	1.4	0.4	0.9	0.7	0	0	0	0
15.9	0	0.5	0.1	0	0	0	0	0	0
21.2	0	0.2	0	0	0	0	0	0	0
26.5	0	0	0	0	0	0	0	0	0
31.8	0	0	0	0	0	0	0	0	0

y

Total 303.9





**Test 19:
Wide Side Impact**

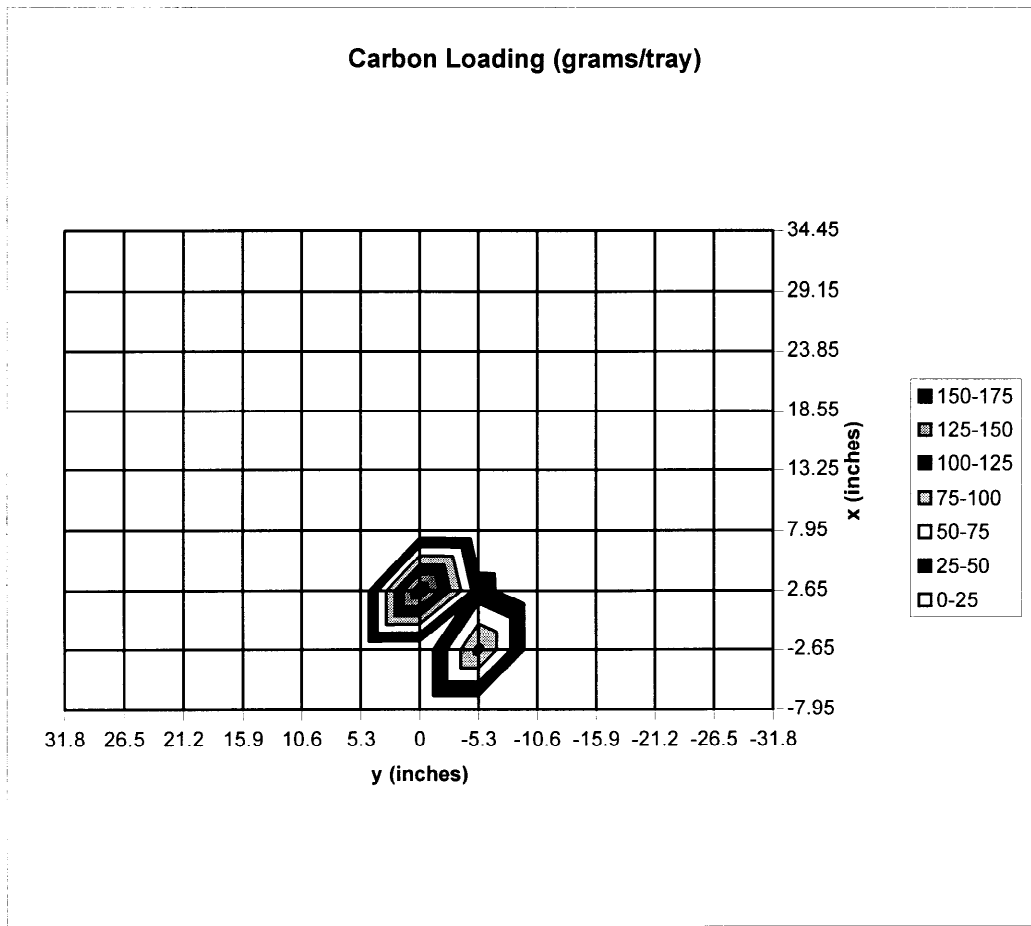
Test 20-Wide Side

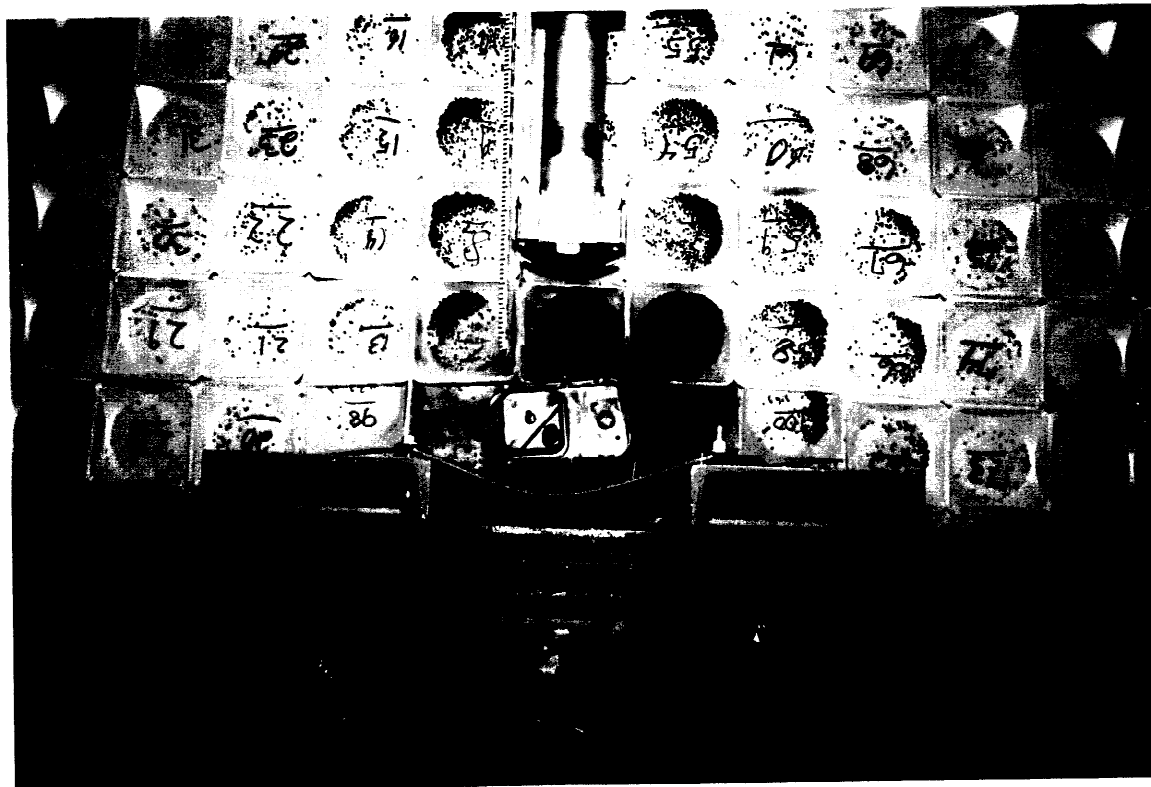
E = 788 ft-lbs

E/E_{min} = 6.11

x ==>	-7.95	-2.65	2.65	7.95	13.25	18.55	23.85	29.15	34.45
-31.8	0	0	0	0	0	0	0	0	0
-26.5	0	0	0	0	0	0	0	0	0
-21.2	0	0	0	0	0	0	0	0	0
-15.9	0	0	0.8	0.6	0	0	0	0	0
-10.6	0	1.8	1.8	0.9	0.5	0	0	0	0
-5.3	0	107.8	34.5	2.5	1.4	1.5	0.5	0	0
0	0	0	171.5	5.5	0.8	0	0	0	0
5.3	0	1.8	1.8	1.8	1.4	1.8	0	0	0
10.6	0	0	0	0.7	0	0	0	0	0
15.9	0	0	0	0	0	0	0	0	0
21.2	0	0	0	0	0	0	0	0	0
26.5	0	0	0	0	0	0	0	0	0
31.8	0	0	0	0	0	0	0	0	0

Total 341.7





Test 20:
Wide Side Impact

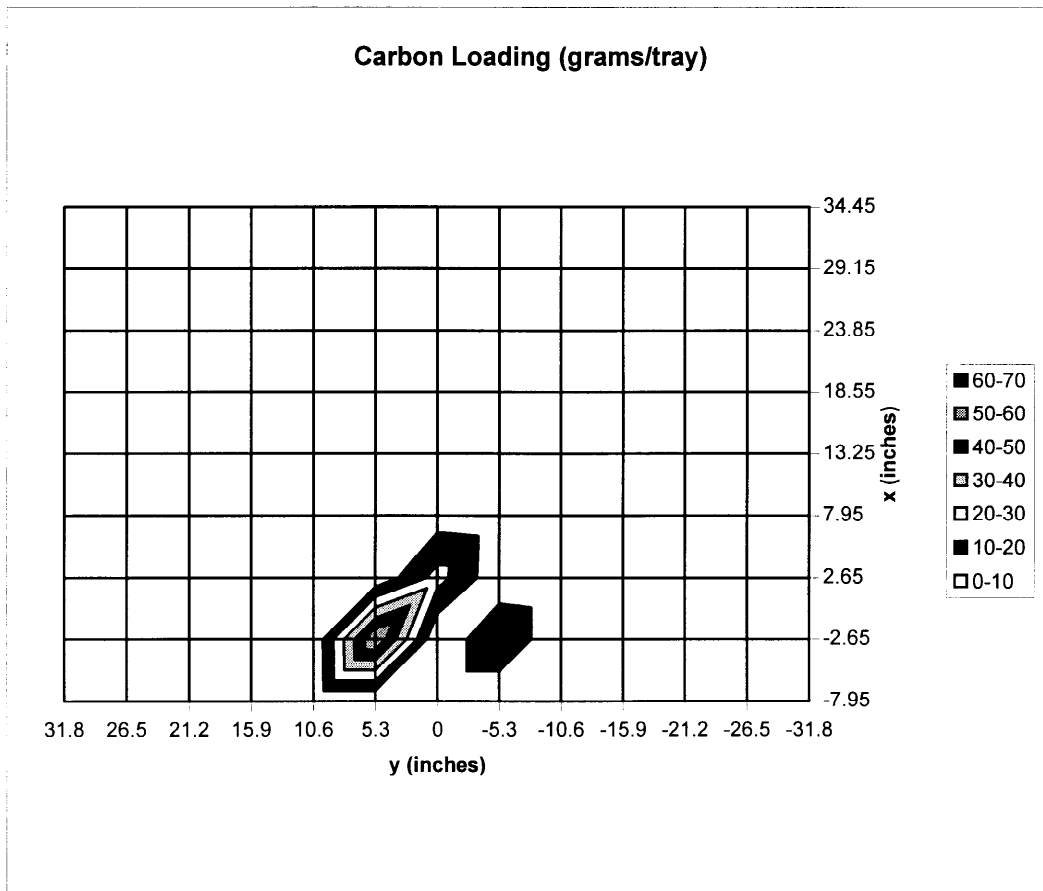
Test 21-Wide Side

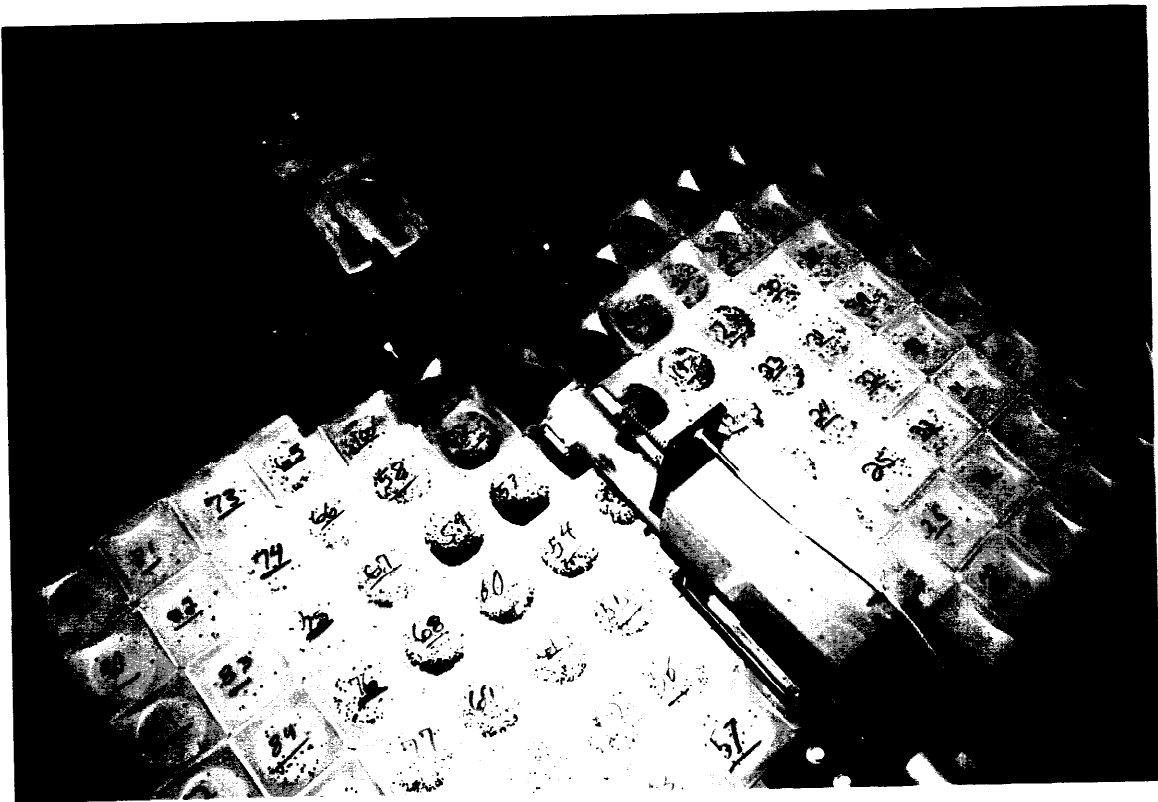
E = 788 ft-lbs

E/E_{min} = 6.11

x ==>	-7.95	-2.65	2.65	7.95	13.25	18.55	23.85	29.15	34.45
-31.8	0	0	0	0	0	0	0	0	0
-26.5	0	0	0	0	0	0	0	0	0
-21.2	0	0	0	0	0	0	0	0	0
-15.9	0	0	0	0	0.7	0	0	0	0
-10.6	0	0	0	2	0.8	0	0	0	0
-5.3	0	20.9	2.4	3	0.7	0	0	0	0
0	0	0	24	4.7	0.9	0	0	0	0
5.3	0	60.2	2	3.6	1.6	0	0	0	0
10.6	0	0.9	1.2	1.1	0	0	0	0	0
15.9	0	0	0	0	0	0	0	0	0
21.2	0	0	0	0	0	0	0	0	0
26.5	0	0	0	0	0	0	0	0	0
31.8	0	0	0	0	0	0	0	0	0

Total 130.7





Test 21:
Wide Side Impact

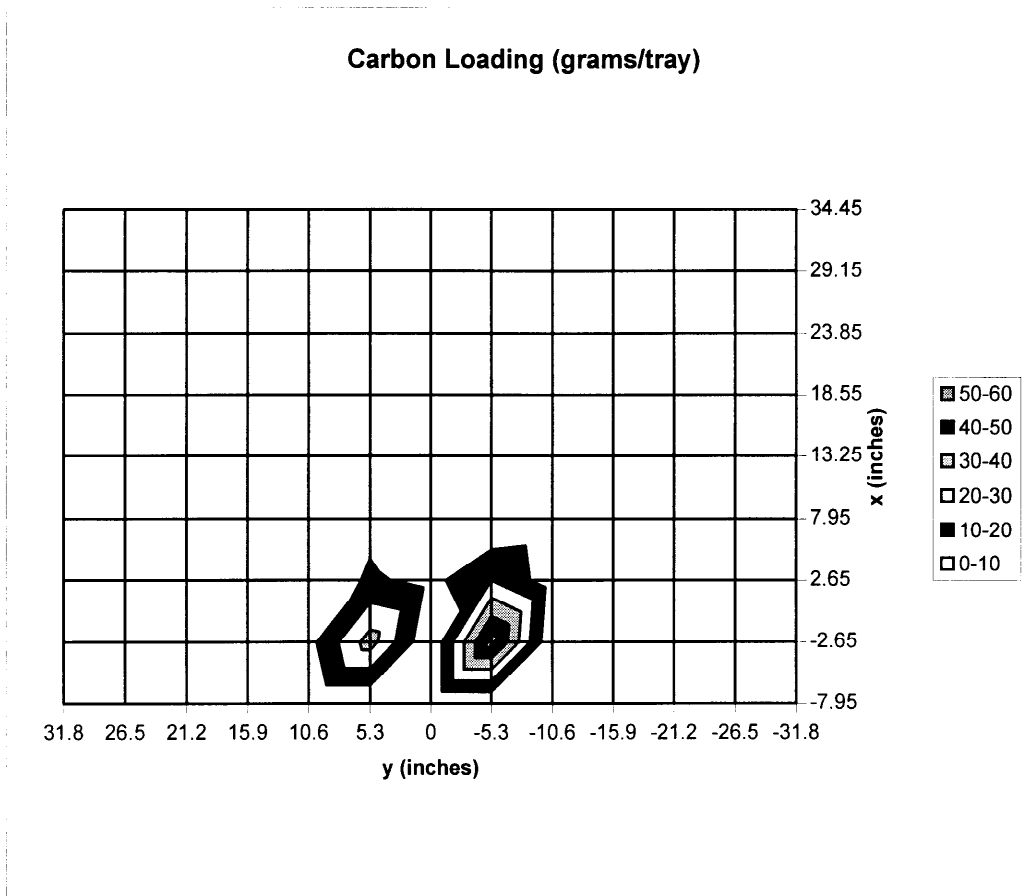
Test 22-Narrow Side

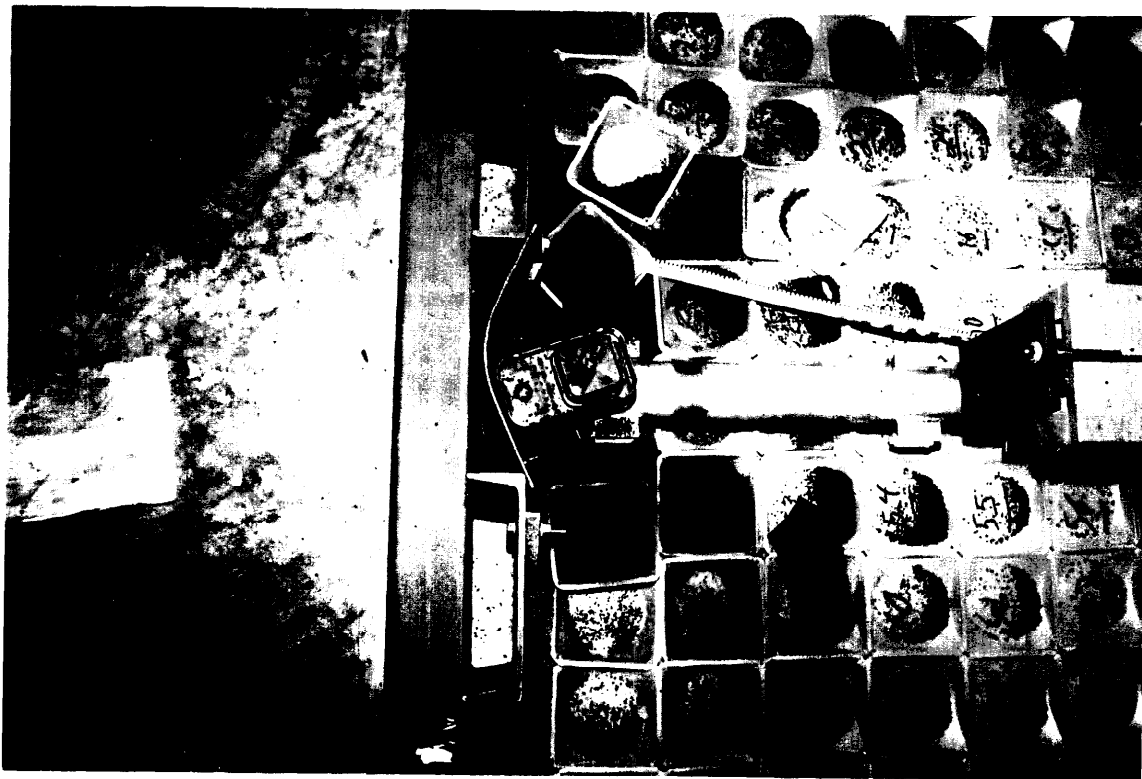
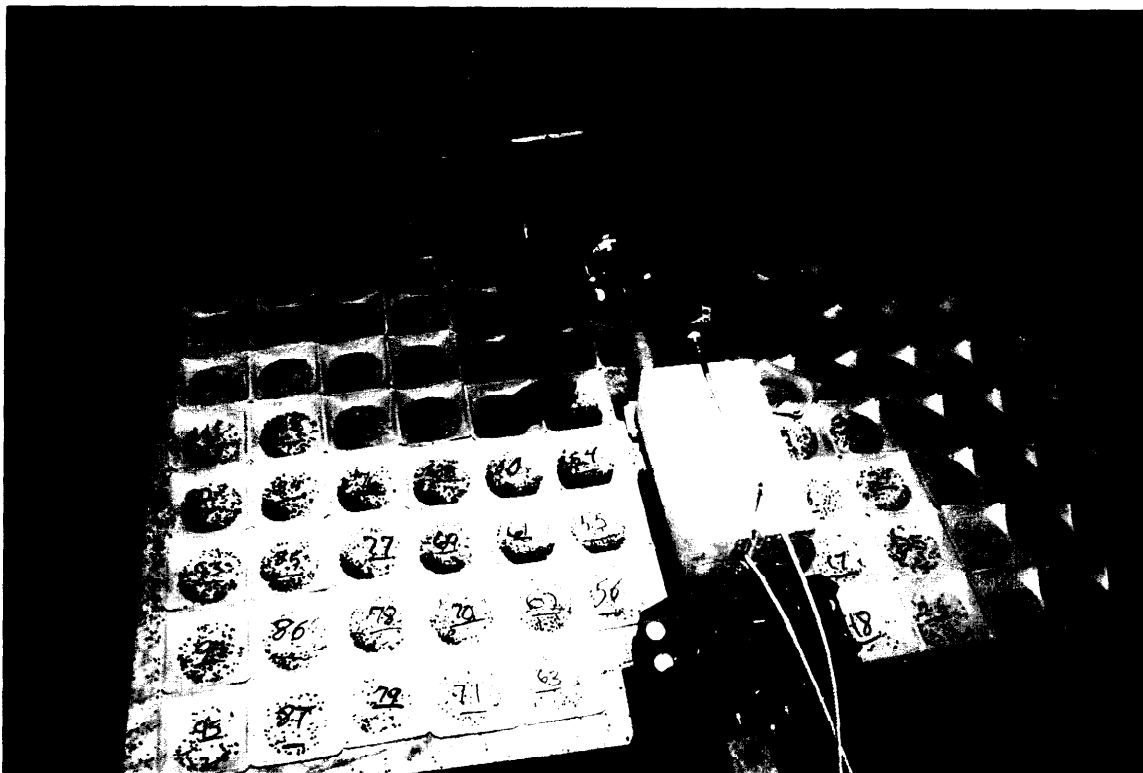
E = 985 ft-lbs

E/E_{min} = 6.26

x ==>	-7.95	-2.65	2.65	7.95	13.25	18.55	23.85	29.15	34.45
-31.8	0	0	0	0.9	1.5	0	0	0	0
-26.5	0	0	0	1	1.1	0.8	0	0	0
-21.2	0	1.2	1.1	1.5	1.2	0.9	0	0	0
-15.9	0	1.7	1.6	1.6	1.2	1.1	0	0	0
-10.6	0	0	4.2	2.2	1.7	1.3	0	0	0
-5.3	0	54.6	20	0	3.9	0.8	0	0	0
0	0	0	6.7	0	0.8	0	0	0	0
5.3	0	34.5	11.7	6.9	1.7	0	0	0	0
10.6	0	6.4	0	0	0	0	0	0	0
15.9	0	0	2.2	1.6	1.1	0	0	0	0
21.2	0	0	1.6	1.3	1.4	0.9	0	0	0
26.5	0	0	1	0	0.9	1.1	1.3	1.6	0
31.8	0	0	1.3	0	0	0	2.1	2.8	0

Total 198





Test 22:
Narrow Side Impact

Test 23-Narrow Side

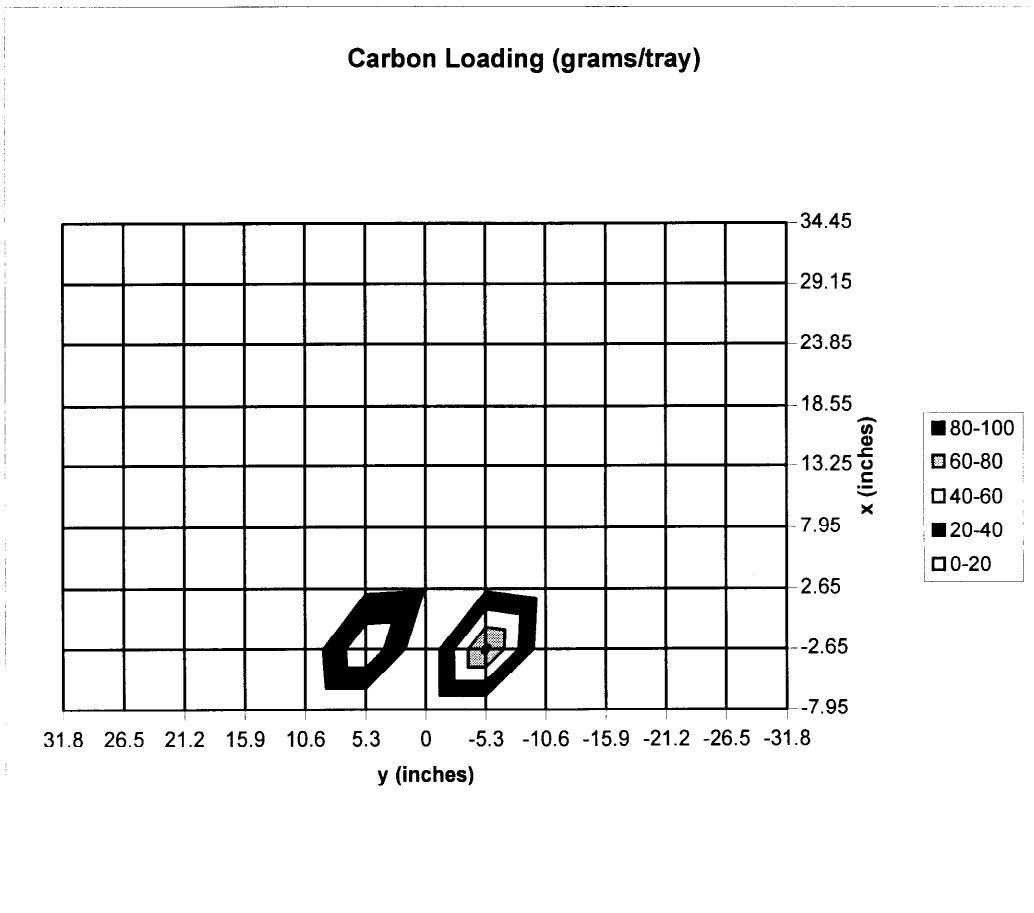
E = 985 ft-lbs

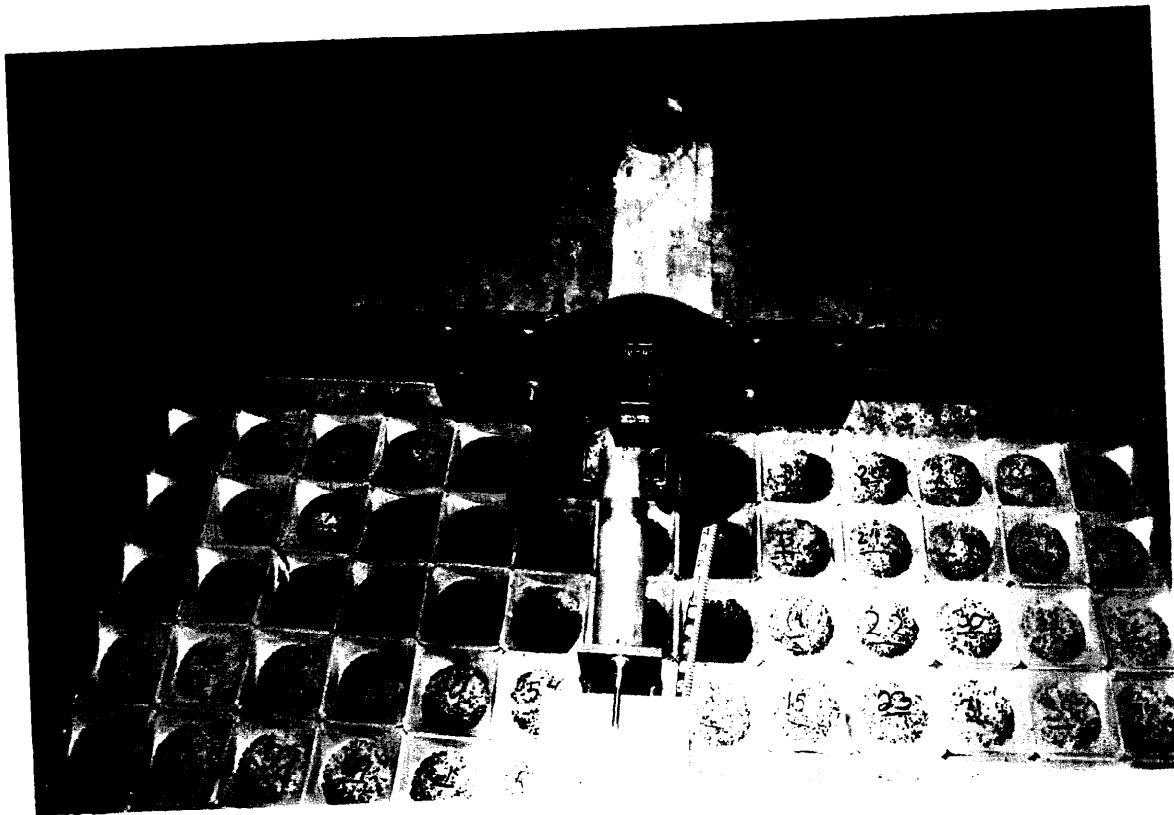
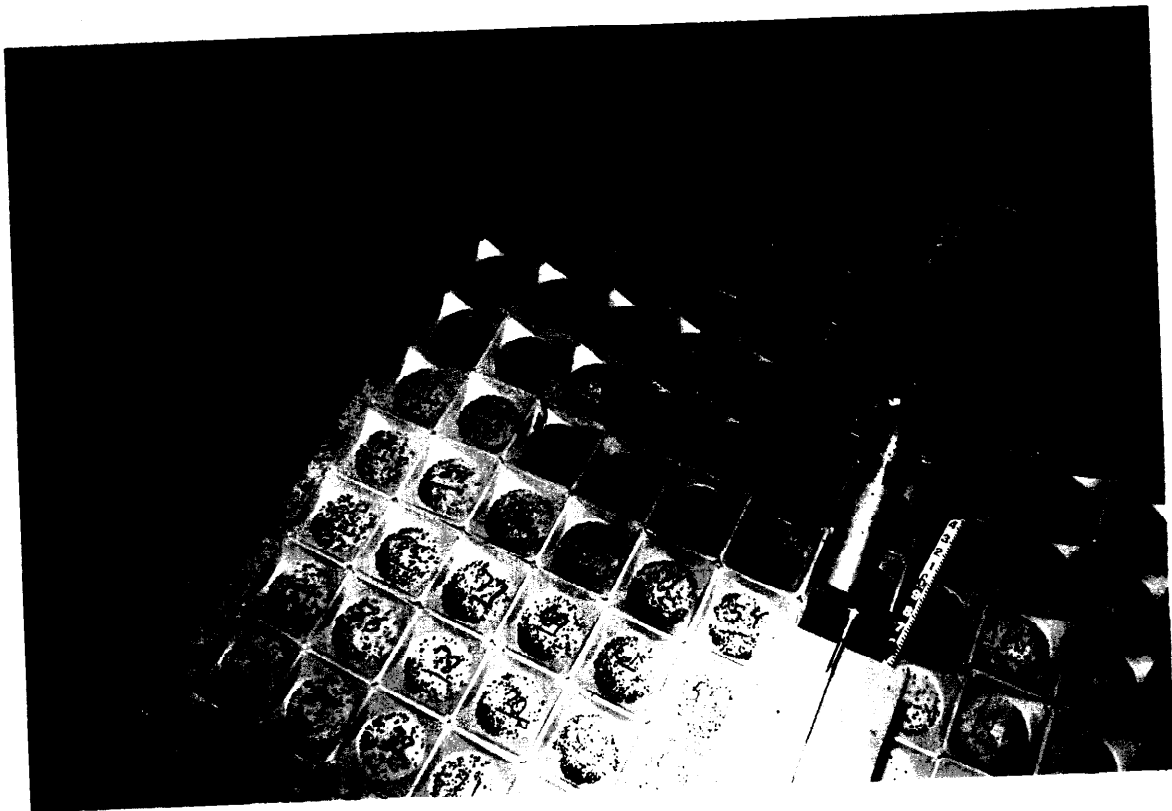
E/E_{min} = 6.26

x ==>	-7.95	-2.65	2.65	7.95	13.25	18.55	23.85	29.15	34.45
-31.8	0	0	0	0	0	0	0.8	0	0
-26.5	0	0	0	0	0.7	1.1	1	0	0
-21.2	0	1.7	0	1.3	1.6	1.3	0.5	0	0
-15.9	0	1.7	2.6	2.8	2	1	0.8	0	0
-10.6	0	3.4	8.2	4.7	1.8	1	1	0	0
-5.3	0	85	16.8	7.9	0	0	0	0	0
0	0	0	18.7	7.7	0	0	0	0	0
5.3	0	57.8	16.4	8.9	0	0	0	0	0
10.6	0	4.1	0	0	0	0	0	0	0
15.9	0	2.2	0	0	0	0	0	0	0
21.2	0	1.3	0	0	0	0	0	0	0
26.5	0	0	0	0	0	0	0	0	0
31.8	0	0	0	0	0	0	0	0	0

y

Total 267.8





**Test 23:
Narrow Side Impact**

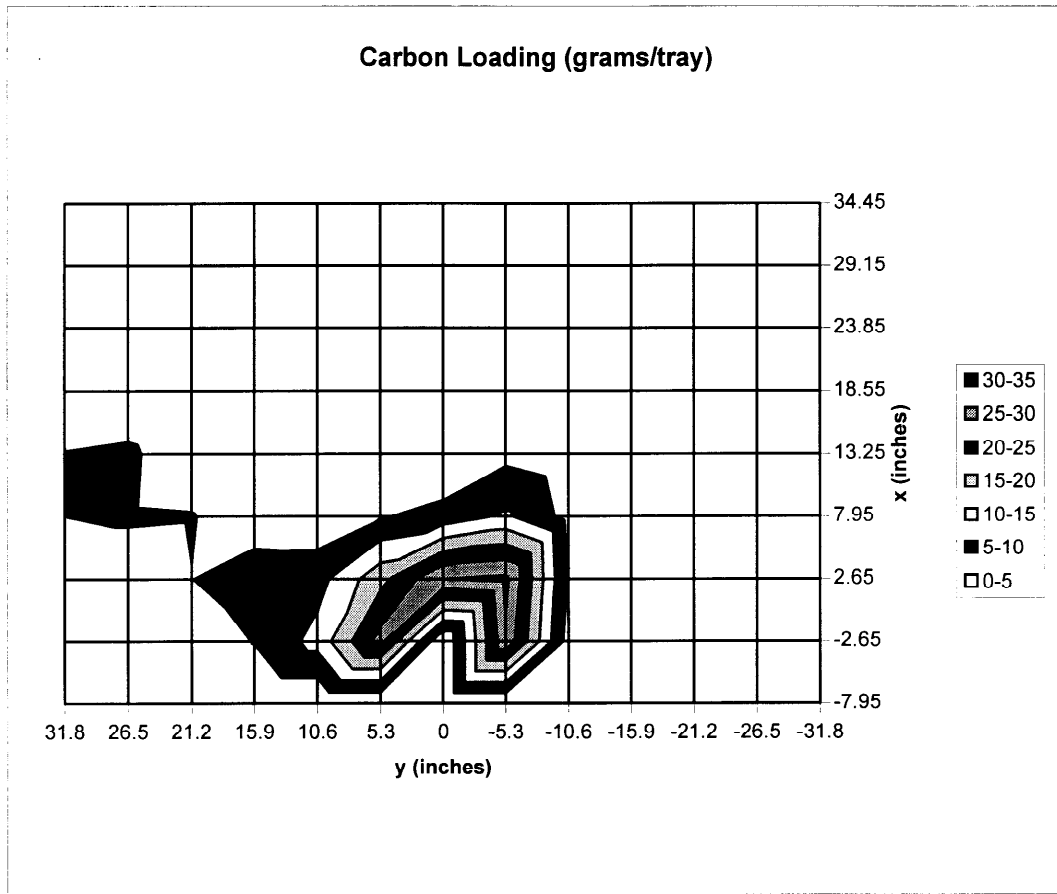
Test 24-Narrow Side

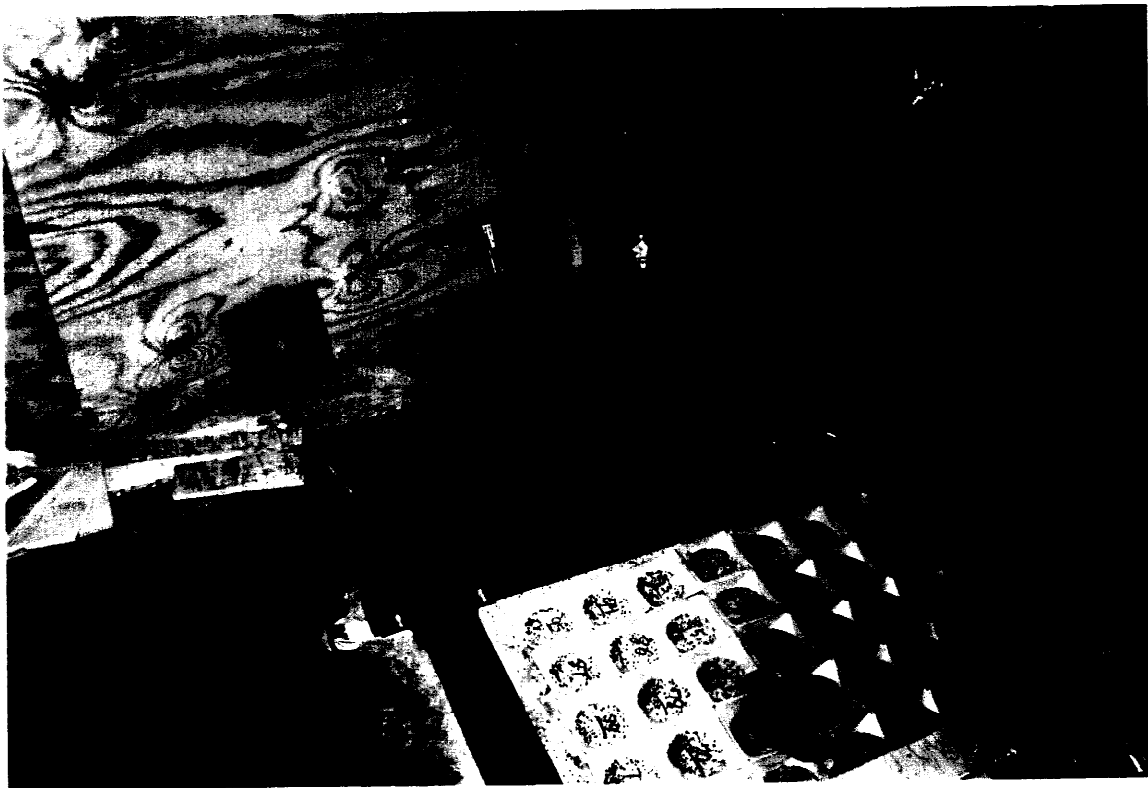
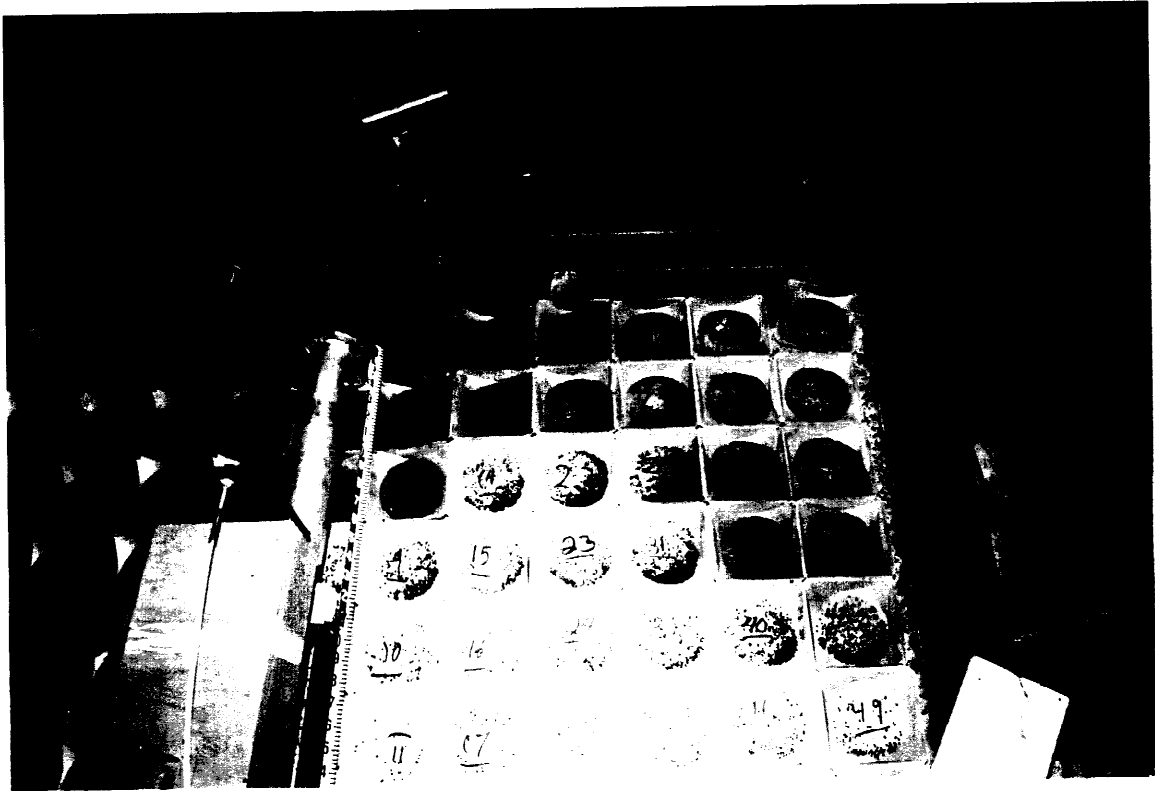
E = 958 ft-lbs

E/E_{min} = 6 10

x ==>	-7.95	-2.65	2.65	7.95	13.25	18.55	23.85	29.15	34.45
-31.8	0	0	1.1	1.1	1.4	0	0	0	0
-26.5	0	0	1.1	1.6	0.8	0	0	0	0
-21.2	0	0	1.8	1.5	0.9	1	0.5	0	0
-15.9	0	0	2.6	1.7	1.2	1	0	0	0
-10.6	0	2.9	4.3	3.4	1.7	1.2	1.2	0	0
-5.3	0	28.9	31.1	10.8	3.6	1.4	0	0	0
0	0	0	29.8	6.8	0	0	0	0	0
5.3	0	26.9	18.5	4.6	0	0	0	0	0
10.6	0	11.8	8.1	1.4	0	0	0	0	0
15.9	0	5.2	7.9	1.8	0	0	0	0	0
21.2	0	1.6	4.9	5.3	1.6	0	0	0	0
26.5	0	0	2.1	5.6	5.9	1.2	0	0	0
31.8	0	2.1	2.3	5	5.2	1.6	0	0	0

Total 277





**Test 24:
Narrow Side Impact**

Appendix B

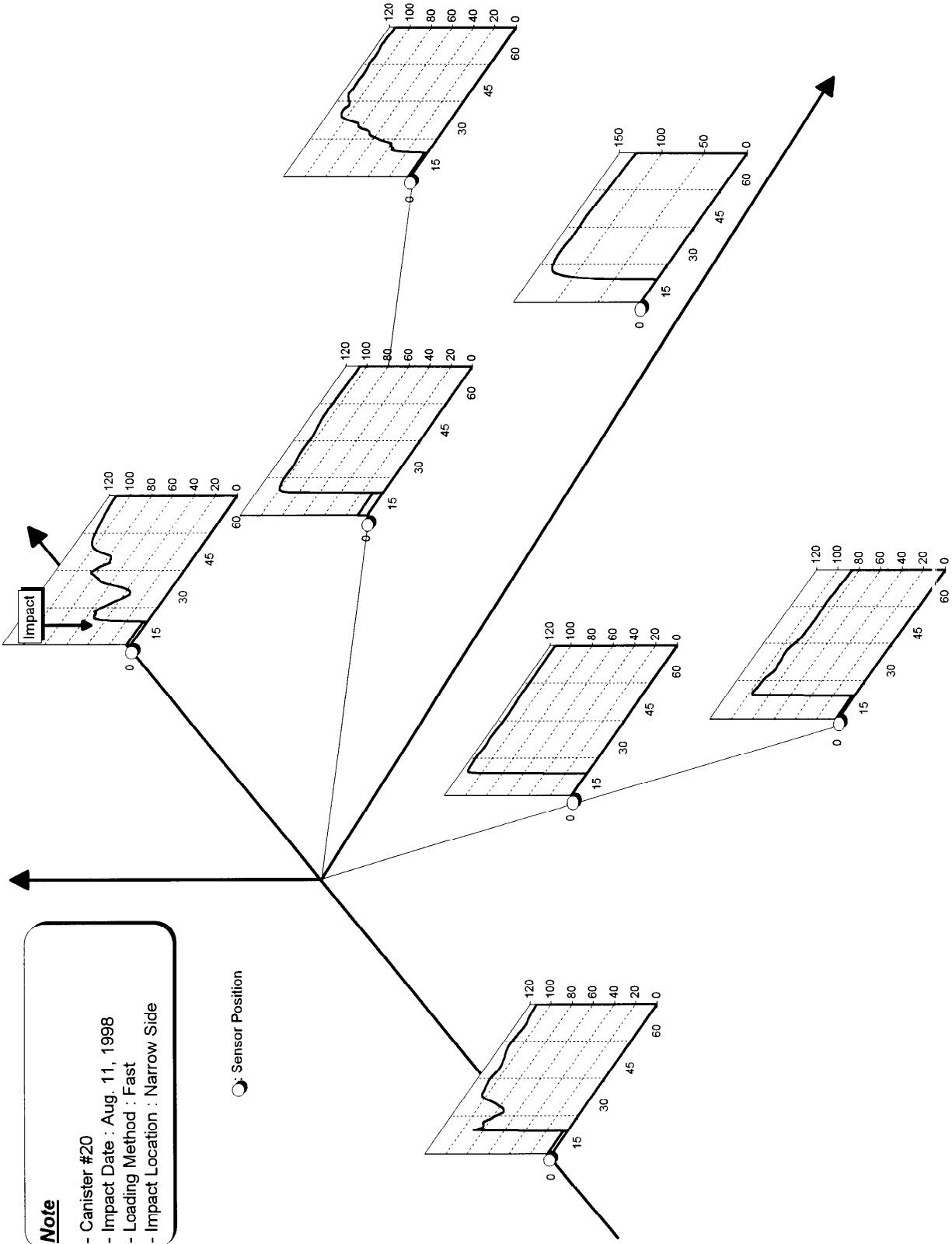
Results from Vapor Concentration Measurement after Canister Rupture Tests

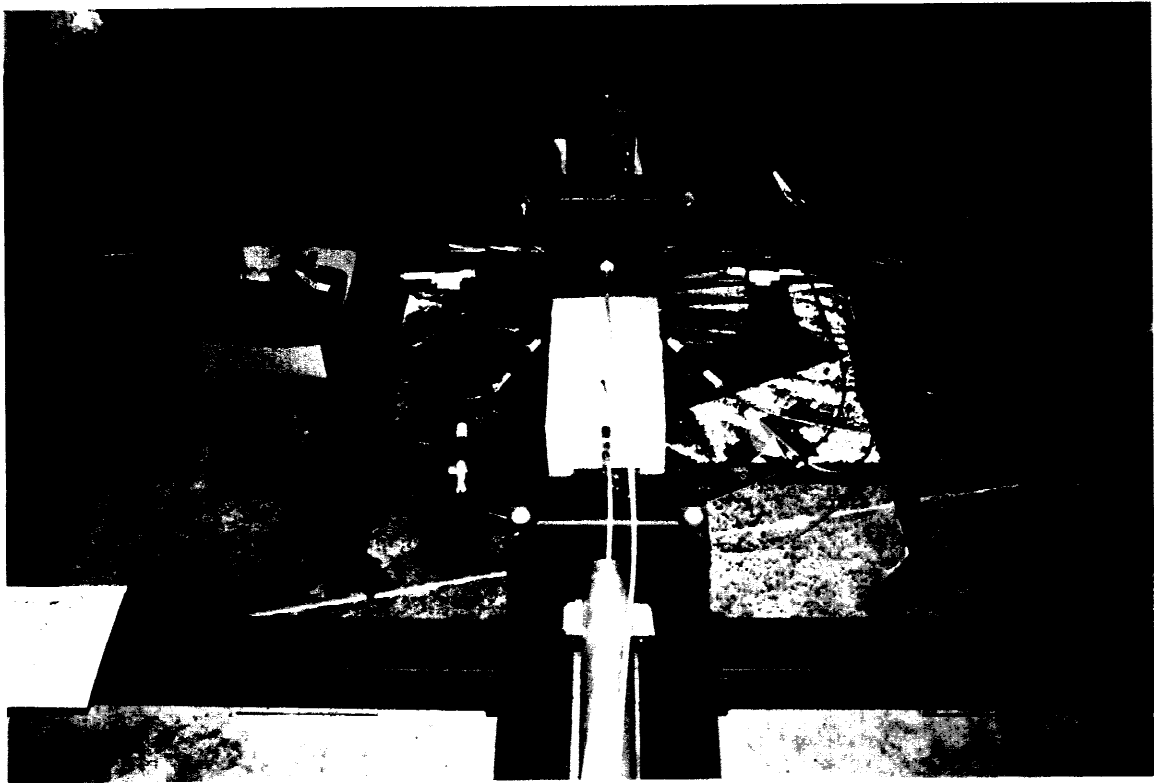
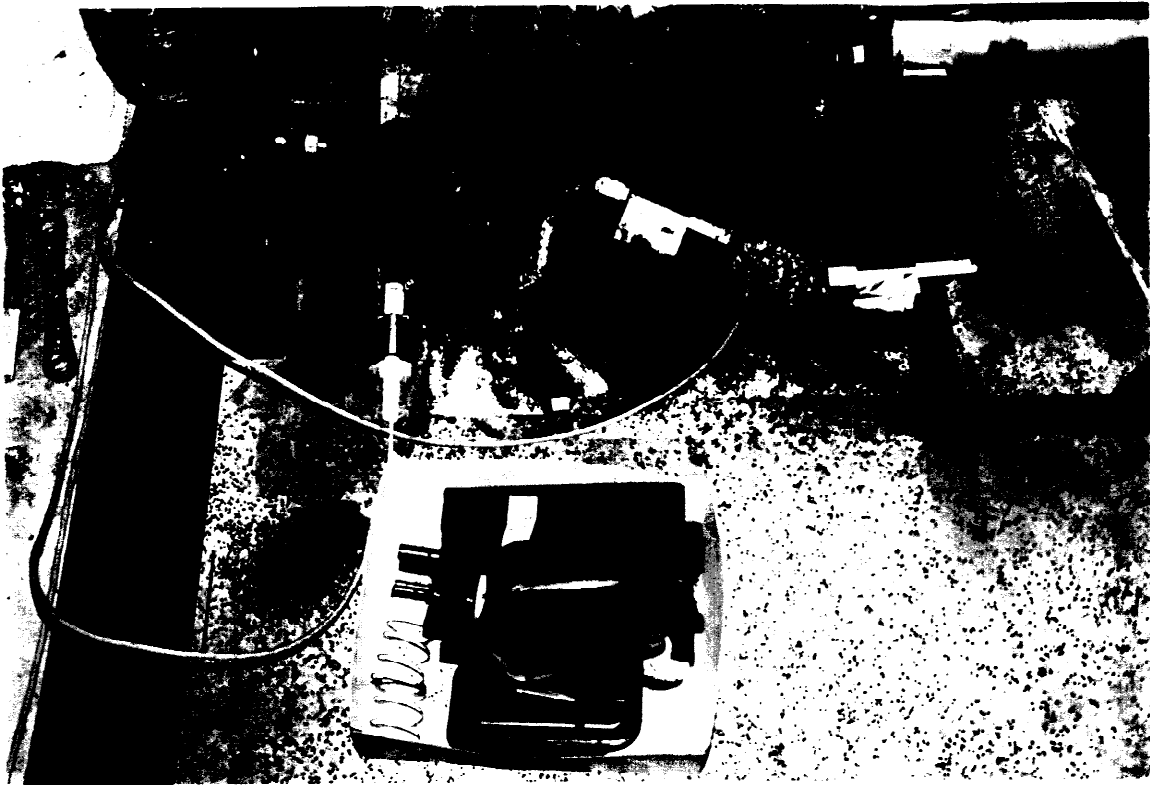
Summary of Vapor Concentration Measurement Test Configurations				
Date	Canister Number	Loading Method	Impact Location	Comments
8/11/98	20	Fast	Narrow Side	
"	21	Fast	Narrow Side	
"	22	Fast	Narrow Side	
8/20/98	23	Slow	Wide Side	
"	30	Slow	Wide Side	
"	31	Slow	Narrow Side	
9/3/98	24	Slow	Bottom	
"	25	Fast	Bottom	
"	27	Fast	Bottom	
9/11/98	32	Fast	Wide Side	Steady Wind 0-50 ft/min Wind Gusts to 200 ft/min
"	28	Fast	Narrow Side	Steady Wind <20 ft/min Wind Gusts 50-100 ft/min

Note

- Canister #20
- Impact Date : Aug. 11, 1998
- Loading Method : Fast
- Impact Location : Narrow Side

○ Sensor Position



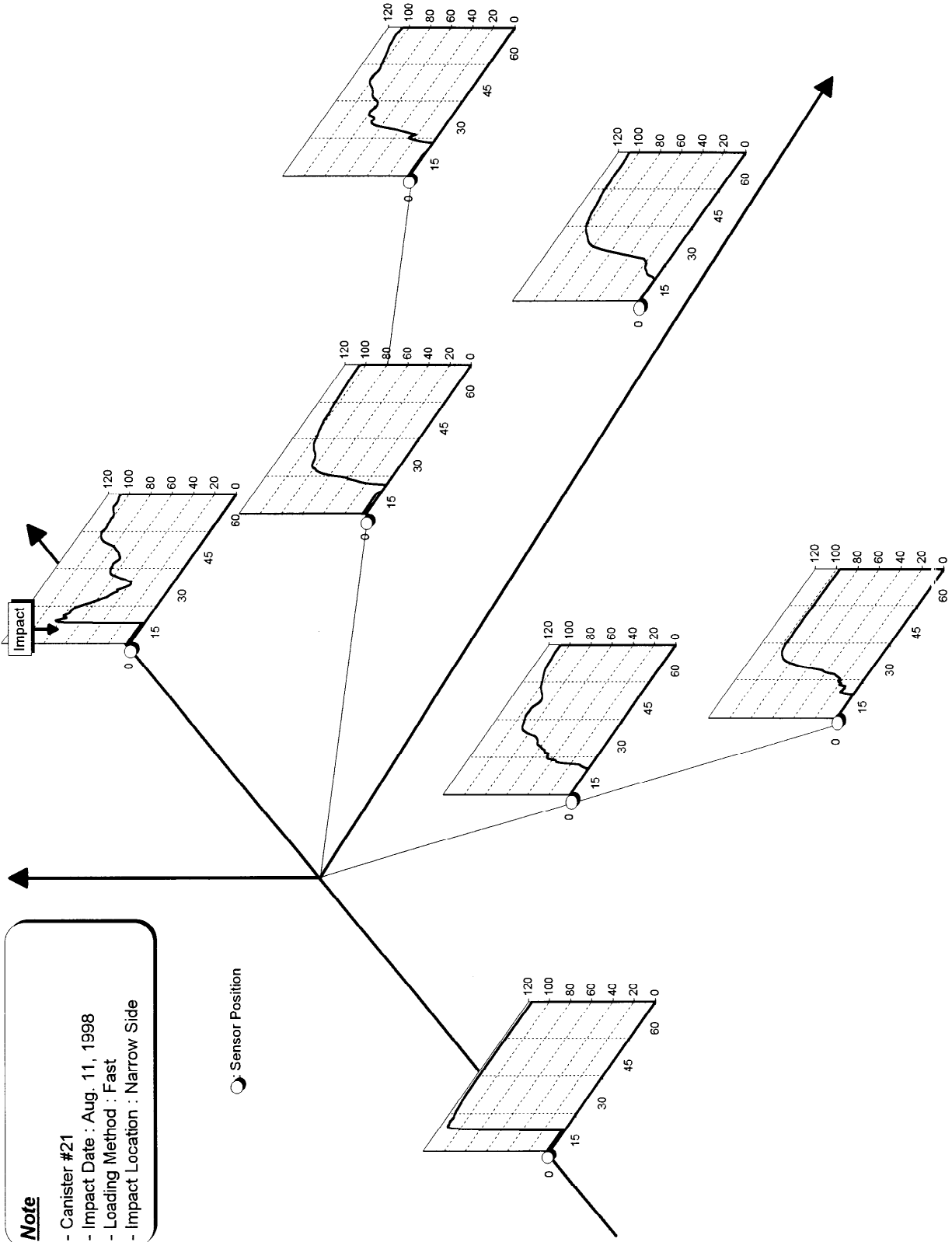


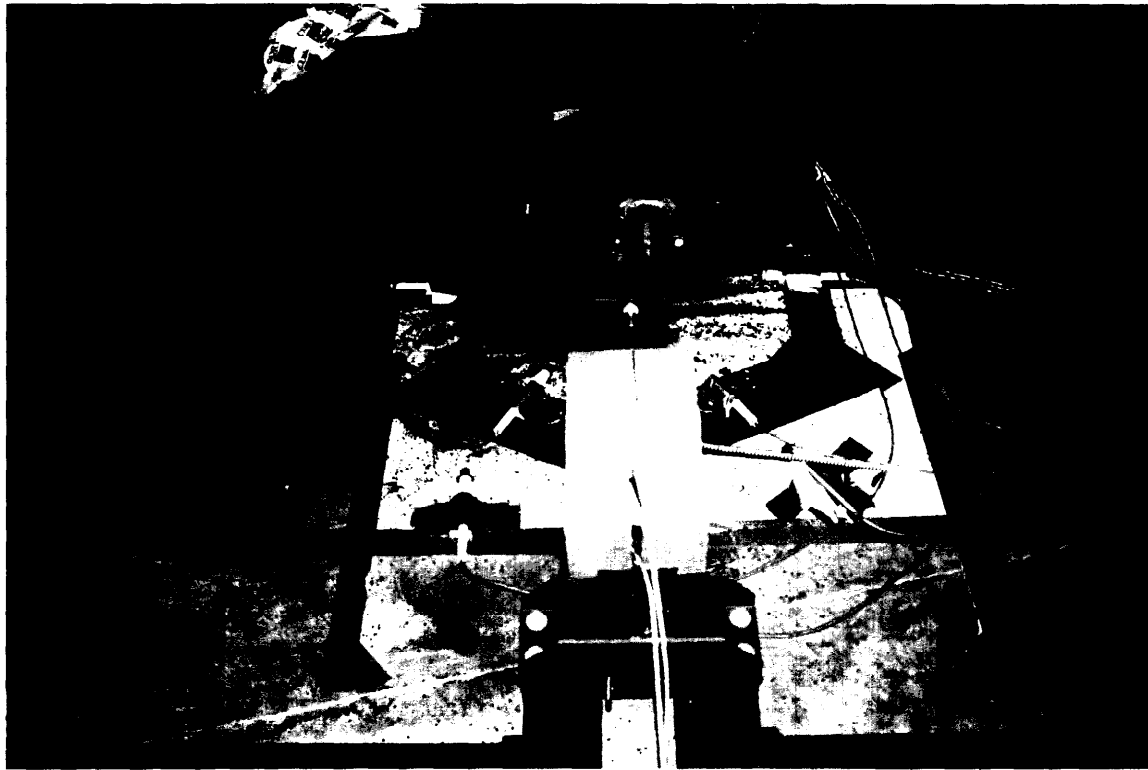
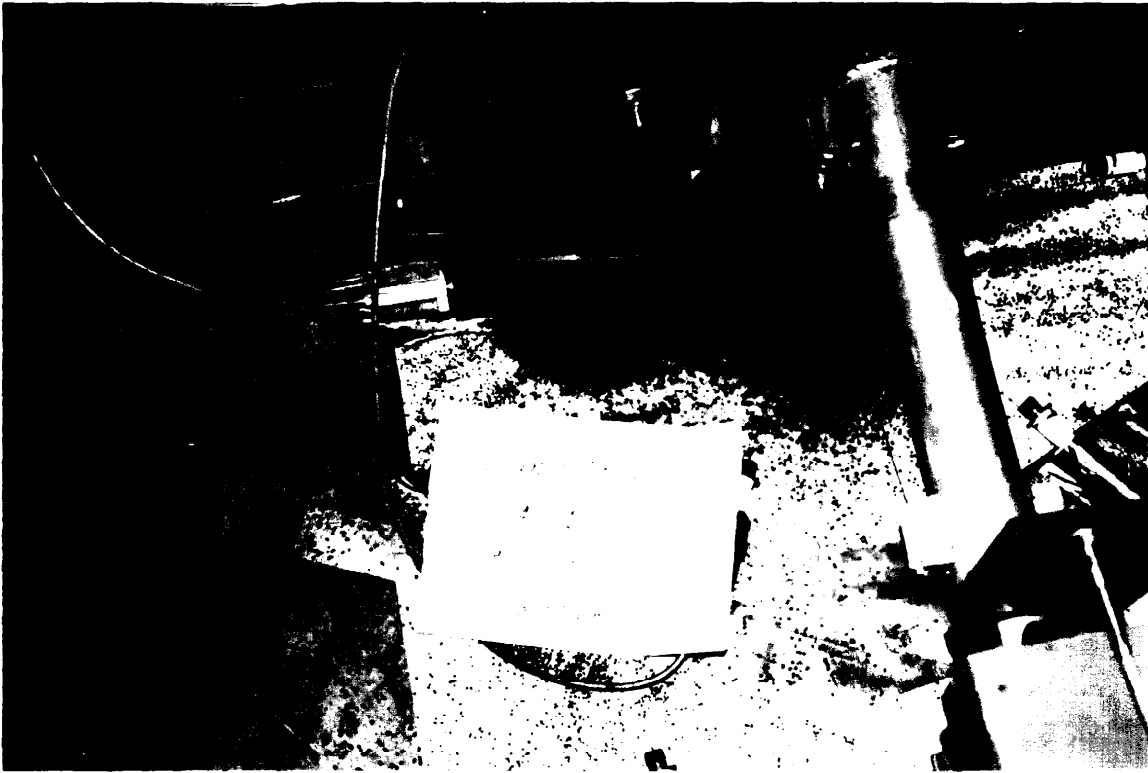
**Canister #20:
Narrow Side Impact
Fast Loading Method**

Note

- Canister #21
- Impact Date : Aug. 11, 1998
- Loading Method : Fast
- Impact Location : Narrow Side

○ Sensor Position



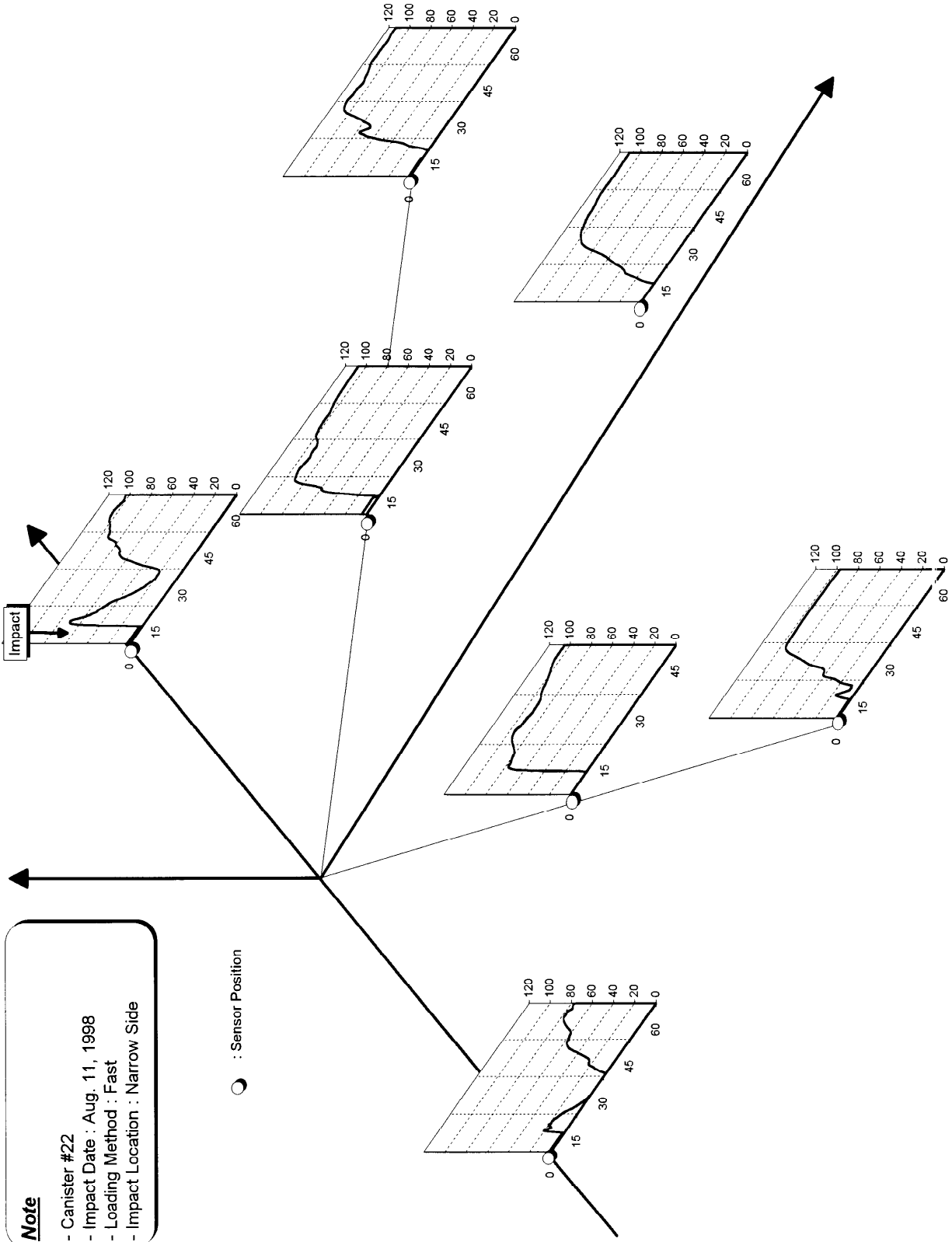


**Canister #21:
Narrow Side Impact
Fast Loading Method**

Note

- Canister #22
- Impact Date : Aug. 11, 1998
- Loading Method : Fast
- Impact Location : Narrow Side

○ : Sensor Position





Canister 22
1/98

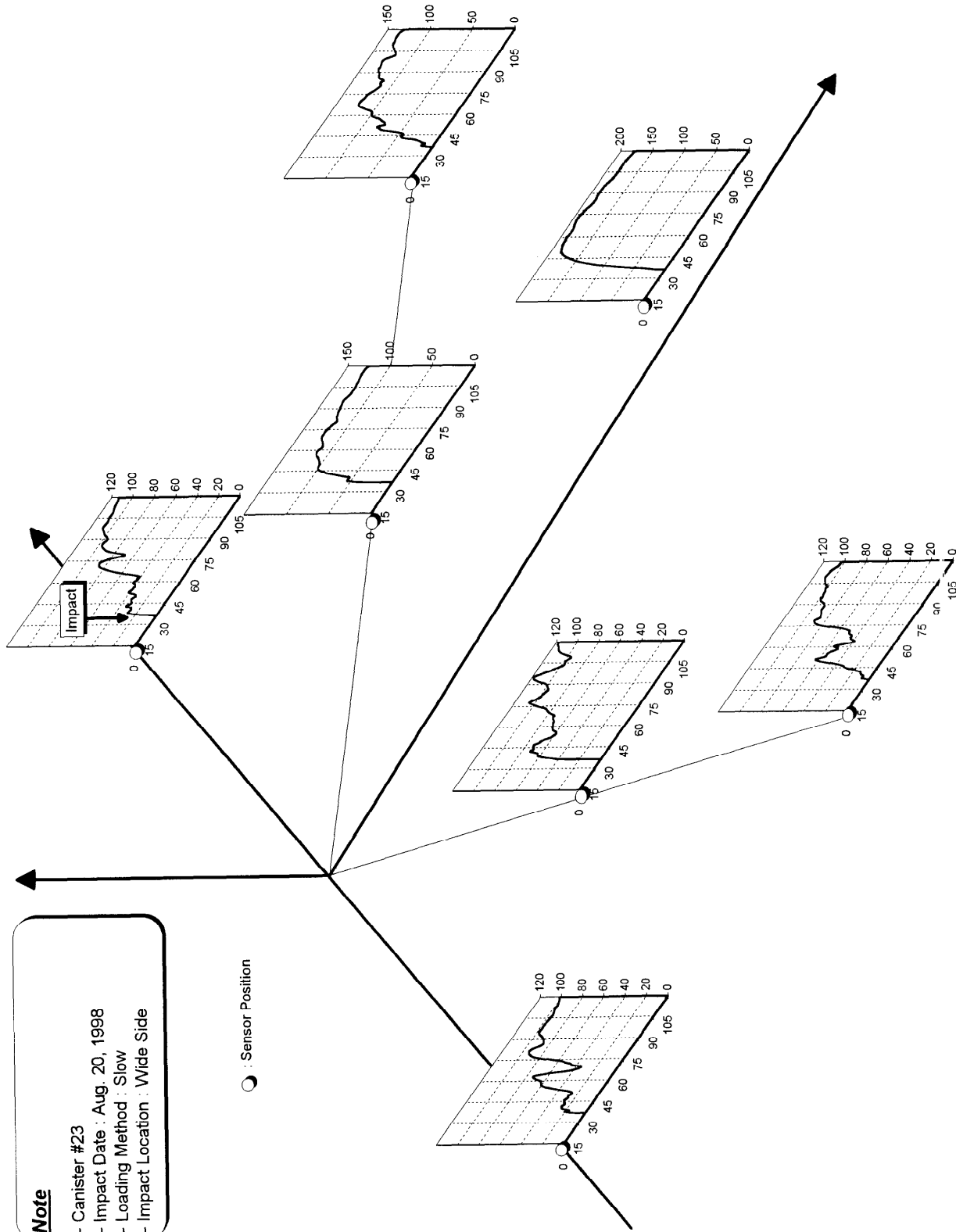


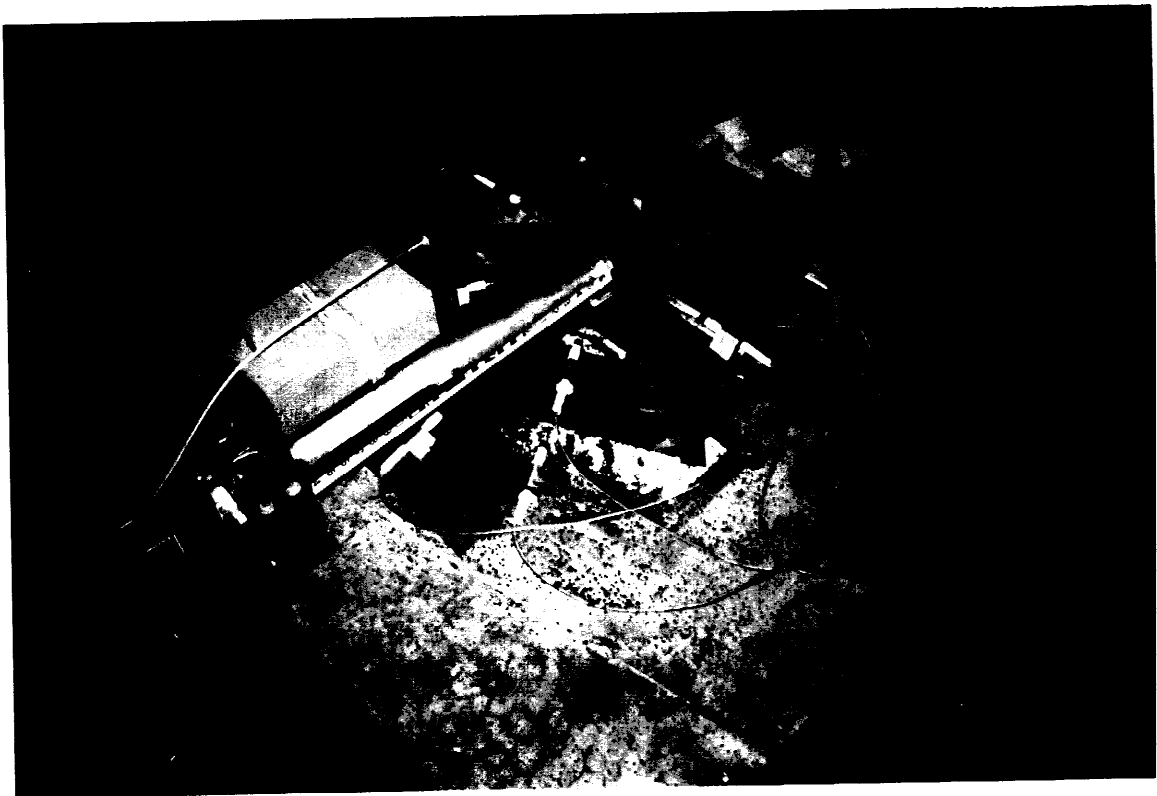
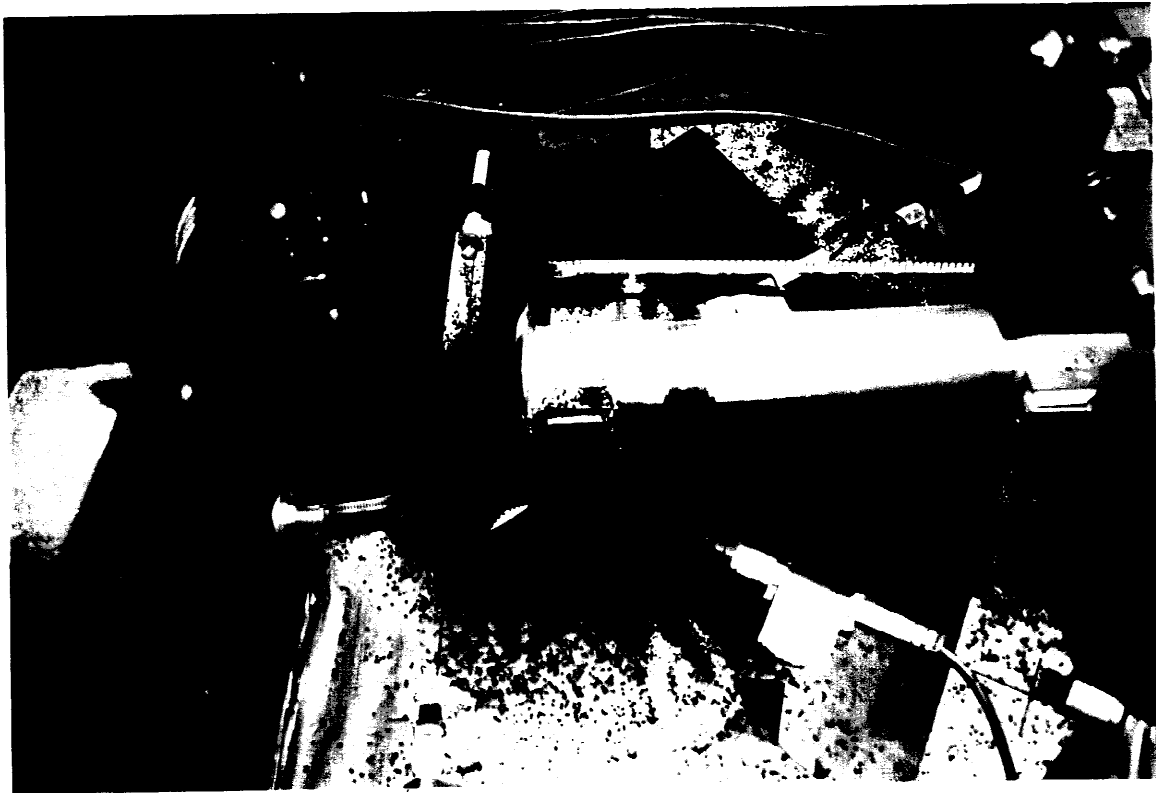
**Canister #22:
Narrow Side Impact
Fast Loading Method**

Note

- Canister #23
- Impact Date : Aug. 20, 1998
- Loading Method : Slow
- Impact Location : Wide Side

○ : Sensor Position



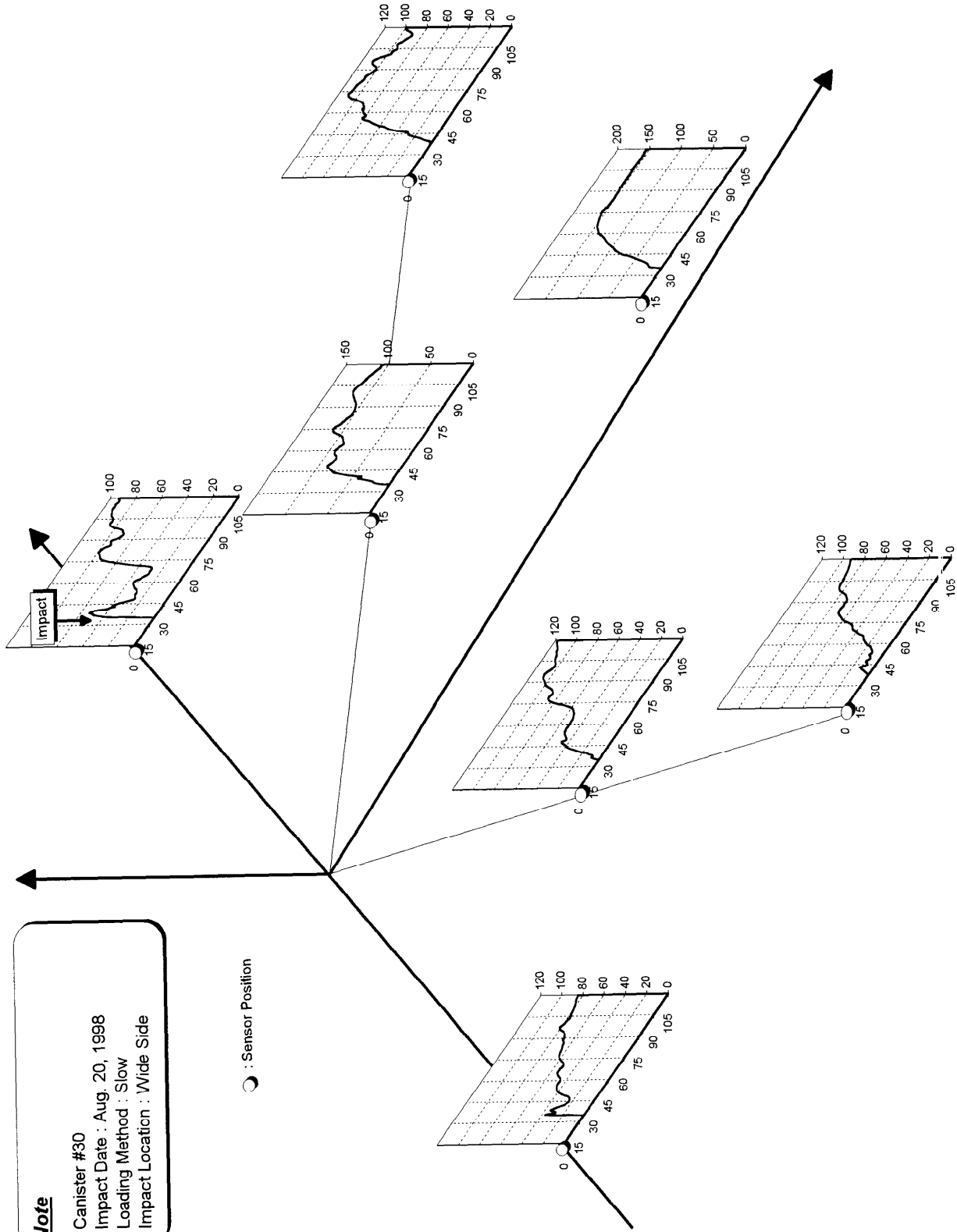


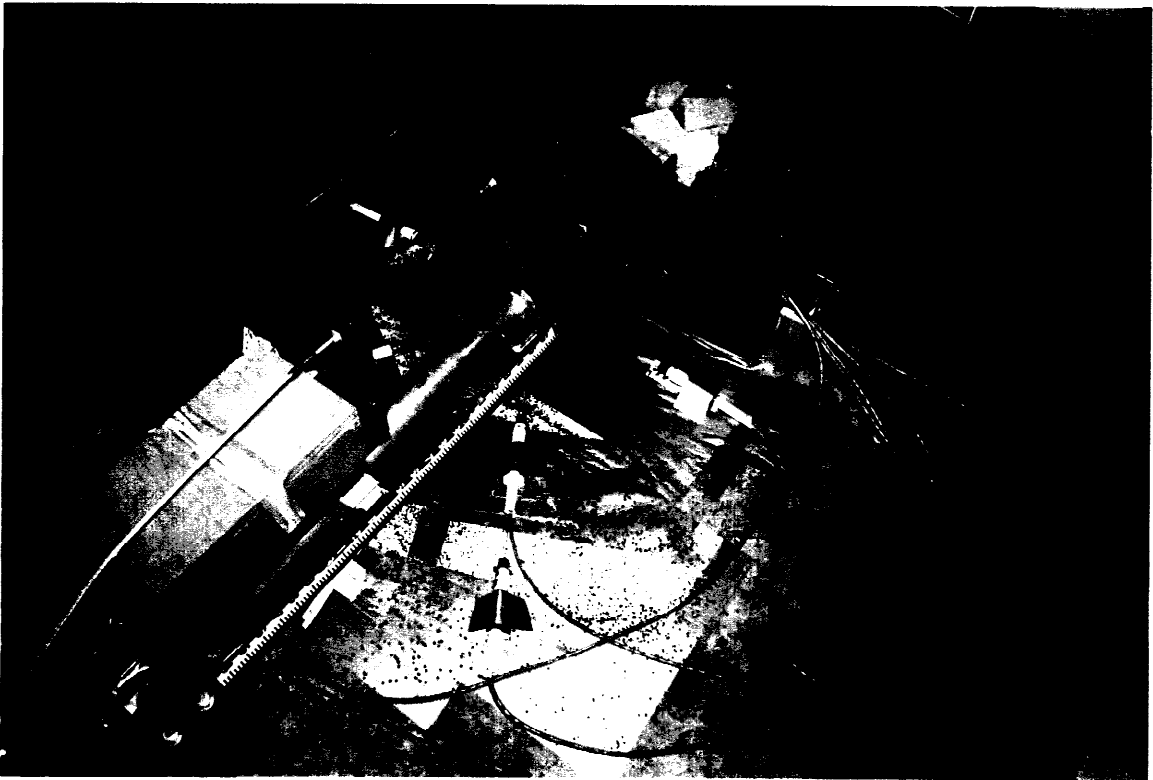
**Canister #23:
Wide Side Impact
Slow Loading Method**

Note

- Canister #30
- Impact Date : Aug. 20, 1998
- Loading Method : Slow
- Impact Location : Wide Side

○ : Sensor Position



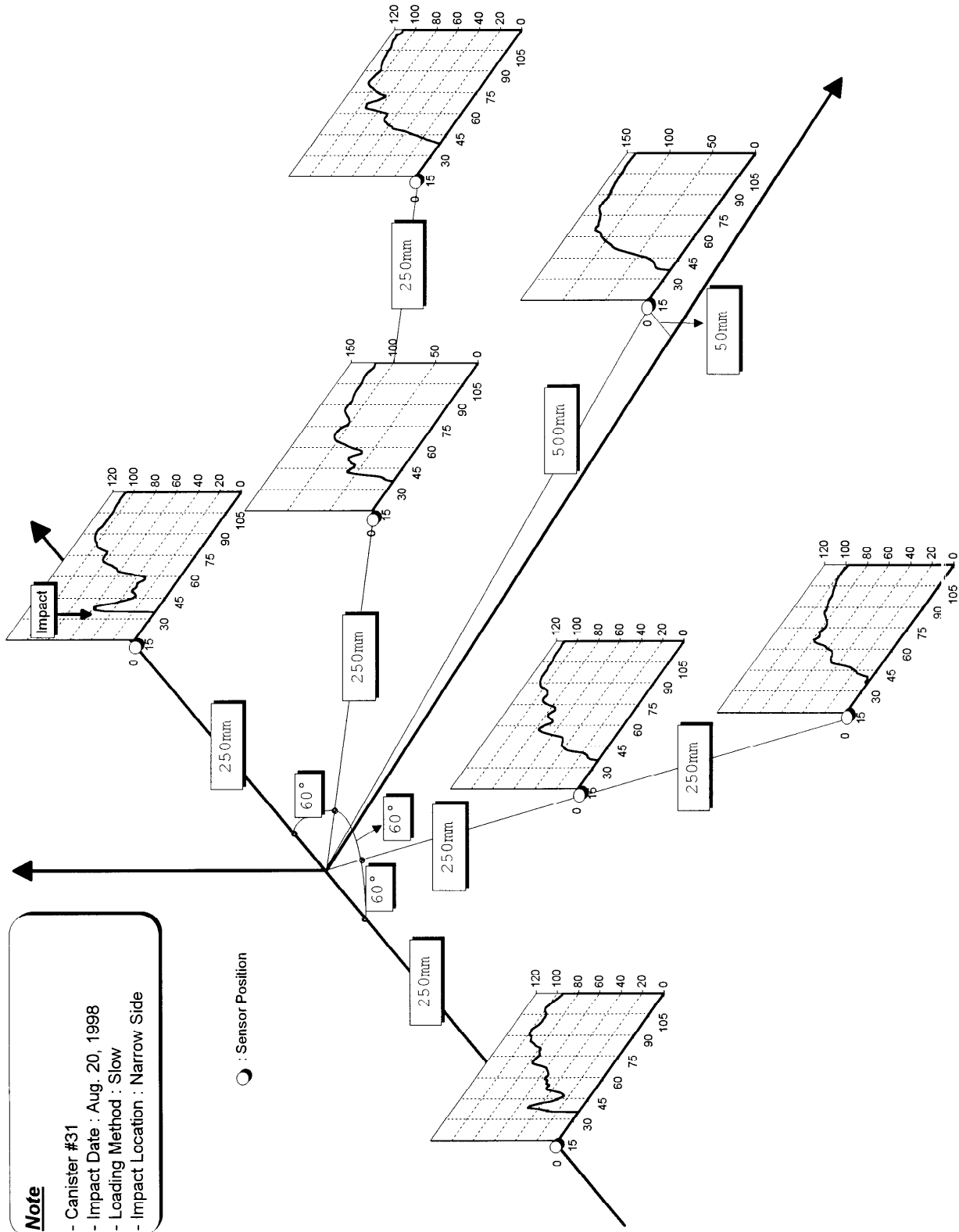


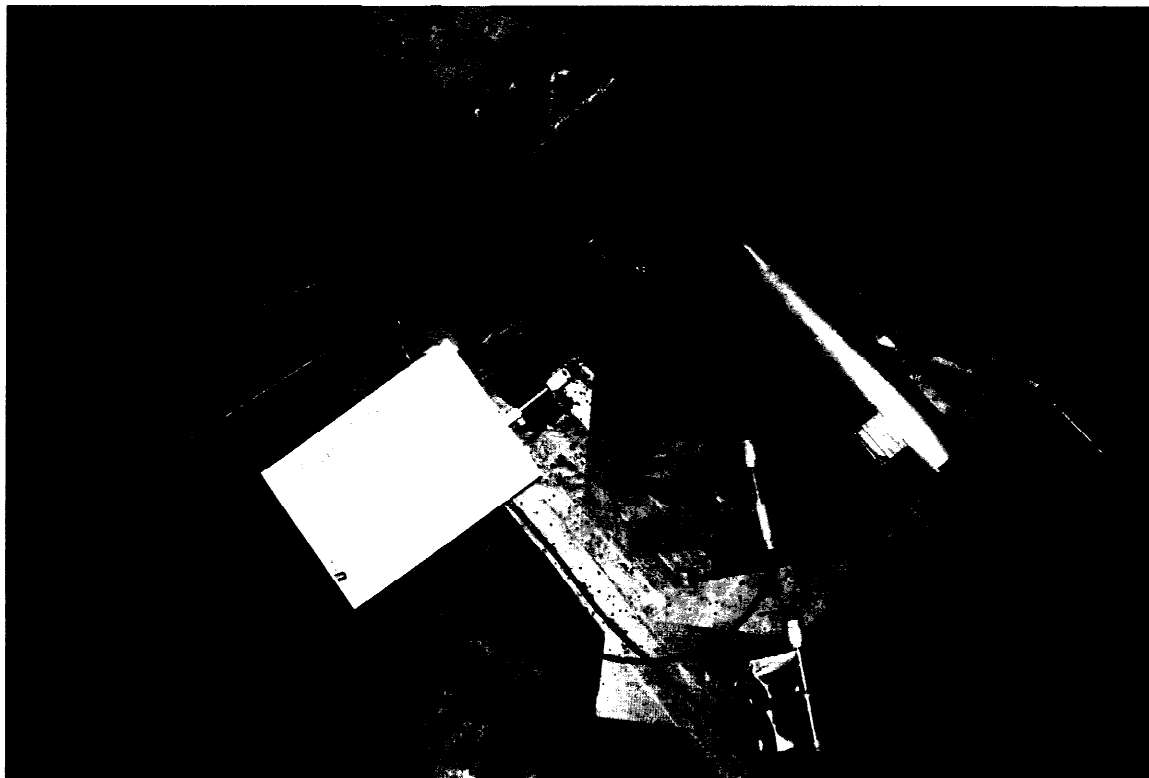
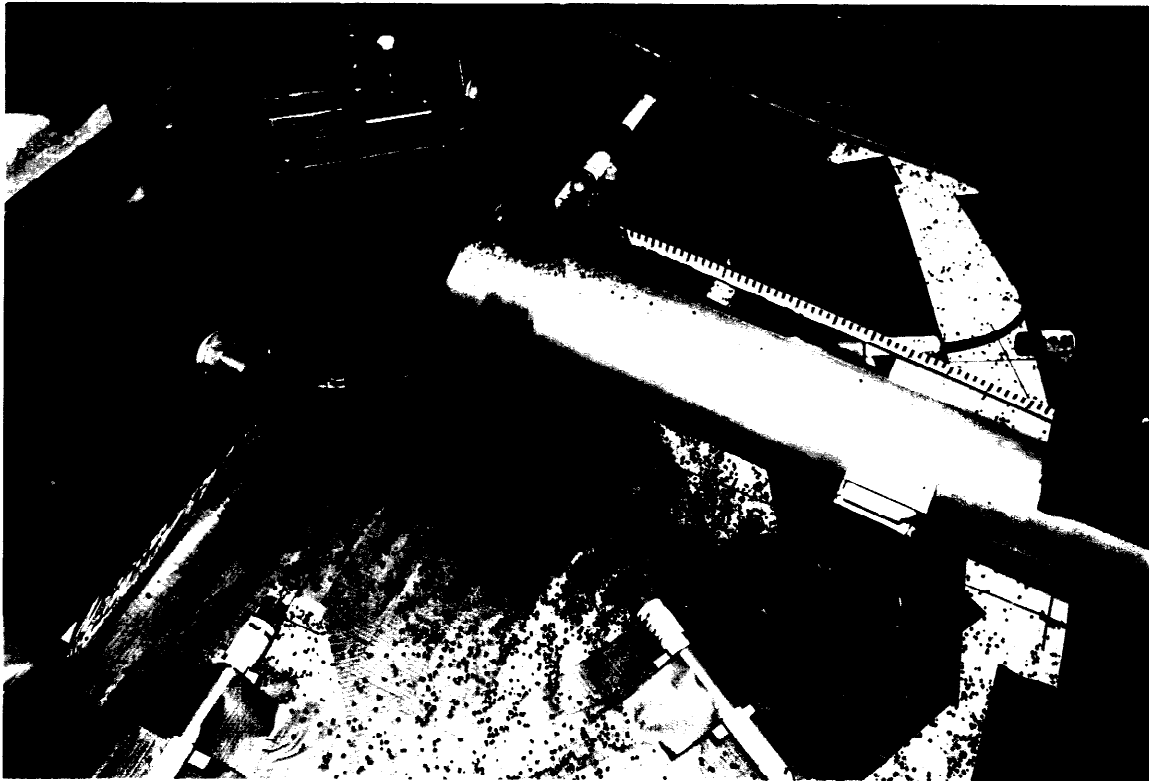
**Canister #30:
Wide Side Impact
Slow Loading Method**

Note

- Canister #31
- Impact Date : Aug. 20, 1998
- Loading Method : Slow
- Impact Location : Narrow Side

○ : Sensor Position



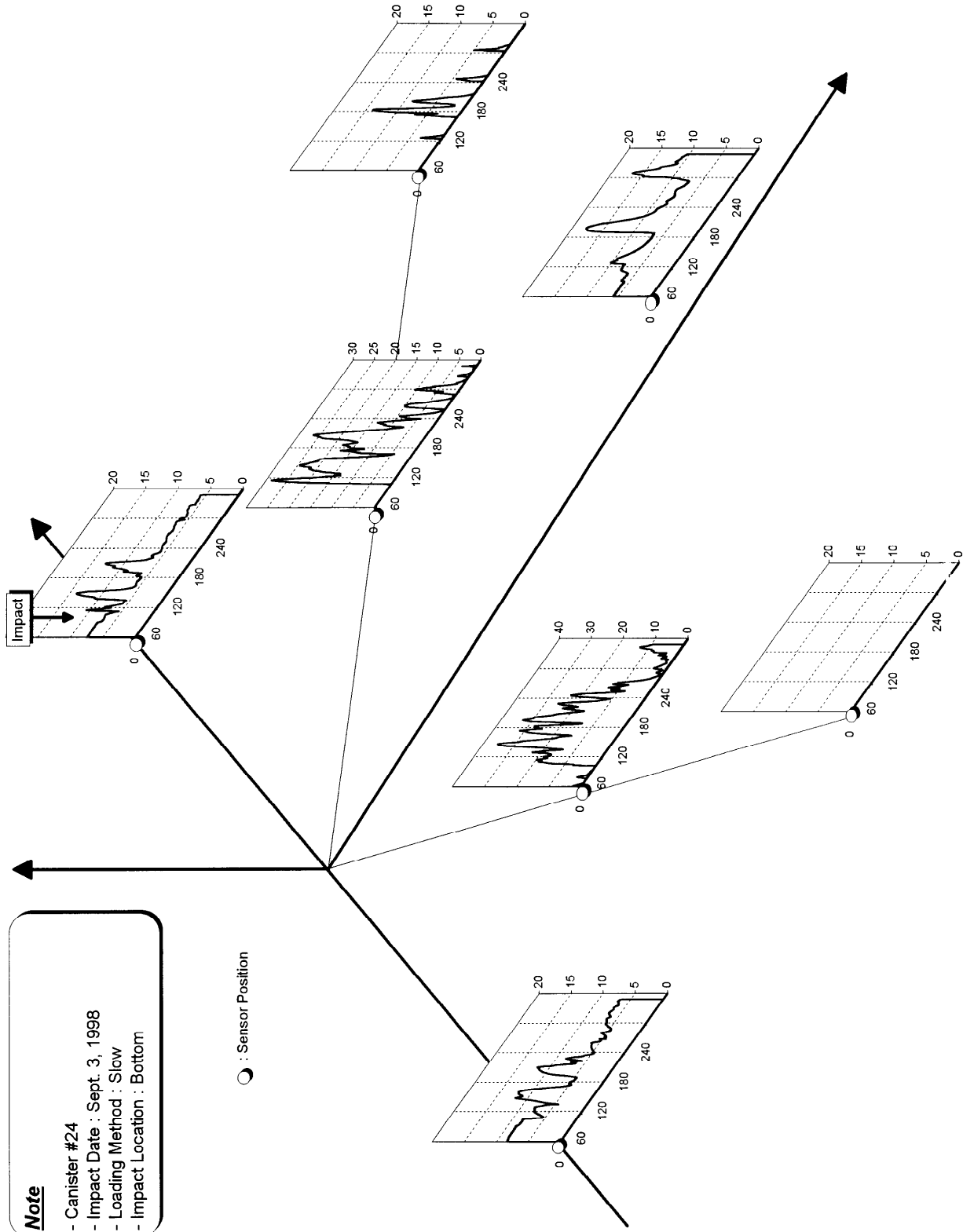


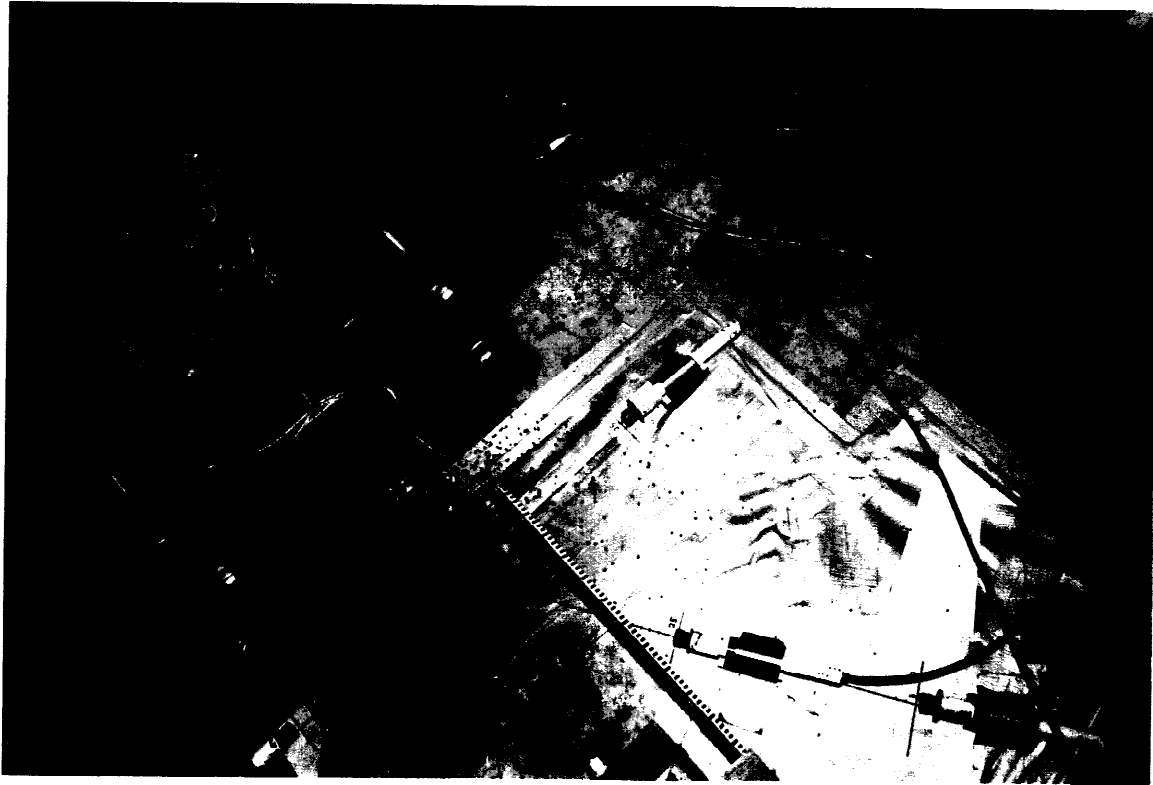
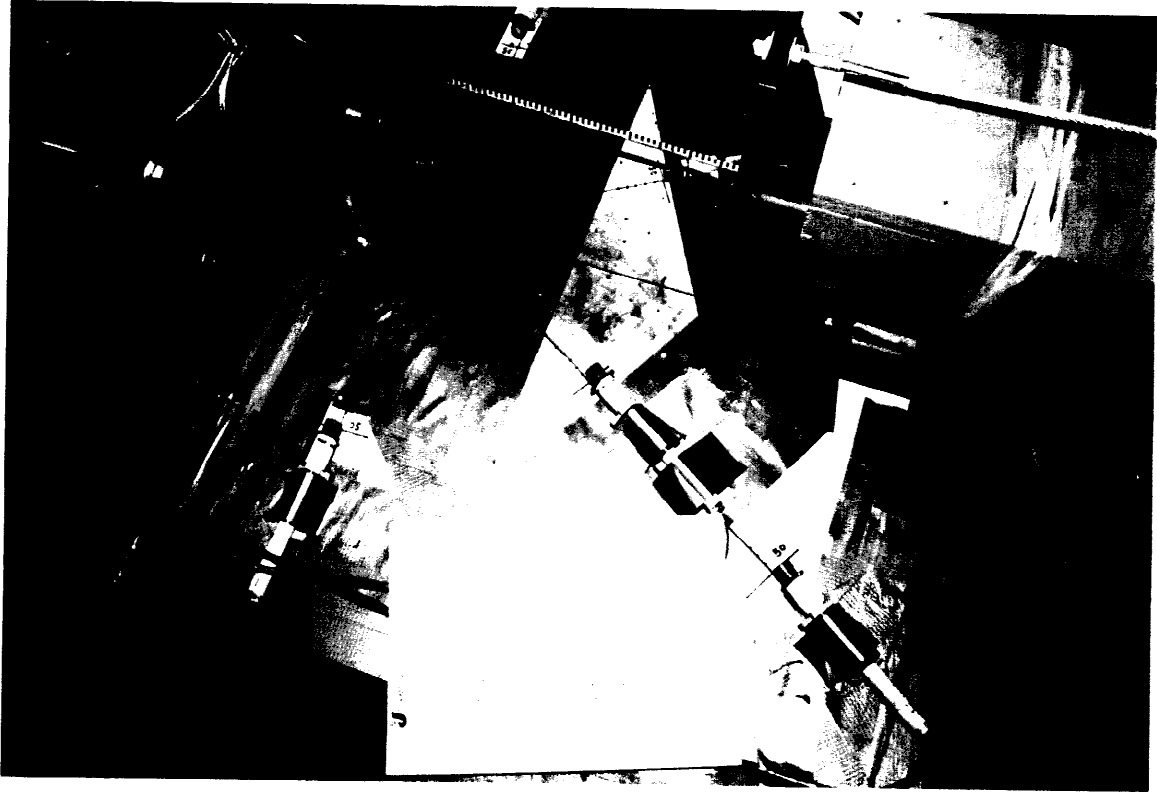
**Canister #31:
Narrow Side Impact
Slow Loading Method**

Note

- Canister #24
- Impact Date : Sept. 3, 1998
- Loading Method : Slow
- Impact Location : Bottom

○ : Sensor Position



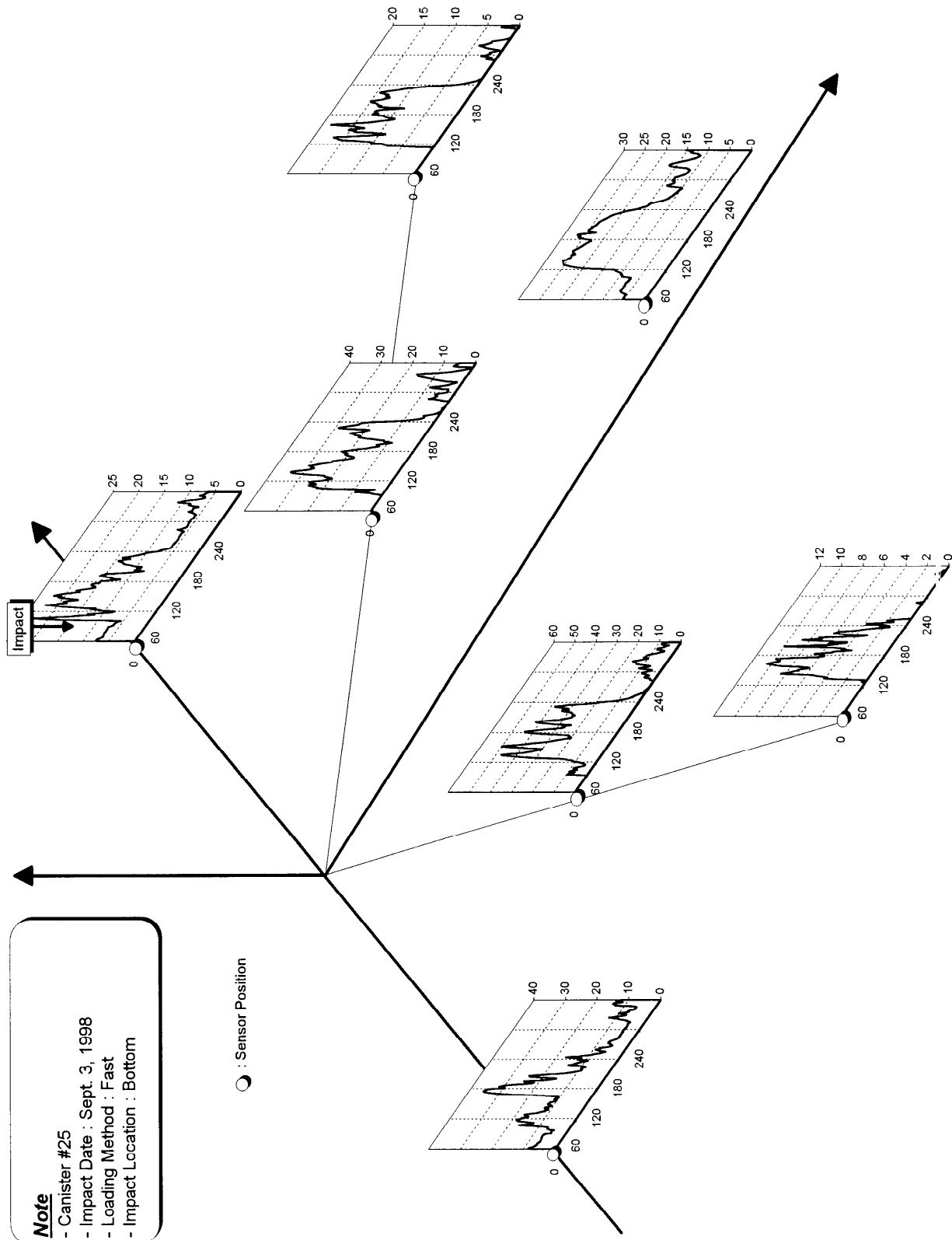


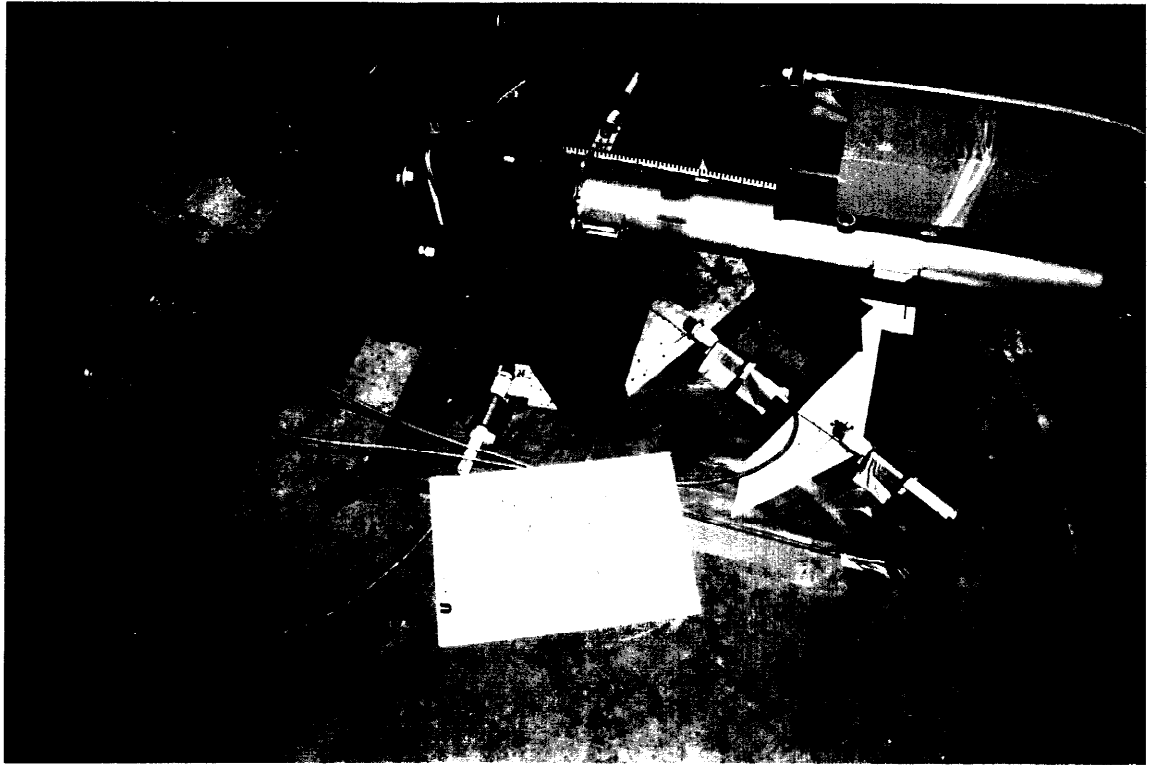
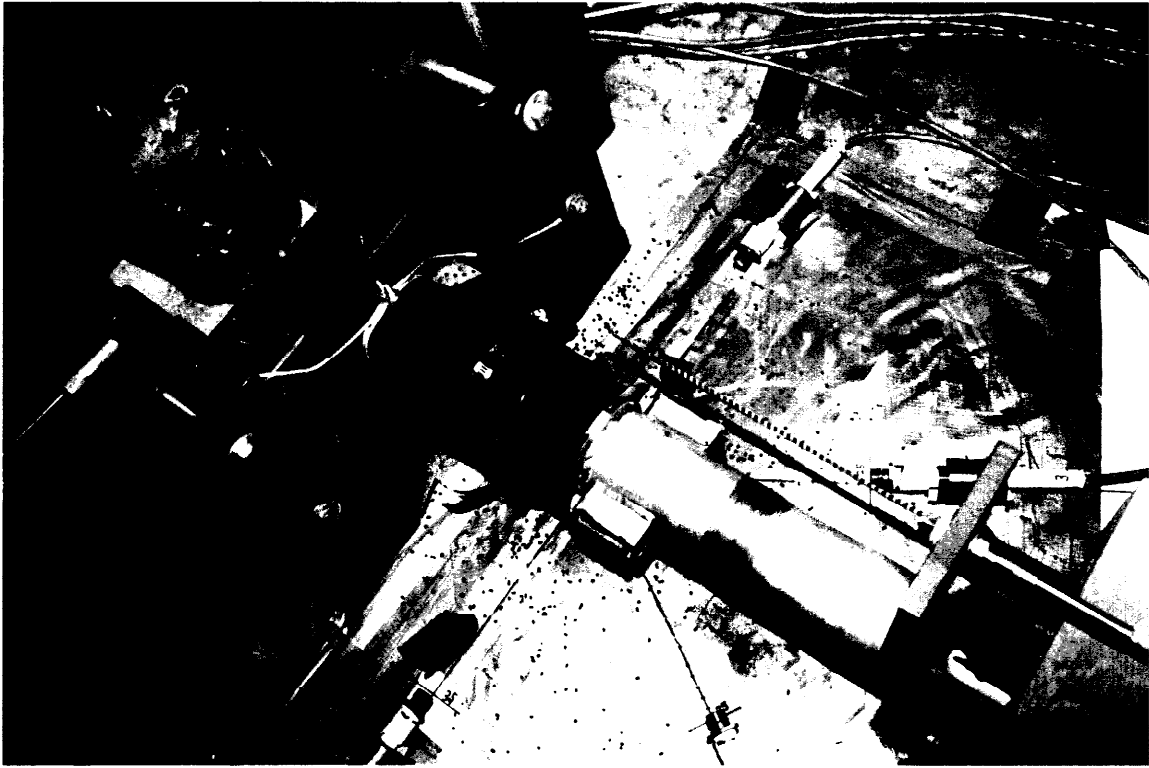
**Canister #24:
Bottom Impact
Slow Loading Method**

Note

- Canister #25
- Impact Date : Sept. 3, 1998
- Loading Method : Fast
- Impact Location : Bottom

○ : Sensor Position



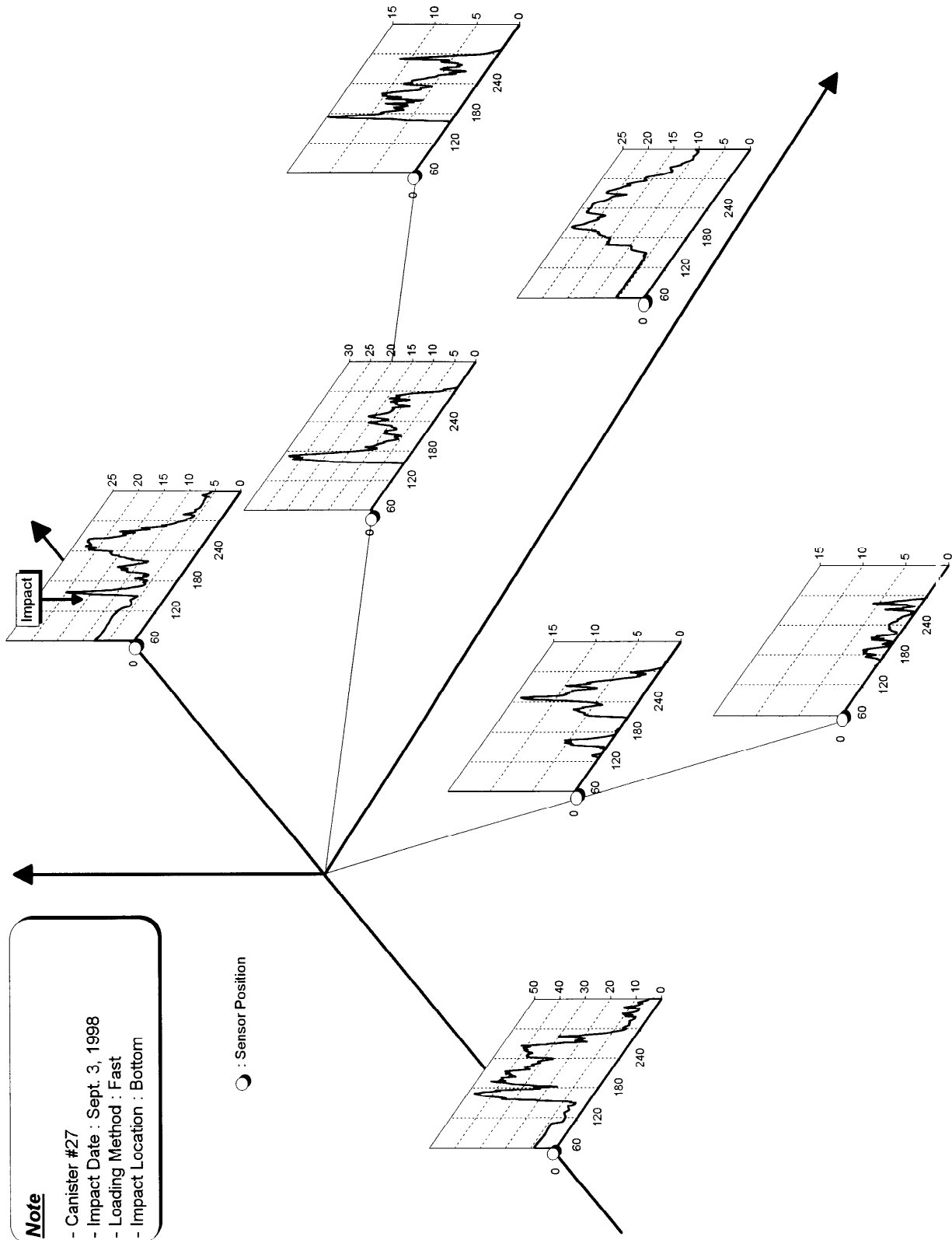


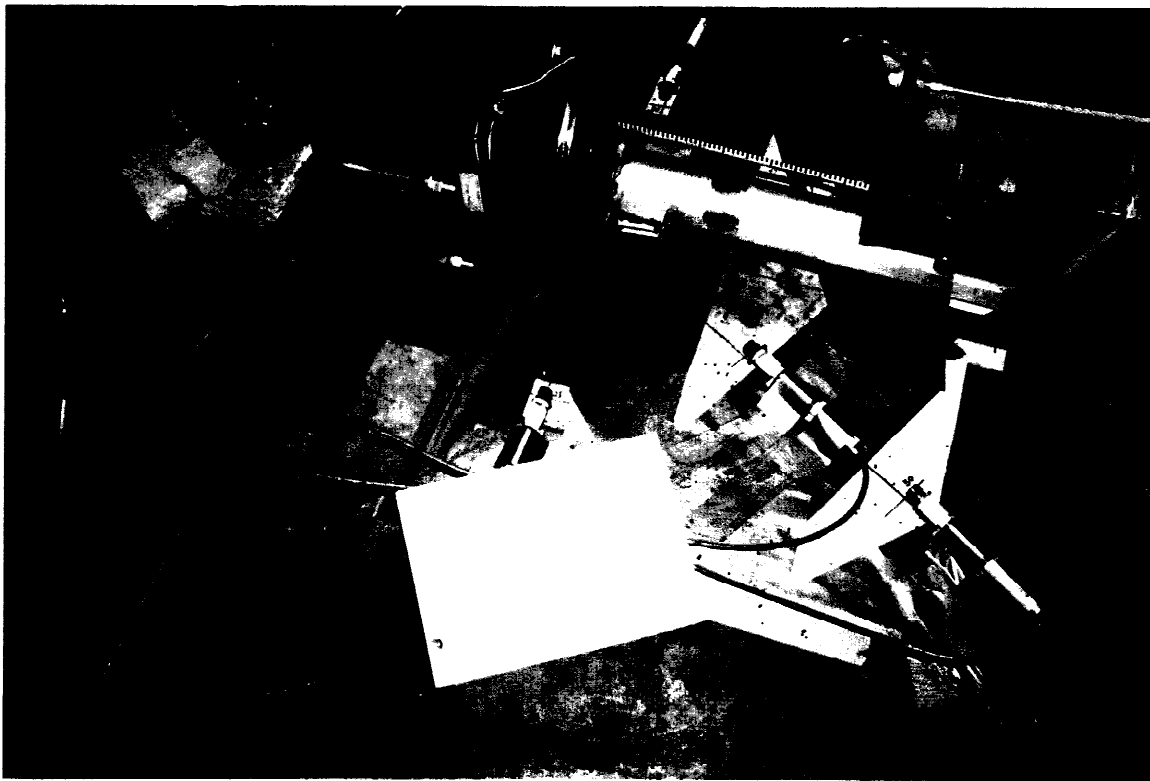
**Canister #25:
Bottom Impact
Fast Loading Method**

Note

- Canister #27
- Impact Date : Sept. 3, 1998
- Loading Method : Fast
- Impact Location : Bottom

○ : Sensor Position



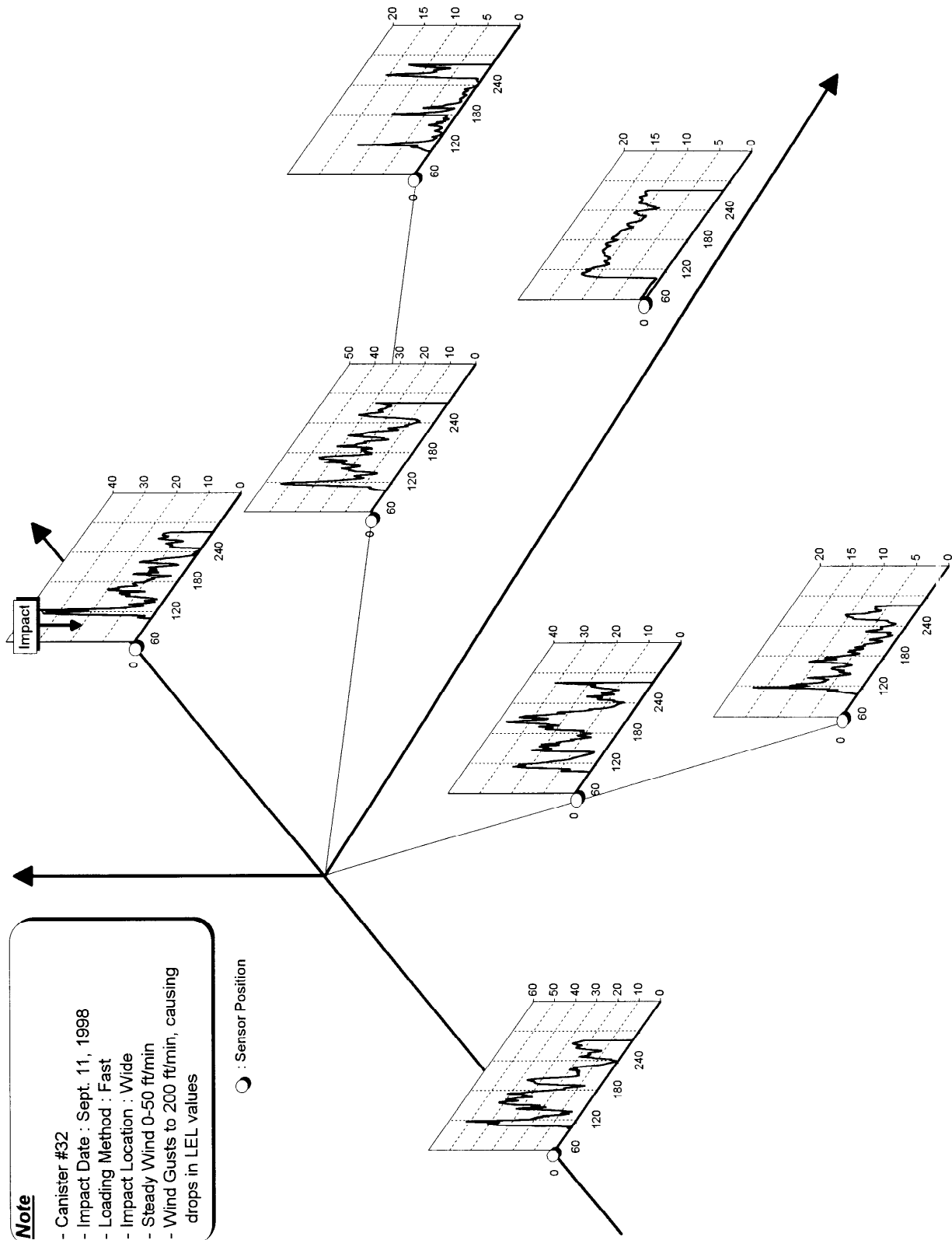


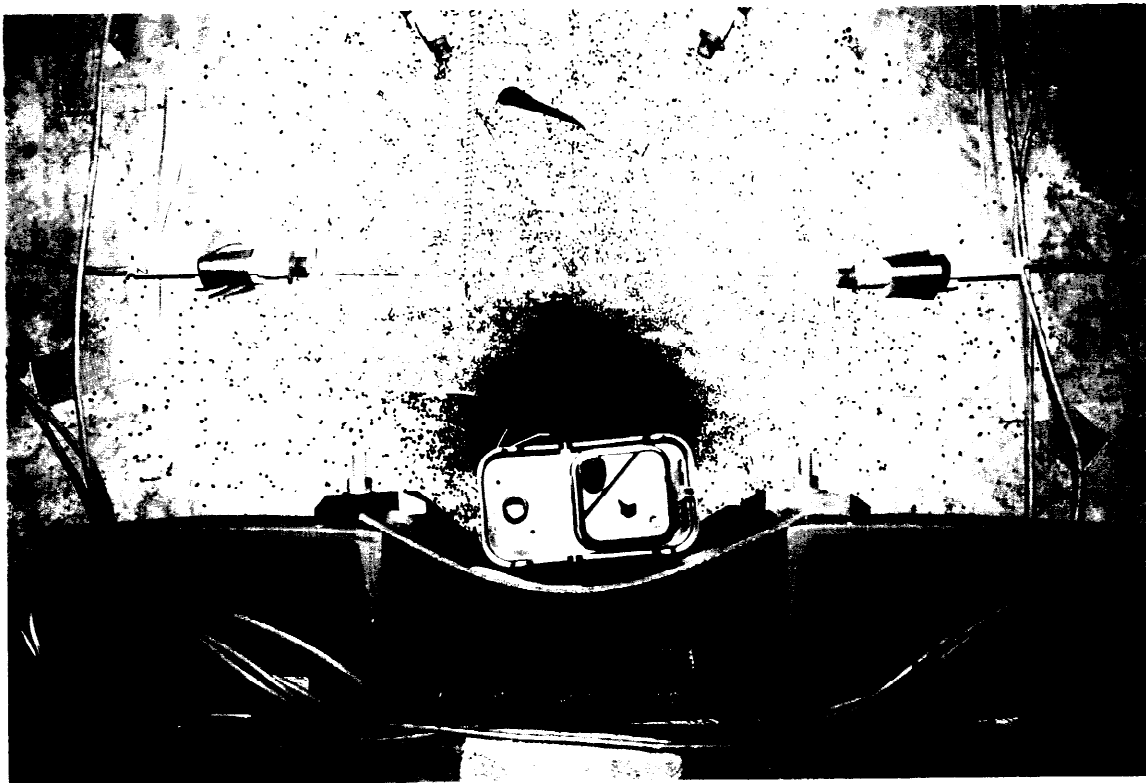
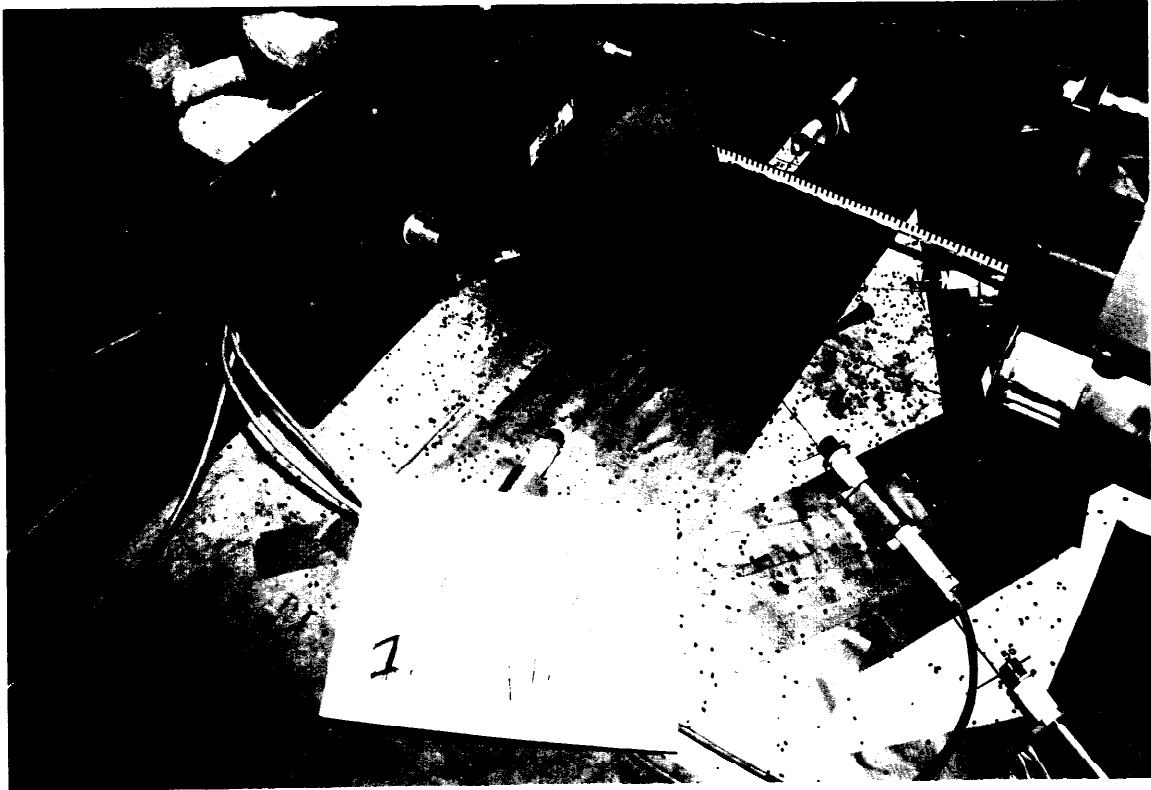
**Canister #27:
Bottom Impact
Fast Loading Method**

Note

- Canister #32
- Impact Date : Sept. 11, 1998
- Loading Method : Fast
- Impact Location : Wide
- Steady Wind 0-50 ft/min
- Wind Gusts to 200 ft/min, causing drops in LEL values

○ : Sensor Position



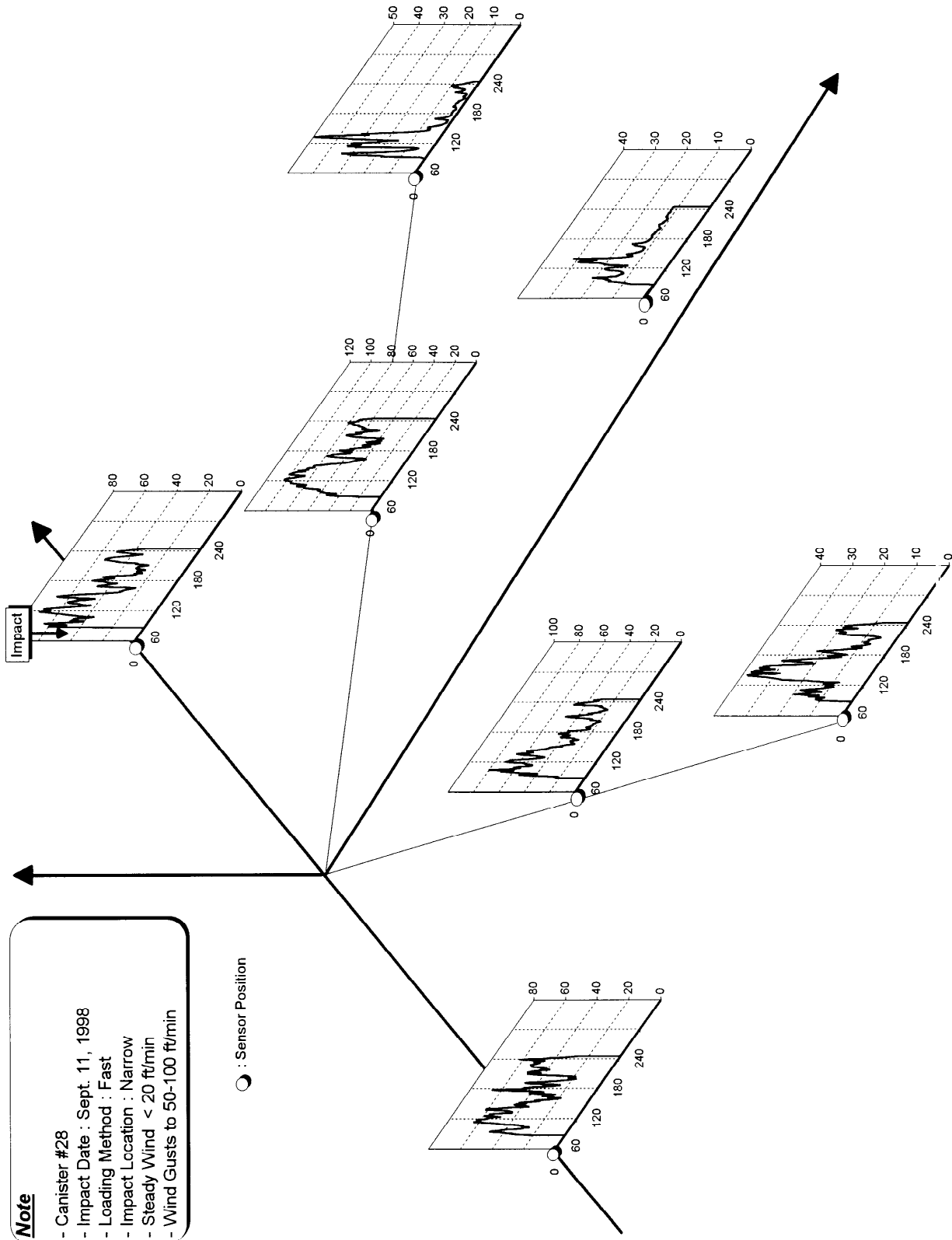


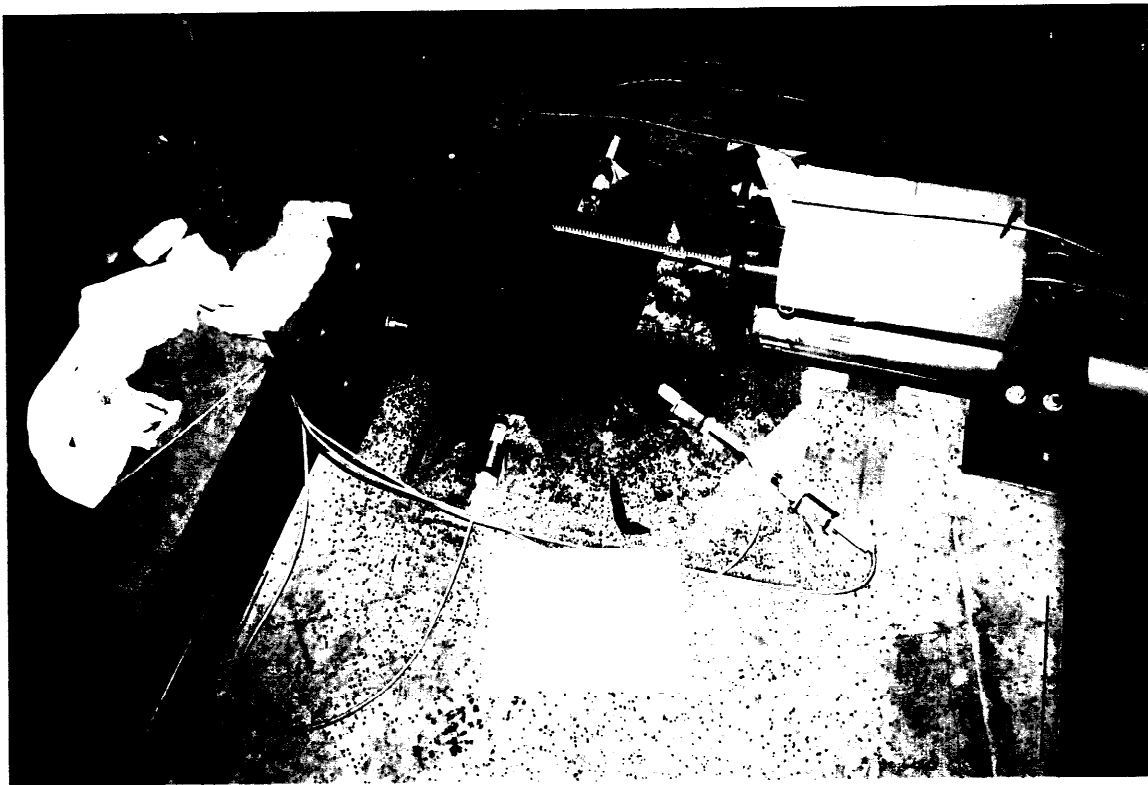
**Canister #32:
Wide Side Impact
Fast Loading Method**

Note

- Canister #28
- Impact Date : Sept. 11, 1998
- Loading Method : Fast
- Impact Location : Narrow
- Steady Wind < 20 ft/min
- Wind Gusts to 50-100 ft/min

○ : Sensor Position





**Canister #28:
Narrow Side Impact
Fast Loading Method**